

**DESIGN OF A SOLAR PHOTO-VOLTAIC POWER CONDITIONING  
SYSTEM AND MPPT WITH SIMULATION, ANALYSIS, AND  
COMPARISON OF ALGORITHMS**

**BY**

**1. SHEIKH MOHAMMAD MOSTAFA**

**ID: 101-33-189**

**2. MD. FOKHRUL ALAM**

**ID: 101-33-129**

This Report Presented in Partial Fulfilment of the Requirements for the Degree  
of Bachelor of Science in Electrical and Electronic Engineering

Supervised By

**Professor Dr. M. Shamsul Alam**

Dean

Faculty of Engineering

Daffodil International University



**DAFFODIL INTERNATIONAL UNIVERSITY**

**DHAKA, BANGLADESH**

**APRIL 2014**

## **APPROVAL**

This Project titled “DESIGN OF A SOLAR PHOTO-VOLTAIC POWER CONDITIONING SYSTEM AND MPPT WITH SIMULATION, ANALYSIS, AND COMPARISON OF ALGORITHMS”, submitted by Sheikh Mohammad Mostafa and Md. Fokhrul Alam to the Department of Electrical and Electronic Engineering, Daffodil International University, has been accepted as satisfactory for the partial fulfilment of the requirements for the degree of B.Sc. in Electrical and Electronic Engineering and approved as to its style and contents. The presentation was held on April 13, 2014.

## DECLARATION

We hereby declare that, this project has been done by us under the supervision of Professor Dr. M. Shamsul Alam, Dean, Faculty of Engineering, Daffodil International University. We also declare that neither this project nor any part of this project has been submitted elsewhere for award of any degree or diploma.

**Supervised by:**

---

**Professor M. Shamsul Alam**

**Dean**

**Department of EEE**

**Daffodil International University**

**Submitted by:**

---

**Sheikh Mohammad Mostafa**

ID: 101-33-189

Department of EEE

Daffodil International University

---

**Md. Fokhrul Alam**

ID: 101-33-129

Department of EEE

Daffodil International University

## ACKNOWLEDGEMENT

First we express our heartiest thanks and gratefulness to almighty Allah for His divine blessing makes us possible to complete this project successfully.

We feel grateful to and wish our profound our indebtedness to **Professor M. Shamsul Alam, Dean**, Faculty of Engineering, Daffodil International University, Dhaka. Deep Knowledge & keen interest of our supervisor in the field of renewable energy influenced us to carry out this project .His endless patience, scholarly guidance ,continual encouragement, constant and energetic supervision, constructive criticism, valuable advice, reading many inferior draft and correcting them at all stages have made it possible to complete this project.

We would like to express our heartiest gratitude to Dr. Md. Fayzur Rahman, Professor and Head, Department of EEE, for his kind help to finish our project and also to other faculty members and the staff of EEE department of Daffodil International University.

We would like to thank our entire course mates in Daffodil International University, who took part in this discussion while completing the course work.

Finally, we must acknowledge with due respect the constant support and patience of our parents.

## ABSTRACT

In this thesis, the advantages of two different maximum power point tracking (MPPT) algorithms has been investigated for a sound solar photovoltaic power conditioning system. By simulation, the performance and efficiency of these algorithms were analyzed by implement in a mppt of a solar photovoltaic power conditioning system as a calculative brain. By using MATLAB's SimPowerSystems block set, we created the model comprised of a solar panel powering a buck-boost converter controlled by the MPPT algorithms driving a resistive load. The main objective was to track the maximum power point (MPP) of the solar array by modulating the buck converter's duty cycle, thereby, optimizing the power output of the panel. The two algorithms observed performance was on par with other real world tests of these algorithms as seen in other published work. The Perturb and Observe (P&O) algorithm performed with a higher overall efficiency and was able to track the MPP quickly, while the Incremental Conductance (InC) algorithm had similar performance but requires more intensive calculations. The analysis of these algorithms led to a greater understanding of where the inefficiencies of this type of system are located, allowing improvement in future work on this subject.

# TABLE OF CONTENTS

<b>CONTENTS</b>	<b>PAGE</b>
Declaration	i
Acknowledgements	ii
Abstract	iii
<b>CHAPTER</b>	
<b>CHAPTER 1: INTRODUCTION</b>	1-26
1.1 Objective	2
1.2 Motivation	3
1.3 Solar Energy	4
1.4 Kinds of Solar Energy	5
1.5 Photovoltaic Solar Power	5
1.6 Photovoltaic Modules	6
1.7 Solar Cell	7
1.7.1 Equivalent Circuit of a Solar Cell	11
1.7.2 Open Circuit Voltage, Short Circuit Current and Maximum Power point	12
1.8 Solar Panel	13
1.9 Solar Array	14
1.10 Kinds of Solar Panel	15
1.10.1 Monocrystalline Solar Cell	16
1.10.2 Poly Crystalline Solar Cell	16
1.10.3 Amorphous Solar Cell	17
1.11 Efficiency Comparison of Different of Solar Cells	17
1.12 Charge Controller	18
1.13 Analog to Digital Converter and Digital to Analog Converter	19
1.14 Pulse-Width Modulation (PWM)	20
1.15 DC-DC Converter	21
1.16 Storage Batteries	22
1.17 The Power Inverter	24

1.17.1 Square Wave Power Inverters	24
1.17.2 Modified Sine Wave Power Inverters	24
1.17.3 True Sine Wave Power Inverters	25
1.17.4 Grid Tie Power Inverters	25

## **CHAPTER 2: LITERATURE SURVEY** 27-30

2.1 Masters Thesis – Hurd	27
2.2 Masters Thesis – Coba	27
2.3 Modeling and Simulation of Photovoltaic Module Using Matlab/Simulink	28
2.4 Advantage of Boost versus Buck Topology for Maximum Power Point Tracker in Photovoltaic Systems	28
2.5 Comparison of MPPT Algorithms for DC-DC Converter Based PV Systems	28
2.6 High Efficiency Switched Capacitor Buck-boost Converter for PV Application	29
2.7 A Novel MPPT Charge Regulator for a Photovoltaic Stand-alone Telecommunication System	29
2.8 Improved Circuit Model of Photovoltaic Array	29
2.9 Comparative Study of Maximum Power Point Tracking Algorithms	30
2.10 Design and Implementation of Maximum Power Point Tracking Algorithm for a Standalone PV System	30

## **CHAPTER 3: SYSTEM OVERVIEW** 32-45

3.1 System Diagram and Description	32
3.2 Modeling of Components under Test	34
3.2.1 Solar Array	34
3.2.2 Buck-boost Converter	36
3.2.3 Load	38
3.2.4 IGBT	39
3.2.5 Pulse Width Modulation Generation	39
3.2.6 DC-AC Converter	40
3.2.7 Low-pass Filter	41
3.2.8 MPPT Algorithms	42

<b>CHAPTER 4: MAXIMUM POWER POINT TRACKER</b>	<b>47-56</b>
4.1 Maximum Power Point Tracking	47
4.2 Effect of Variation of Solar Irradiation	50
4.3 Effect of Variation of Temperature	51
4.4 Comparison of the tracking power for different MPPT system	52
4.5 Sensing Circuits	53
4.5.1 Voltage Sensor	53
4.5.2 Current Sensor	54
4.6 Duty Cycle	54
4.7 Methods for MPPT	55
4.7.1 Perturb and Observe Method	55
4.7.2 Incremental Conductance Method	55
4.7.3 Parasitic Capacitance Method	56
4.7.4 Constant Voltage Method	56
4.7.5 Constant Current Method	56
<b>CHAPTER 5: MPPT ALGORITHMS TEST AND DATA ANALYSIS</b>	<b>58-80</b>
5.1 Matlab Code for Perturb and Observe Algorithm	58
5.1.1 Run Result	59
5.1.2 Duty Cycle versus Power	61
5.2 Matlab Code for Incremental Conductance Algorithm	61
5.2.1 Run Result	63
5.2.2 Duty Cycle versus Power	65
5.3. Comparison	65
5.3.1 P&O versus Inc	65
5.4 Verification of the Conditions of the Algorithms	67
5.4.1 Perturb and Observe Algorithm	67
5.4.2 Incremental Conductance Algorithm	68
5.5 Correlation	71
5.5.1 Correlation between Input Power & Duty Cycle (P & O algorithm)	71
5.5.2 Correlation between Input Power & Duty Cycle (InC algorithm)	74
5.5.3 Correlation between Duty Cycles obtained from P&O and InC algorithms	77



<b>CHAPTER 6: SIMULATION RESULTS AND COMPARISON</b>	<b>82-95</b>
6.1 Simulink Model	82
6.1.1 Simulink Model using P&O Algorithm	82
6.1.2 Simulink Model using Inc Conductance Algorithm	83
6.2 Effect of Irradiance and Temperature on PV Voltage, Current and Power	84
6.3 Waveforms for P&O Algorithm	87
6.3.1 PV Voltage and Current	87
6.3.2 PV Power	88
6.3.3 Input and Output Voltage of Buck-boost Converter	88
6.3.4 Duty Cycle	89
6.3.5 AC Voltage Output	89
6.4 Waveforms for Inc Conductance Algorithm	90
6.4.1 PV Voltage and Current	90
6.4.2 PV Power	90
6.4.3 Input and Output Voltage of Buck-boost Converter	91
6.4.4 Duty Cycle	91
6.4.5 AC Voltage Output	92
6.5 Comparison	92
6.5.1 Comparison of the tracking power,voltage,current with different MPPT system for different temperature and irradiance	92
6.5.2 Comparison of the tracking power,voltage,current without MPPT system for different temperature and irradiance	93
6.5.3 Comparison of the tracking power,voltage,current between NO MPPT and MPPT(PO) for different temperature and irradiance	93
6.5.4 Comparison of the tracking power,voltage,current between NO MPPT and MPPT(INC) for different temperature and irradiance	94
6.5.5 Comparison of the elapsed time for different MPPT system	95

<b>CHAPTER 7: CONCLUSION AND FUTURE WORK</b>	97-99
7.1 Conclusion	97
7.2 Future Work	98
7.2.1 UAV Flight Endurance	98
7.2.2 Second Stage Constant Voltage Output	99
7.2.3 Test MPPT on Real Hardware	99
<b>APPENDIX</b>	100-105
<b>REFERENCES</b>	106-108

## LIST OF FIGURES

Fig1.1: Solar Power System	4
Fig1.2: Photovoltaic Solar Power	5
Fig1.3: PV Module typical construction	6
Fig1.4: Solar cell	7
Fig1.5: Structure of Solar cell	8
Fig1.6: I-V characteristics of the PV cell	9
Fig1.7: P-V characteristics of the PV cell	10
Fig1.8: Equivalent circuit of a solar cell	12
Fig1.9: Important points in the characteristic curves of a solar panel	13
Fig1.10: Solar panel	14
Fig1.11: Solar array	15
Fig 1.12: Different Solar Cells	16
Fig 1.13: The relationship between the current and the voltage during the 3 phases of the charge cycle	18
Fig 1.14: Analog to Digital and Digital to Analog Conversion	19
Fig1.15: PWM signals of varying duty cycles	21
Fig1.16: DC-DC Converter with MPPT	22
Fig 1.17: Storage Batteries	23
Fig 1.18: Power Inverter	24
Fig 3.1: The functional portion of the model under test in Simulink, which includes the solar array, buck-boost converter, resistive load, inverter and LC filter	33
Fig 3.2: The pv panel used for the simulation of the system	34
Fig 3.3: The Current versus Voltage and Power versus Voltage plots from the Panel Modeled	36
Fig 3.4: Overview of the buck-boost converter model in Simulink	36
Fig 3.5: The two operating states of a buck–boost converter	38
Fig 3.6: Output load resistor with measurement blocks connected	39
Fig 3.7: IGBT block from MATLAB SimPowerSystems	39
Fig 3.8: PWM signal with triangle wave and duty cycle example	40
Fig 3.9: DC-AC Converter used in the system	41
Fig 3.10: Low-pass Filter used in the system	42
Fig 3.11: Flow chart of Perturb and Observe Algorithm	43

Fig 3.12: Flow chart of the InC Algorithm	44
Fig 4.1: Solar Photovoltaic system with maximum power point tracker	48
Fig 4.2: Maximum power point tracker: DC-DC converter	48
Fig 4.3: Control circuit diagram	49
Fig 4.4: I-V characteristics curve	49
Fig 4.5: Variation of P-V curve with solar irradiation	50
Fig 4.6: Variation of I-V curve with solar irradiation	51
Fig 4.7: Variation of P-V curve with temperature	51
Fig 4.8: Variation of I-V curve with temperature	52
Fig 4.9: Voltage Sensor	53
Fig 4.10: Current Sensor	54
Fig 5.1: Perturb and Observe-Duty cycle versus Power	61
Fig 5.2: Incremental conductance-Duty cycle versus Power	65
Fig 5.3: Duty Cycle vs Power Curves of P&O & InC Algorithms	71
Fig 6.1: The functional portion of the model under test in Simulink using Perturb and Observe Algorithm	82
Fig 6.2: The functional portion of the model under test in Simulink using Inc Conductance Algorithm	83
Fig 6.3: Effect of Irradiance and Temperature on PV Current	84
Fig 6.4: Effect of Irradiance and Temperature on PV Voltage	85
Fig 6.5: Effect of Irradiance and Temperature on PV Power	85
Fig 6.6: Effect of Irradiance and Temperature on PV Voltage, Current and Power	86
Fig 6.7: Waveforms of PV Voltage (Top) and Current (Bottom) versus Time	87
Fig 6.8: Waveform of Photo-Voltaic Power versus Time	88
6.9: Waveforms of Input (Bottom) and Output Voltage (Top) of Buck-Boost Converter versus Time	88
6.10: Waveform of Duty Cycle versus Time	89
Fig 6.11: Waveforms of AC Voltage after Filtering (Top) and before Filtering (Bottom) versus Time	89
Fig 6.12: Waveforms of PV Voltage (Top) and Current (Bottom) versus Time	90
Fig 6.13: Waveform of Photo-Voltaic Power versus Time	90

Fig 6.14: Waveforms of Input (Bottom) and Output Voltage (Top) of Buck-Boost Converter versus Time	91
Fig 6.15: Waveform of Duty Cycle versus Time	91
Fig 6.16: Waveforms of AC Voltage after Filtering (Top) and before Filtering (Bottom) versus Time	92

## LIST OF TABLES

Table: 1.1: Efficiency Comparison of Different of Solar Cells	17
Table 4.4: Comparison of the tracking power for different MPPT system	52
Table 5.1: Input Current, Input Voltage, Input Power and Corresponding Duty Cycle after Each Step for P&O Algorithm	60
Table 5.2: Input Current, Input Voltage, Input Power and Corresponding Duty Cycle after Each Step for Inc Conductance Algorithm	63
Table 5.3: Input Current, Input Voltage, Input Power and Corresponding Duty Cycle after Each Step for P&O and Inc Conductance Algorithm	65
Table 5.4: Correlation between Input Power & Duty Cycle (P & O algorithm)	71
Table 5.5: Correlation between Input Power & Duty Cycle (InC algorithm)	74
Table 5.6: Correlation between Duty Cycles obtained from P&O and InC algorithms	77
Table 6.5.1: Comparison of the tracking power,voltage,current wiyh different MPPT system for different temperature and irradiance	92
Table 6.5.2: Comparison of the tracking power,voltage,current without MPPT system for different temperature and irradiance	93
Table 6.5.3: Comparison of the tracking power,voltage,current between NO MPPT and MPPT(PO) for different temperature and irradiance	93
Table 6.5.4: Comparison of the tracking power,voltage,current between NO MPPT and MPPT(PO) for different temperature and irradiance	94
Table 6.5.5: Comparison of the elapsed time for different MPPT system	95

## **LIST OF ACRONYMS AND ABBREVIATIONS**

D	Duty Cycle
DC	Direct Current
AC	Alternating Current
InC	Incremental Conductance
P&O	Perturb and Observe
CCM	Continuous Conduction Mode
MPP	Maximum Power Point
MPPT	Maximum Power Point Tracker
PWM	Pulse Width Modulation

# **CHAPTER 1**

## **INTRODUCTION**

One of the major concerns in the power sector is the day-to-day increasing power demand but the unavailability of enough resources to meet the power demand using the conventional energy sources. Demand has increased for renewable sources of energy to be utilized along with conventional systems to meet the energy demand. Renewable sources like wind energy and solar energy are the prime energy sources which are being utilized in this regard. The continuous use of fossil fuels has caused the fossil fuel deposit to be reduced and has drastically affected the environment depleting the biosphere and cumulatively adding to global warming.

Solar energy is abundantly available that has made it possible to harvest it and utilize it properly. Solar energy can be a standalone generating unit or can be a grid connected generating unit depending on the availability of a grid nearby. Thus it can be used to power rural areas where the availability of grids is very low. Another advantage of using solar energy is the portable operation whenever wherever necessary.

In order to tackle the present energy crisis one has to develop an efficient manner in which power has to be extracted from the incoming solar radiation. The power conversion mechanisms have been greatly reduced in size in the past few years. The development in power electronics and material science has helped engineers to come up very small but powerful systems to withstand the high power demand. But the disadvantage of these systems is the increased power density. Trend has set in for the use of multi-input converter units that can effectively handle the voltage fluctuations. But due to high production cost and the low efficiency of these systems they can hardly compete in the competitive markets as a prime power generation source.

The constant increase in the development of the solar cells manufacturing technology would definitely make the use of these technologies possible on a wider basis than what the scenario is presently. The use of the newest power control mechanisms called the Maximum Power Point Tracking (MPPT) algorithms has led to the increase in the efficiency of operation of the solar modules and thus is effective in the field of utilization of renewable sources of energy[1],[2].



Maximum power point trackers (MPPTs) play an important role in photovoltaic (PV) power systems because they maximize the power output from a PV system for a given set of conditions, and therefore maximize the array efficiency. Thus, an MPPT can minimize the overall system cost. MPPTs find and maintain operation at the maximum power point, using an MPPT algorithm. Many such algorithms have been proposed. However, two particular algorithms, the perturb-and-observe (P&O) method and Incremental Conductance (INC) method, claimed by many in the literature to be inferior to others, continues to be by far the most widely used method in commercial PV MPPTs[3].

## 1.1 Objective

The objective of this thesis is to determine the most cost effective and efficient method for maximum power point tracking (MPPT). Many optimizations can be done to a system. Knowing which will bring about the greatest change is truly the challenge.

Since fossil fuels are detrimental to the environment and also non-renewable, there has been an upsurge of interest in clean and renewable energy. While more than one option is available to fill that void, the most interesting and widespread so far is photovoltaics. Photovoltaics are semiconductor devices which convert solar irradiation in the visible spectrum to generate direct current (DC). With recent advances in technology and discoveries of new materials, solar cells are increasing in efficiency and flexibility. This change in what solar panels are composed of has greatly increased the applications of these panels. The surface they are supported on no longer needs to be rigid and planar, and due to this they are now able to be used in applications that previously could not use photovoltaics. In order to fully harness the power of the sun, we need to optimize the output from the solar panels. In the simplest terms a solar panel is a current source when short circuited and has a voltage while in open circuit configuration. The key to attaining the greatest output from the panels is to maintain an output impedance so that the solar panels operate at a point that corresponds to its maximum power point (MPP). The MPP is the operating point required to optimize the output power of the panels. Depending on weather conditions, the output power is proportional to the amount of incident light on the surface of the photovoltaics, as well as being inversely proportional to the temperature of the panels. This means that the hotter the panels get the less current they can provide at the output.

In order to convert the power from the solar array, we require a power converter that will be able to extract the most power from the array. By connecting a buck boost converter to the

output of the solar array, we are then able to control the voltage of the solar array by varying the duty cycle ( $D$ ) of the buck boost converter. When one is changing  $D$ , we want the voltage and current to provide the most power at a specific voltage level. In order to reach this voltage level, a control algorithm is implemented to track and follow the highest input power from the solar array. When this algorithm is functioning correctly, it is said to be an MPPT[4].

## 1.2 Motivation

Photovoltaic power control is one of the burning research fields these days. Researchers are working round the clock to develop better solar cell materials and efficient control mechanisms. The challenge of the project and the new area of study were the motivations behind the project.

Clean and renewable energy has greatly increased funding for supporting areas in research and development. Today, energy is necessary for nearly everything. We need a more efficient method of transformation of DC for different voltages and power levels. By analyzing the power transfer in a buck converter, we will be able to better understand how and why these converters function so well. In our modern society, it has become increasingly necessary to shift away from non-renewable resources. A change might occur if energy prices were to increase drastically, but by then it might be too late to switch our focus and essentially rebuild our machines to run off of fuel that is readily available. The effect can be seen today in the car industry as currently it is driven by petroleum. With every increase in petroleum prices, a public outcry is heard and more and more people are replacing their inefficient vehicles with modern hybrid or electric drive vehicles. We can reduce the effect of petroleum pollution by shifting to renewable resources, such as photovoltaics. In addition to this need for renewable resources, there is also a similar need for efficient transformation of power from one form to another. Since solar panels are quite inefficient to begin with, any method of improving power transfer from these panels is a worthwhile gain in overall efficiency. One method to accomplish this is to operate the panels at their MPP. By connecting a solar array to a buck boost converter, we can control the output voltage of the panels. The parameter to be controlled is the percentage of time a switch is active during each control cycle. In order to compare the performance of different algorithms designed to control the buck boost converter, a simulation was made to compare the algorithms[4].

### 1.3 Solar Energy

Solar energy is the energy derived from the sun through the form of solar radiation. Solar powered electrical generation relies on photovoltaic and heat engines. A partial list of other solar applications includes space heating and cooling through solar architecture, day lighting, and solar hot water, solar cooking, and high temperature process heat for industrial purposes.

Solar technologies are broadly characterized as either passive solar or active solar depending on the way they capture, convert and distribute solar energy. Active solar techniques include the use of photovoltaic panels and solar thermal collectors to harness the energy. Passive solar techniques include orienting a building to the Sun, selecting materials with favourable thermal mass or light dispersing properties, and designing spaces that naturally circulate air[5].

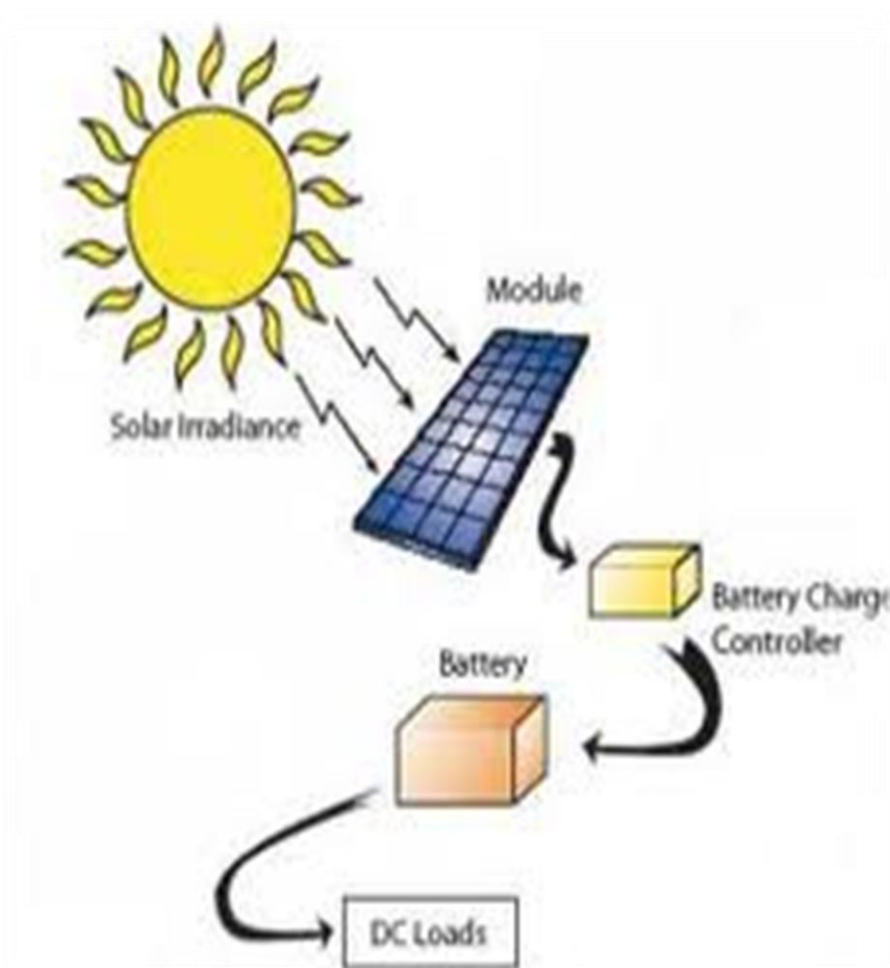


Fig1.1: Solar power system. Image from [5]

## 1.4 Kinds of Solar Energy

There are two kinds of solar energy.

Electricity Production (Photovoltaic or PV Technology)

Water Heating (Solar Thermal or Flat Plate Technology).

## 1.5 Photovoltaic Solar Power

Solar energy is energy that is present in sunlight. It has been used for thousands of years in many different ways by people all over the world. As well as its traditional human uses in heating, cooking, and drying, it is used today to make electricity where other power supplies are absent, such as in remote places and in space. It is becoming cheaper to make electricity from solar energy and in many situations it is now competitive with energy from coal or oil.

The most common kind of solar energy is photovoltaic cells, which directly convert light to electricity. Photovoltaic (PV) cells utilize semiconductor technology to convert solar radiation directly into an electric current which can be used immediately or stored for future use.[6] PV cells are often grouped in the form of “modules” to produce arrays which have the capability to produce power for orbiting satellites and other spacecraft.

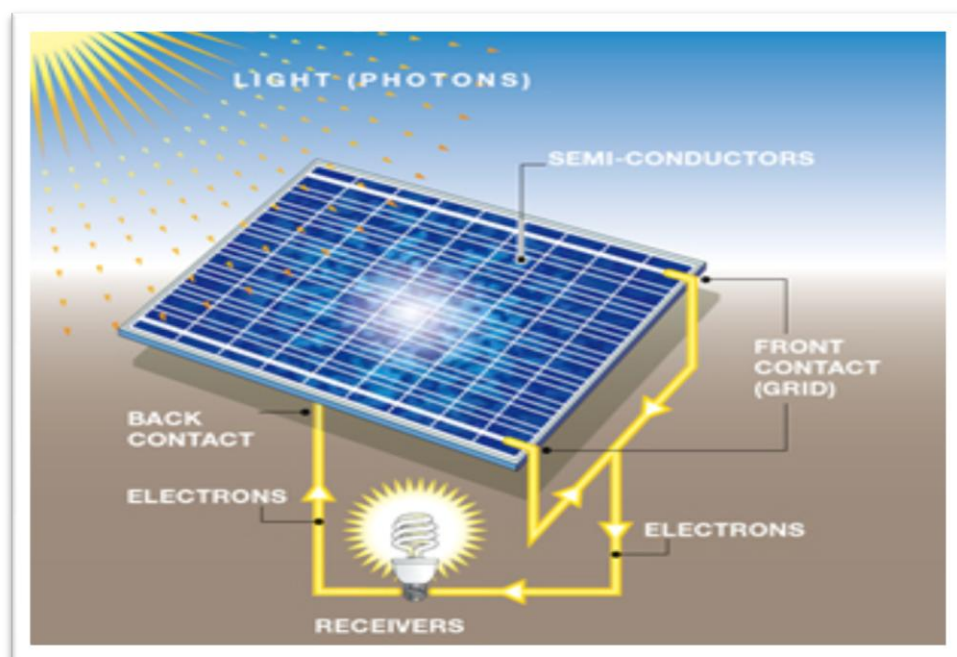


Fig1.2: Photovoltaic solar power .Image from [6]

Recently, with the continual decline of manufacturing costs (declining 3% to 5% per year in recent years)[6], uses of PV technology have grown to include home power generation, and grid-connected electricity generation. Installations of PV systems have also been increasing due in large part to comprehensive incentive programs which help reduce the costs of these systems and also allow users to sell excess electricity back to the public grid.

## 1.6 Photovoltaic Modules

PV modules are made from solar cells connected in series and parallel to obtain the desired current and voltage levels. Solar cells are encapsulated as they have to be weatherproofed and electric connections also have to be robust and corrosion free. The typical construction of a PV module can be seen in figure 1.3.

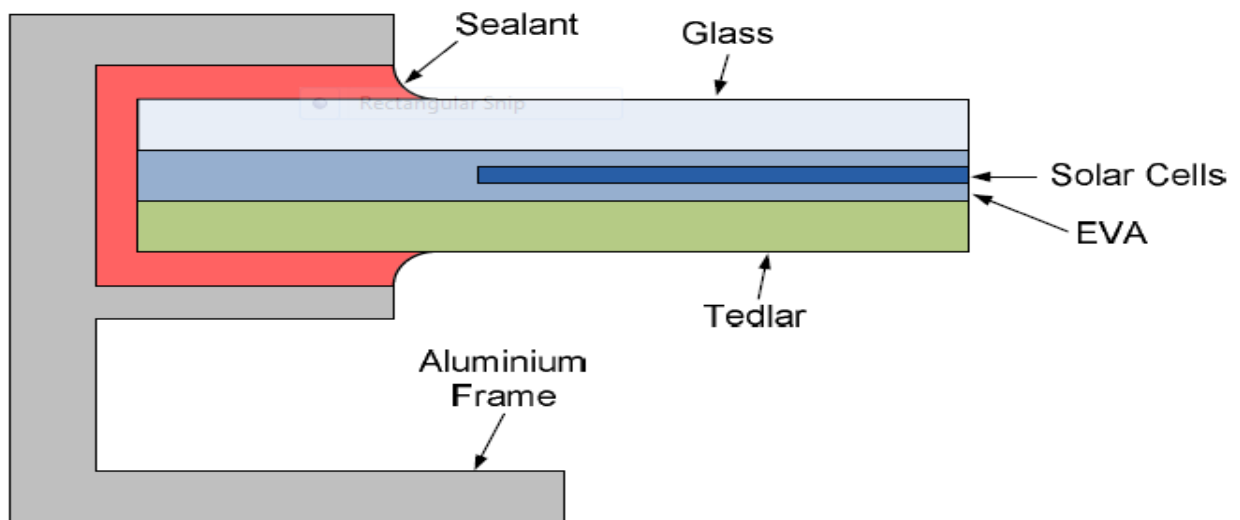


Figure1.3: PV Module typical construction. Image from [7]

As the cells are brittle, they are encapsulated in an airtight layer of ethylene vinyl acetate (EVA), a polymer, so the cells are cushioned and in that way are protected during transport and handling. The top cover is a tempered glass treated with an antireflection coating so the maximum light is transmitted to the cell. The underneath is a sheet of polyvinyl fluoride (PVF), also known Tedlar, a synthetic polymer  $(CH_2CHF)_n$  that constitutes a barrier to moisture and prevents the cell from chemical attack. An aluminium frame is used to simplify

mounting and handling and to give extra protection. Frameless modules are sometimes used in facades for aesthetic reasons. This typical construction is used because the PV module has to “survive” outdoors for at least 20-25 years under different weather conditions, sometimes extreme[4]. This construction assures at least the lifetime of the PV modules. In fact, PV panel manufacturers provide a guarantee of at least 20 years, for example BP Solar assures 85 % of minimum warranted power output after 25 years of service, 93 % of the minimum warranted power output at 12 years and a five-year warranty of materials and workmanship[7]. Such a long guarantee is extremely long compared to most products and is due to the exceptional construction of PV modules.

## 1.7 Solar Cell

A solar cell (also called photovoltaic cell or photoelectric cell) is a solid state electrical device that converts the energy of light directly into electricity by the photovoltaic effect. Assemblies of cells used to make solar modules which are used to capture energy from sunlight, are known as solar panels. The energy generated from these solar modules, referred to as solar power, is an example of solar energy.[8]



Fig1.4: Solar cell. Image from [8]

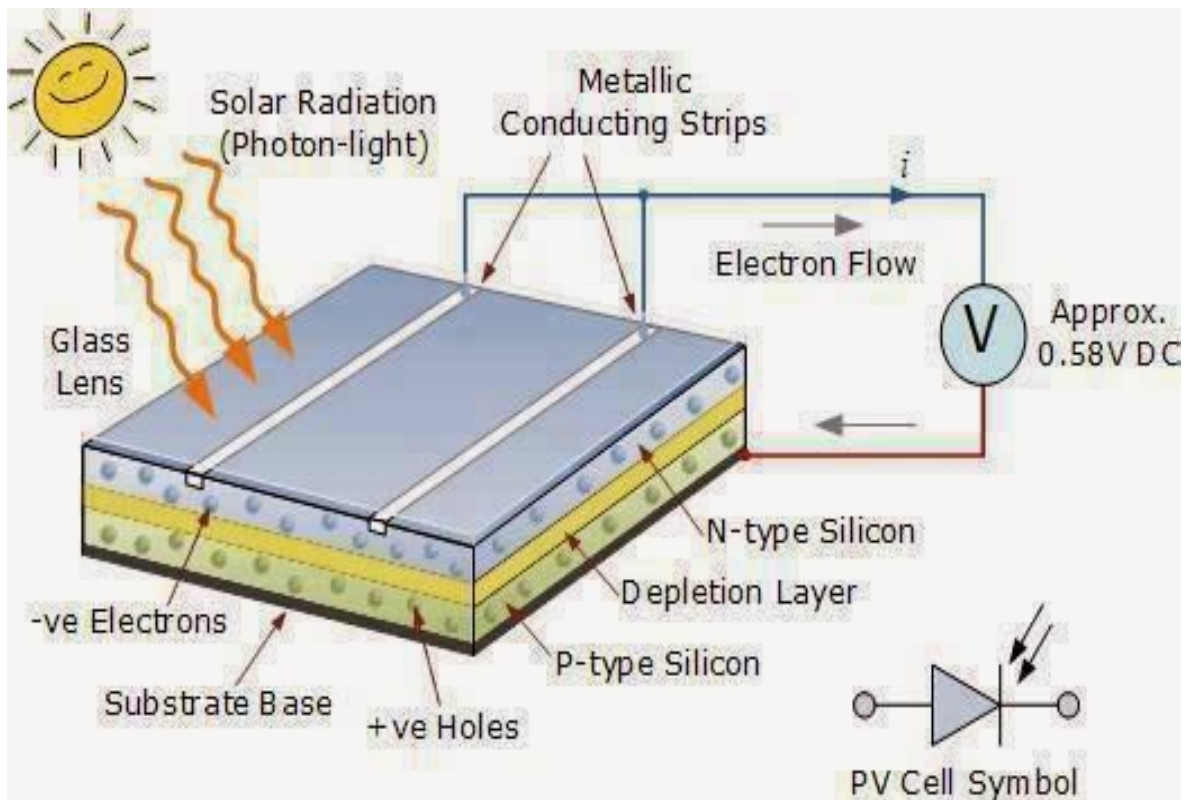
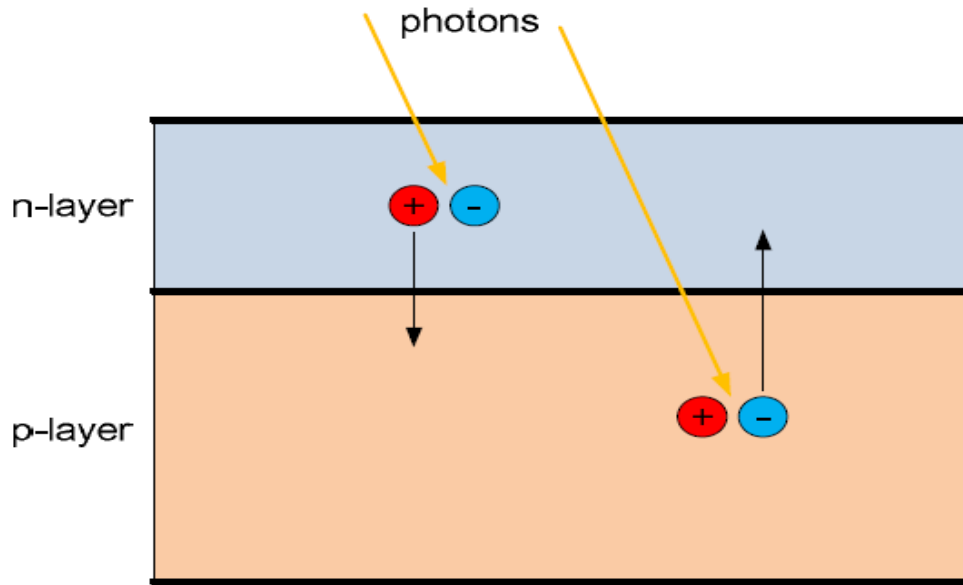


Fig 1.5: Structure of Solar cell. Image from [8]



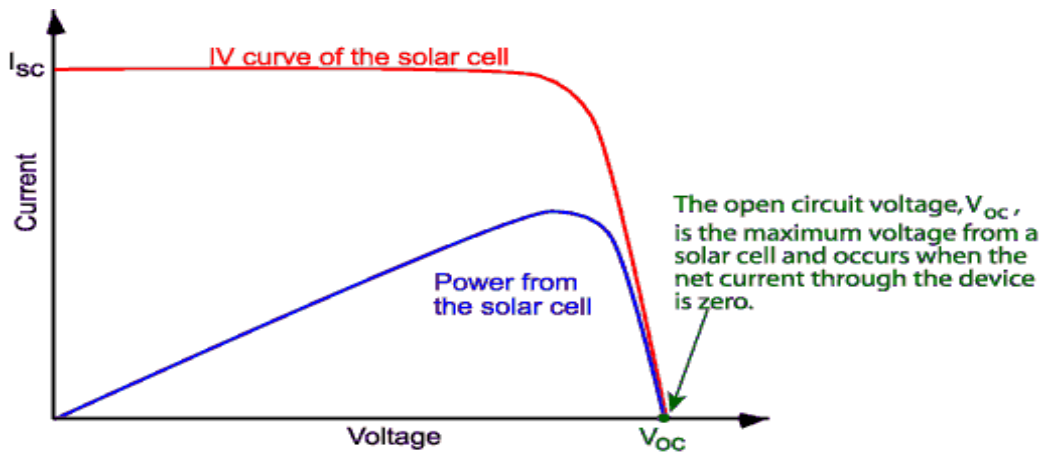
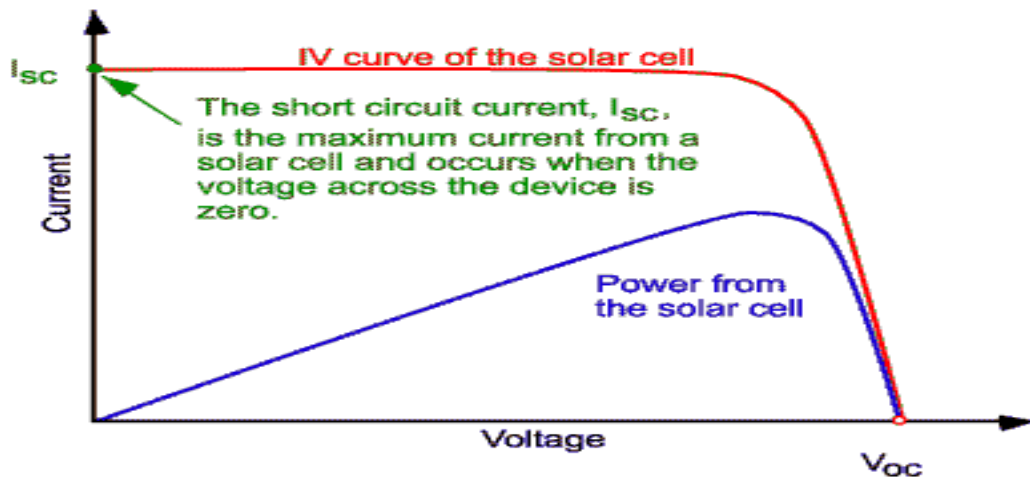
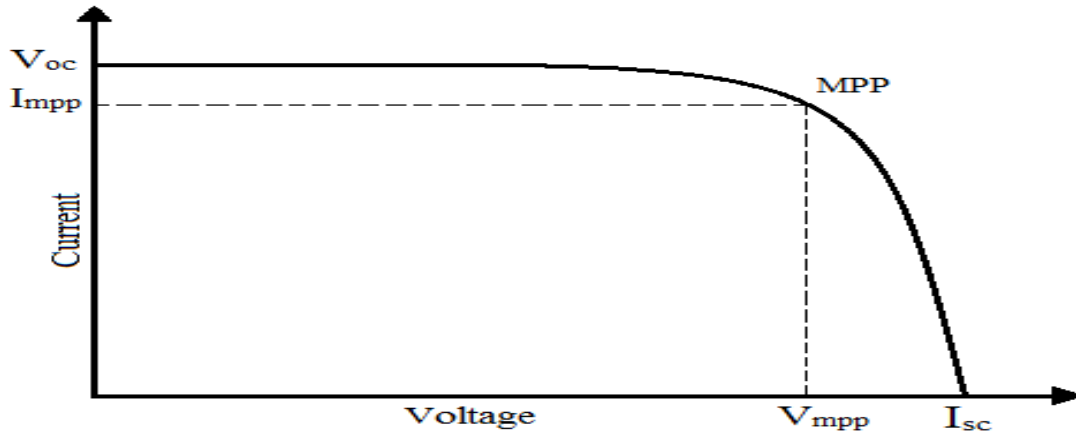


Figure1.6: I-V characteristics of the PV cell. Image from [8]



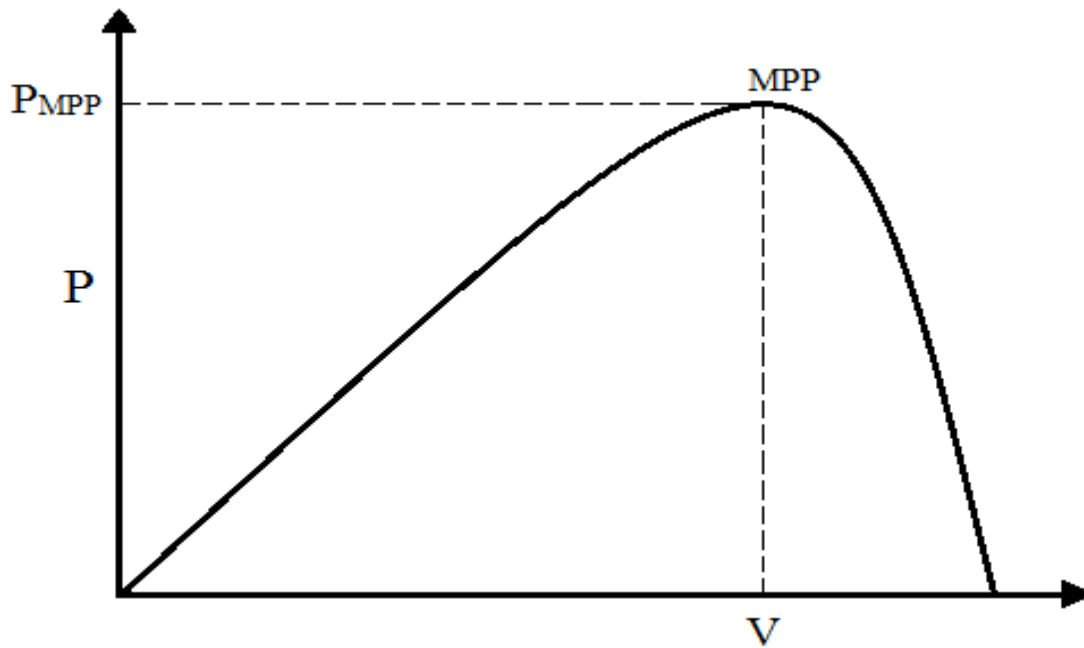


Figure1.7: P-V characteristics of the PV cell. Image from [8]

The first solar powered satellite was the TIROS-1 launched in 1960 [7]. Previous satellites used batteries that were charged before heading to space and had no way to be recharged in space. Since technology for batteries was in its early stages of development, the power capacity for these small communications relays was quite low until they had a way to recharge the batteries while in space. Seven years later, in 1967, Soyuz 1 was the first manned spacecraft to have its power replenished by solar panels [8]. From that point onward, nearly all satellites have been solar powered.

In 1980, thin film solar cells were developed by a team at the University of Delaware [6]. Thin film cells can use one of four different absorbing semiconductors: amorphous-Si, CdTe, CuInSe<sub>2</sub>, and Cu<sub>2</sub>S. Depending on which absorbing material is chosen, the efficiency and cost can be greatly affected. The lower cost of manufacturing and low mass encouraged more research into thin film solar cells. In many of today's integrated applications, thin film solar cells are an important component. Their importance is derived from their flexibility and their thinness. Current bulk-silicon-based photovoltaics have a very thick profile and cannot be bent or deformed even a small amount without shattering. Recently, there have been many innovations that have allowed photovoltaics with efficiencies greater than 40% to be created by the University of Delaware [7].

Photovoltaics is the field of technology and research related to the practical application of photovoltaic cells in producing electricity from light, though it is often used specifically to refer to the generation of electricity from sunlight. Cells are described as photovoltaic cells when the light source is not necessarily sunlight. These are used for detecting light or other electromagnetic radiation near the visible range, for example infrared detectors, or measurement of light intensity.

By knowing the total amount of power in the light that is incident on the surface of the cells, the efficiency can be found from

$$\eta = (P_{out}/P_{in}) 100\%;$$

where  $P_{out}$  is the output power and  $P_{in}$  is the input power. In order to get the correct efficiency measurement of the solar array, we need to normalize based on area. By dividing energy by the area, we obtain the normalized energy output

$$\epsilon_{norm} = \epsilon/A$$

where  $\epsilon$  is solar irradiance energy and  $A$  is area of the solar array.

### 1.7.1 Equivalent Circuit of a Solar Cell

The solar cell can be represented by the electrical model shown in figure. Its current voltage characteristic is expressed by the following equation

$$I = I_L - I_0 \left( e^{\frac{q(V-IR_S)}{AkT}} - 1 \right) - \frac{V-IR_S}{R_{SH}}$$

Where  $I$  and  $V$  are the solar cell output current and voltage respectively,  $I_0$  is the dark saturation current,  $q$  is the charge of an electron,  $A$  is the diode quality (ideality) factor is the Boltzmann constant,  $T$  is the absolute temperature and  $R_s$  and  $R_{sh}$  are the series and shunt resistances of the solar cell.  $R_s$  is the resistance offered by the contacts and the bulk semiconductor material of the solar cell. The origin of the shunt resistance  $R_{sh}$  is more difficult to explain. It is related to the non ideal nature of the p-n junction and the presence of impurities near the edges of the cell that provide a short-circuit path around the junction. In an ideal case  $R_s$  would be zero and  $R_{sh}$  infinite. However, this ideal scenario is not possible and manufacturers try to minimize the effect of both resistances to improve their products.

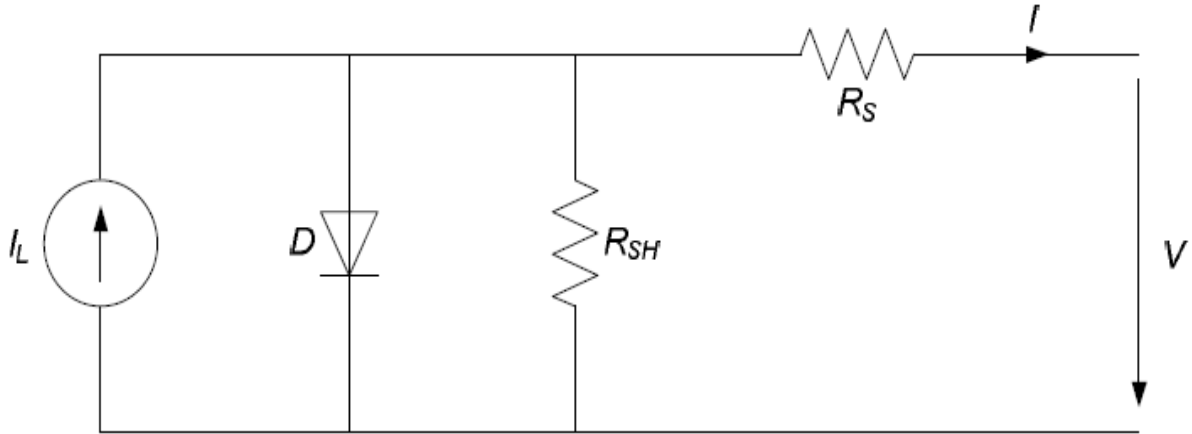


Figure1.8: Equivalent circuit of a solar cell. Image from [9]

Sometimes, to simplify the model, the effect of the shunt resistance is not considered, i.e.  $R_{SH}$  is infinite, so the last term is neglected. A PV panel is composed of many solar cells, which are connected in series and parallel so the output current and voltage of the PV panel are high enough to the requirements of the grid or equipment. Taking into account the simplification mentioned above, the output current-voltage characteristic of a PV panel is expressed by the following equation, where  $n_p$  and  $n_s$  are the number of solar cells in parallel and series respectively.

$$I \approx n_p I_L - n_p I_0 \left( e^{\frac{q(V - IR_S)}{AkT}} - 1 \right)$$

## 1.7.2 Open Circuit Voltage, Short Circuit Current and Maximum Power point

Two important points of the current-voltage characteristic must be pointed out: the open circuit voltage  $V_{OC}$  and the short circuit current  $I_{SC}$ . At both points the power generated is zero.  $V_{OC}$  can be approximated from (1) when the output current of the cell is zero, i.e.  $I=0$  and the shunt resistance  $R_{SH}$  is neglected. It is represented by equation. The short circuit current  $I_{SC}$  is the current at  $V = 0$  and is approximately equal to the light generated current  $I_L$  as shown in equation.

$$V_{OC} \approx \frac{AkT}{q} \ln\left(\frac{I_L}{I_0} + 1\right)$$

$$I_{SC} \approx I_L$$

The maximum power is generated by the solar cell at a point of the current-voltage characteristic where the product  $VI$  is maximum. This point is known as the MPP and is unique, as can be seen in figure, where the previous points are represented.

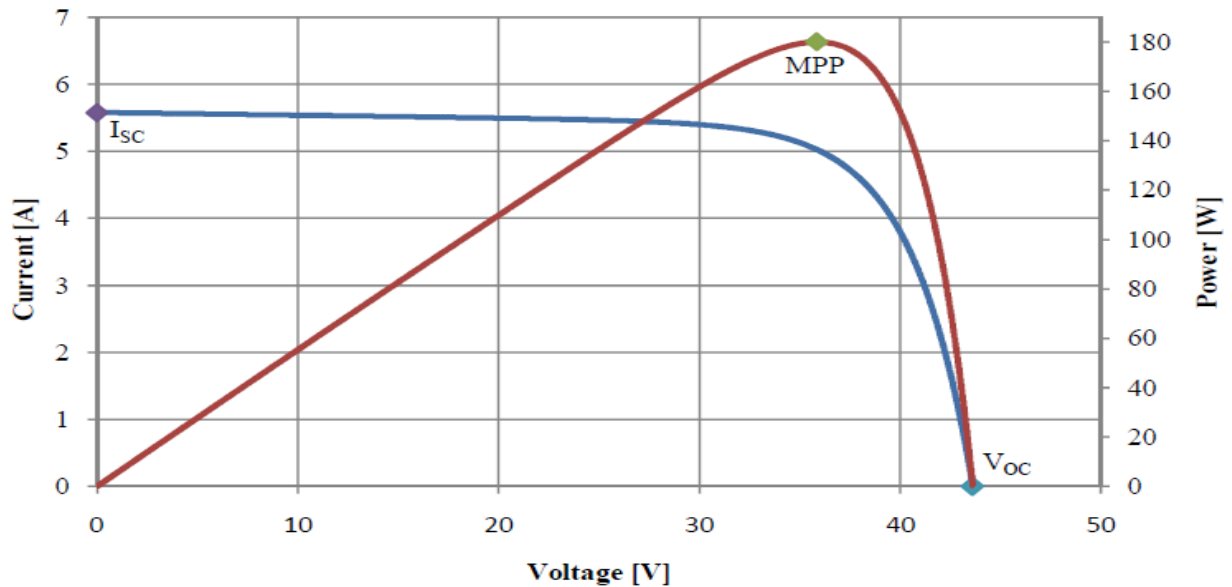


Figure1.9: Important points in the characteristic curves of a solar panel. Image from [9]

## 1.8 Solar Panel

A solar panel (photovoltaic module or photovoltaic panel) is a packaged, connected assembly of solar cells, also known as photovoltaic cells. The solar panel can be used as a component of a larger photovoltaic system to generate and supply electricity in commercial and residential applications. Because a single solar panel can produce only a limited amount of power, many installations contain several panels.

Generally in a solar panel there are 36 solar cells in connected in series which has 0.56v each. From one solar panel we get  $(36 \times 0.56) = (19\text{--}21)$  V and the value of current is depend on the volume of the solar cell. A photovoltaic system typically includes an array of solar panels, an inverter, and sometimes a battery and interconnection wiring.



Fig1.10: Solar panel. Image from [7]

## **1.9 Solar Array**

A number of solar cells electrically connected to each other and mounted in a support structure or frame is called a photovoltaic module. Modules are designed to supply electricity at a certain voltage, such as a common 12 volts system. The current produced is directly dependent on how much light strikes the module. Multiple modules can be wired together to form an array. In general, the larger the area of a module or array, the more the electricity will be produced. Photovoltaic modules and arrays produce direct-current (dc) electricity. They can be connected in both series and parallel electrical arrangements to produce any required voltage and current combination.

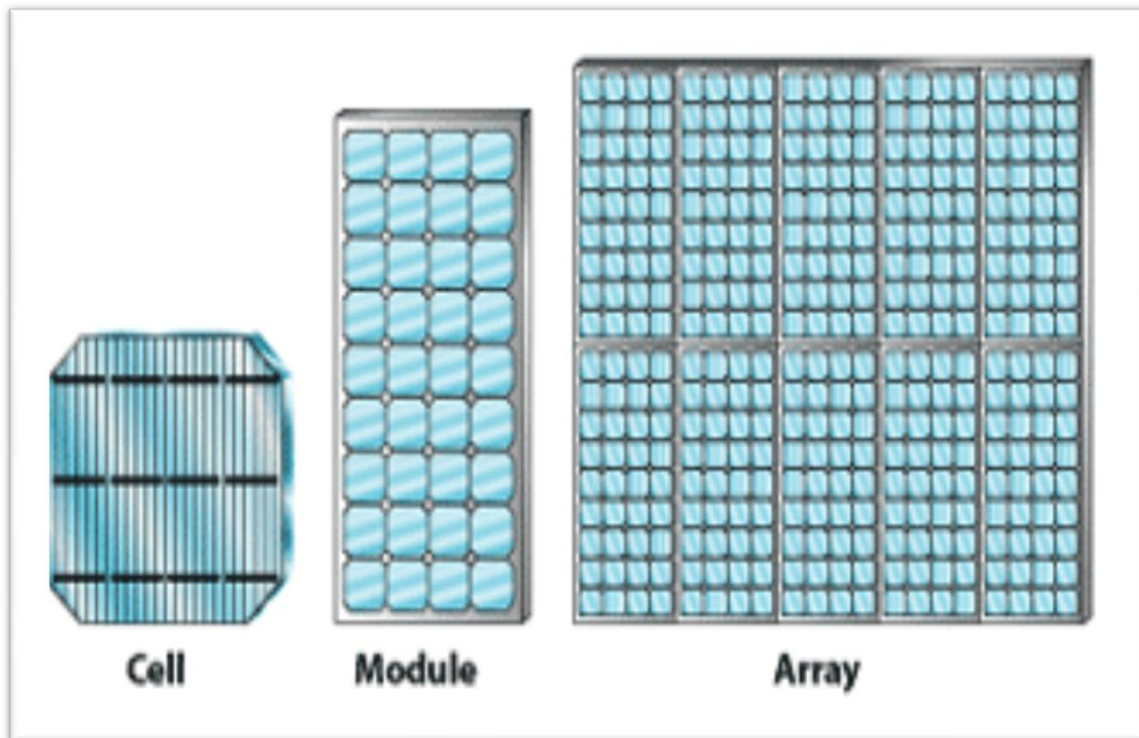


Fig1.11: Solar array. Image from [7]

For this component, we created a model of the solar array based on

$$I_d = I_{sat} \left( e^{\frac{qV_d}{kT}} - 1 \right)$$

where  $I_d$  is the diode current (A),  $V_d$  is the voltage across the diode (V),  $I_{sat}$  is the diode reverse saturation current (A),  $q$  is the electron charge ( $1.602 \times 10^{-19} \text{C}$ ),  $k$  is Boltzmann's constant ( $1.381 \times 10^{-23} \text{J/K}$ ),  $T$  is the junction temperature (K), and  $e$  is Napier's Constant (approximately 2.71828).

## 1.10 Kinds of Solar Panel

There are different kinds of solar panel such as

Single /mono crystalline

Multi /poly crystalline

Thin Film /Amorphous solar module

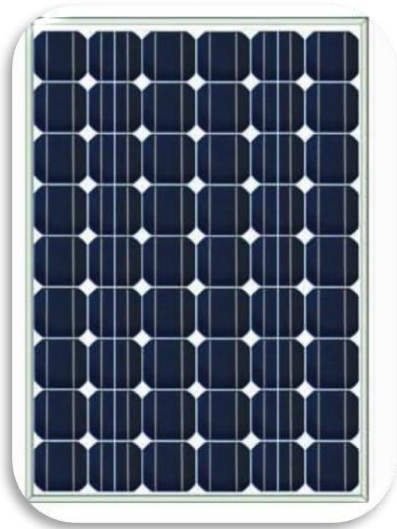


Fig.a: Monocrystalline solar cell

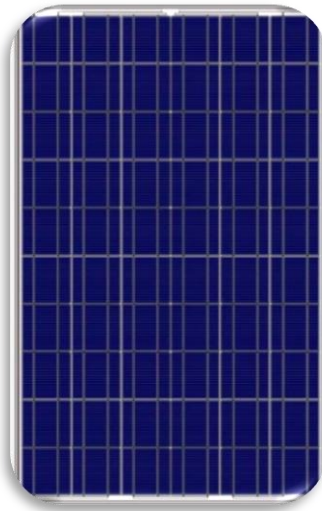


Fig.b: Polycrystalline solar cell



Fig.c: Amorphous solar cell

Fig 1.12: Different Solar Cells. Image from [10]

### **1.10.1 Monocrystalline Solar Cell**

Monocrystalline silicon is also used in the manufacturing of high performance solar cells. Since, however, solar cells are less demanding than microelectronics for as concerns structural imperfections, monocrystalline solar grade (Sog-Si) is often used, single crystal is also replaced by the cheaper polycrystalline or multicrystalline silicon. Monocrystalline solar cells can achieve 17% efficiency whereas other types of less expensive cells including thin film and poly crystalline are only capable of achieving around 10% efficiency[10].

### **1.10.2 Poly Crystalline Solar Cell**

The silicon used for polycrystalline cells is cast into a mould rather than grown as a single crystal. As a result multiple smaller crystals form that gives the cell a 'galvanized' appearance. The electrical properties of those multiple crystals are usually not quite as good as those of the single crystal used in monocrystalline cells, resulting in lower overall cell efficiency. Efficiencies are still good enough to consider these cells, but mainly when they offer significant cost advantages[10].

### 1.10.3 Amorphous Solar Cell

An amorphous solar cell is a type of solar cell that is relatively cheap to produce and widely available. They are named so because of their composition at the microscopic scale. Amorphous means "without shape". When the term is applied to solar cells it means that the silicon material that makes up the cell is not highly structured or crystallized. Amorphous solar cells are usually created by applying doped silicon material to the back of a plate of glass. The cells usually appear dark brown on the sun-facing side and silvery on the conductive side. When produced as a solar panel (a collection of many solar cells) it will appear to have several thin parallel lines running across its surface. These thin lines are actually breaks in the N and P layers of the silicon substrate and they create the boundaries of individual cells in the panel. Amorphous solar panels usually come without any obvious hook-up points or wires. It can be very puzzling to figure out how to use them[10].

### 1.11 Efficiency Comparison of Different of Solar Cells

Table: 1.1: Efficiency Comparison of Different of Solar Cells[10]

Types of cell	Efficiency (%)	Research needs
Monocrystalline silicon	24	Higher production yields, lowering of cost and energy content
Multicrystalline silicon	18	Lower manufacturing cost and complexity
Amorphous silicon	13	Lower production costs, increase production volume and stability
Organic solar cells	2-3	Improve stability and efficiency



## 1.12 Charge Controller

A Charge Controller is necessary since the brighter the sunlight, the more voltage the solar cells produce; the excessive voltage could damage the batteries. A charge controller is used to maintain the proper charging voltage on the batteries. As the input voltage from the solar array rises, the charge controller regulates the charge to the batteries preventing any overcharging. Modern multi-stage charge controllers most quality charge controller units have what is known as a 3 stage charge cycle that goes like this:

1. **BULK:** During the Bulk phase of the charge cycle, the voltage gradually rises to the Bulk level (usually 14.4 to 14.6 volts) while the batteries draw maximum current. When Bulk level voltage is reached the absorption stage begins[11].

2. **ABSORPTION:** During this phase the voltage is maintained at Bulk voltage level for a specified time (usually an hour) while the current gradually tapers off as the batteries charge up.

3. **FLOAT:** After the absorption time passes the voltage is lowered to float level (usually 13.4 to 13.7 volts) and the batteries draw a small maintenance current until the next cycle.

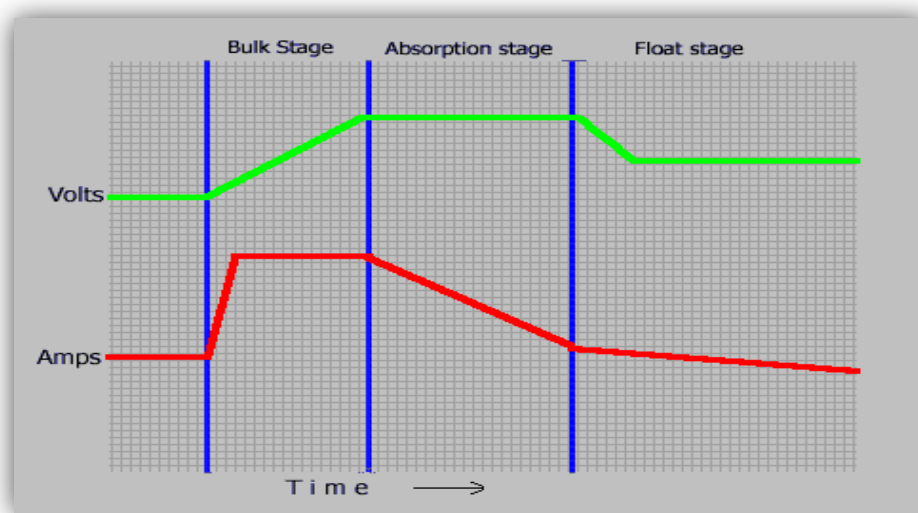


Fig 1.13: The relationship between the current and the voltage during the 3 phases of the charge cycle. Image from [11]

## 1.13 Analog to Digital Converter and Digital to Analog Converter

An analog-to-digital converter is a device that converts a continuous physical quantity (usually voltage) to a digital number that represents the quantity's amplitude.

The input to the A/D converter is a voltage. A/D converters may be designed for voltages from 0 to 10v, from -5 to +5v, etc., but they almost always take a voltage input. In any event, the input is an analog voltage signal for most cases. The output of the A/D converter is a binary signal, and that binary signal encodes the analog input voltage. So, the output is some sort of digital number.

Digital-to-analog converter is a device that converts a digital number to a continuous physical quantity (usually voltage). A common example is the processing, by a modem, of computer data into audio-frequency (AF) tones that can be transmitted over a twisted pair telephone line. The circuit that performs this function is a digital-to-analog converter (DAC).

Basically, digital-to-analog conversion is the opposite of analog-to-digital conversion. In most cases, if an analog-to-digital converter (ADC) is placed in a communications circuit after a DAC, the digital signal output is identical to the digital signal input. Also, in most instances when a DAC is placed after an ADC, the analog signal output is identical to the analog signal input. [12]

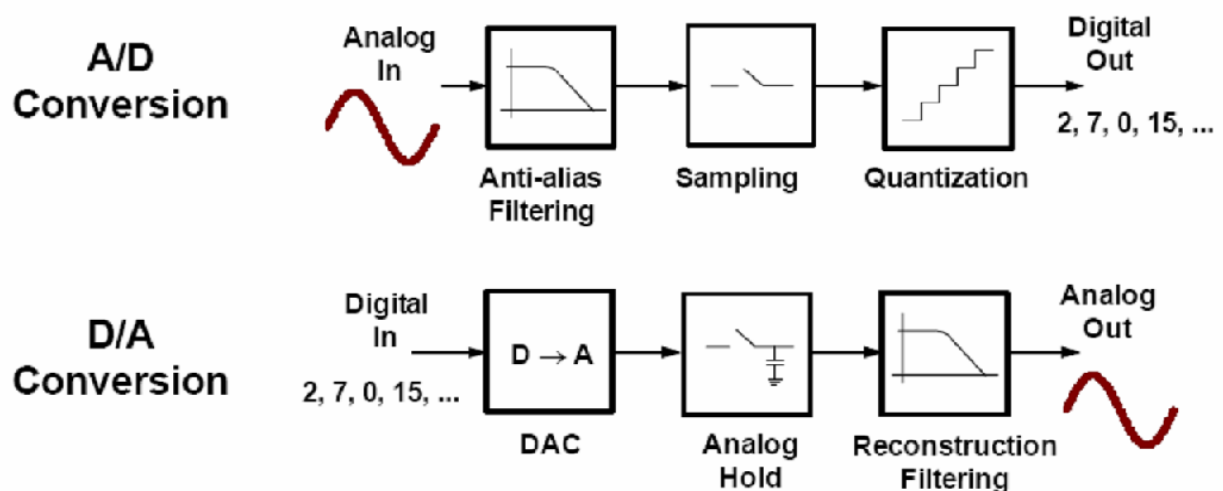


Fig 1.14: Analog to Digital and Digital to Analog Conversion. Image from [12]

## 1.14 Pulse-Width Modulation (PWM)

Pulse-width modulation (PWM) is a modulation technique that conforms the width of the pulse, formally the pulse duration, based on modulator signal information. Although this modulation technique can be used to encode information for transmission, its main use is to allow the control of the power supplied to electrical devices, especially to inertial loads such as motors. In addition, PWM is one of the two principal algorithms used in photovoltaic solar battery chargers, the other being MPPT.

The term duty cycle describes the proportion of 'on' time to the regular interval or 'period' of time; a low duty cycle corresponds to low power, because the power is off for most of the time. Duty cycle is expressed in percent, 100% being fully on.

The main advantage of PWM is that power loss in the switching devices is very low. When a switch is off there is practically no current, and when it is on, there is almost no voltage drop across the switch. Power loss, being the product of voltage and current, is thus in both cases close to zero. PWM also works well with digital controls, which, because of their on/off nature, can easily set the needed duty cycle.

Figure 1.15 shows three different PWM signals. Figure 1.15a shows a PWM output at a 10% duty cycle. That is, the signal is on for 10% of the period and off the other 90%. Figures 1.15b and 1.15c show PWM outputs at 50% and 90% duty cycles respectively. These three PWM outputs encode three different analog signal values, at 10%, 50%, and 90% of the full strength. If, for example, the supply is 9V and the duty cycle is 10%, a 0.9V analog signal results[13].

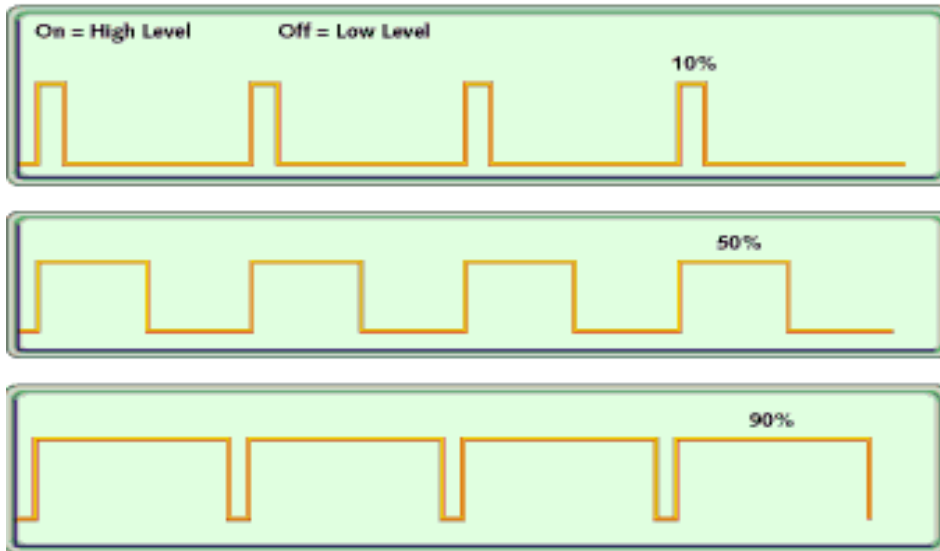


Figure1.15: PWM signals of varying duty cycles. Image from [13]

## 1.15 DC-DC Converter

A DC-to-DC converter is an electronic circuit which converts a source of direct current from one voltage level to another. It is a class of power converter. Electronic switch-mode DC to DC converters operate by storing the input energy temporarily and then releasing that energy to the output at a different voltage and current. Just like a transformer, they essentially just change the input energy into a different impedance level. So whatever the output voltage level, the output power all comes from the input; there's no energy manufactured inside the converter. In fact some energy is used by the converter circuitry and components while doing their job. It is this principle that makes a DC-DC Converter essential for MPPT. The converter presents an electrical load to the solar panel that varies as the output voltage of the converter varies. This load variation in turn causes a change in the operating point (current and voltage characteristics) of the panel. Thus by intelligently controlling the operation of the DC-DC converter, the power output of the panel can be intelligently controlled and made to output the maximum possible.

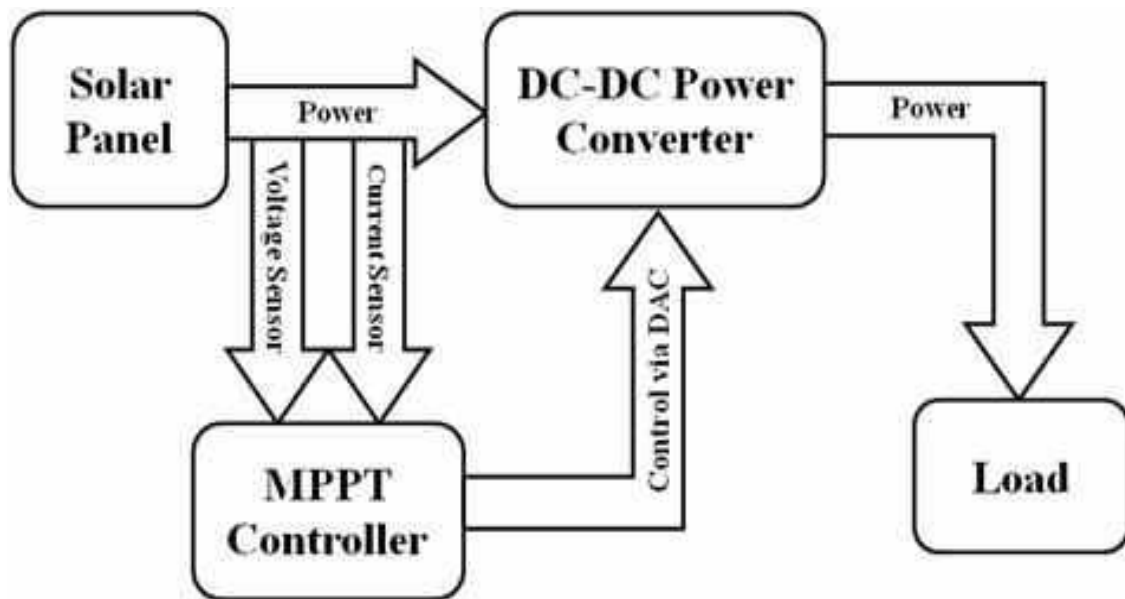


Fig1.16: DC-DC Converter with MPPT .Image from [14]

## 1.16 Storage Batteries

The fuel tank of your solar power system without batteries to store energy you would only have power when the sun was shining or the generator was running. This tutorial describes the 4 basic types of batteries & provides some good tips on the care & feeding of your batteries to maximize their performance and life.

### INDUSTRIAL STRENGTH:

The next 3 types are the heavier industrial type batteries. They are all also considered Deep Cycle and are usually Lead Acid types with much thicker internal plates that can withstand many deep discharge cycles. These next 3 are all designed for alternative energy systems.

### FLOODED TYPE:

These are Lead acid batteries that have caps to add water. Many manufacturers make these types for Solar Energy use. They are reasonably priced and work well for many years. All flooded batteries release gas when charged and should not be used indoors. If installed in an enclosure, a venting system should be used to vent out the gases which can be explosive.

## GEL:

Not to be confused with maintenance free batteries, sealed gel batteries have no vents and will not release gas during the charging process like flooded batteries do. Venting is therefore not required and they can be used indoors. This is a big advantage because it allows the batteries to maintain a more constant temperature and perform better.

## AGM:

Absorbed Glass Mat batteries are in my opinion the best available for Solar Power use. A woven glass mat is used between the plates to hold the electrolyte. They are leak/spill proof, do not out gas when charging, and have superior performance. They have all the advantages of the sealed gel types and are higher quality, maintain voltage better, self discharge slower, and last longer. The Sun Extender series by Concorde Battery is an excellent example of AGM batteries. They are more expensive, but you usually get what you pay for. You will find this type of battery used in airplanes, hospitals, and remote telephone/cell tower installations.



Fig 1.17: Storage Batteries. Image from[15]

## 1.17 The Power Inverter

Unless we plan on using battery power for everything, We will need a Power Inverter. Since the majority of modern conveniences all run on 240 volts AC, the Power Inverter will be the heart of your Solar Energy System. It not only converts the low voltage DC to the 240 volts AC that runs most appliances, but also can charge the batteries if connected to the utility grid or a AC generators as in the case of a totally independent stand-alone solar power system.



Fig 1.18: Power Inverter. Image from[16]

### 1.17.1 Square Wave Power Inverters

This is the least expensive and least desirable type. The square wave it produces is inefficient and is hard on many types of equipment. These inverters are usually fairly inexpensive, 500 watts or less. Don't even consider one of these types of power inverters for a home system[16].

### 1.17.2 Modified Sine Wave Power Inverters

This is probably the most popular and economical type of power inverter. It produces an AC waveform somewhere between a square wave and a pure sine wave. Modified Sine Wave inverters, sometimes called Quasi-Sine Wave inverters are not real expensive and work well in all but the most demanding applications and even most computers work well with a Modified Sine Wave inverter. However, there are exceptions. Some appliances that use motor speed controls or that use timers may not work quite right with a Modified Sine Wave inverter. And since more and more consumer products are using speed controls & timers, I

would only recommend this type of inverter for smaller installations such as a camping cabin[16].

### **1.17.3 True Sine Wave Power Inverters**

A True Sine Wave power inverter produces the closest to a pure sine wave of all power inverters and in many cases produces cleaner power than the utility company itself. It will run practically any type of AC equipment and is also the most expensive. Many True Sine Wave power inverters are computer controlled and will automatically turn on and off as AC loads ask for service. I believe they are well worth the extra cost. I use a True Sine Wave power inverter myself and find that its automatic capabilities make it seem more like Utility Company power[16].

### **1.17.4 Grid Tie Power Inverters**

If we are connected to normal Utility company power and just want to add some Free Sun Power electricity to reduce your electric bill and if we do not need a totally independent system, it is possible that a Grid Tie power inverter will suit our needs. With a Grid Tie power inverter, whatever electricity that your solar panels produce will reduce the amount supplied by the utility company, in effect lowering our bill[16].



THIS PAGE INTENTIONALLY LEFT BLANK

## **CHAPTER 2**

### **LITERATURE SURVEY**

#### **2.1 Masters Thesis – Hurd**

In this thesis, William R. Hurd documented his best effort to use solar cells to increase the endurance of a unmanned air vehicle (UAV). In order to optimize the output of his solar panels, he needed to use an MPPT. The MPPT he chose also contained a battery charging circuit. This simplified his designs to allow him to focus on the actual mounting and positioning of the solar cells. The panels he used were removed from the manufacturer's encapsulation. He then laminated the cells to the top of the air vehicle's wing. A major difference between his project and the one described in this thesis is the voltages of his solar array input and the voltage of his battery system. While his system had a higher battery voltage, the one considered in this thesis has a higher solar array voltage. His design required a boost converter, while the one considered in this thesis requires a buck converter.[17]

#### **2.2 Masters Thesis – Coba**

This thesis was very similar in content to William R. Hurd's thesis. Javier V. Coba was attempting to continue the work of Mr. Hurd. Javier Coba was focused on a specific production UAV, the Raven RQ-11B. While Mr.Hurd did have the Raven UAV in mind, he did not have the chance to test his addition in the field. By their calculations, they nearly doubled the endurance of the unmodified UAV. This improvement did come at a cost as the solar wing they fabricated was too large to fold and store in the original manned portable UAV package. Because of this, they concluded that any solar array extension of the Raven RQ-11B wing system should be done by the company when the wings are manufactured so as to provide a reliable and scaled form factor and still enable a two-man crew to deploy the UAV in field.[18]

## **2.3 Modelling and Simulation of Photovoltaic Module Using Matlab/Simulink**

The steps taken to measure the output of two specific solar array modules, MSX60 and MSX64, were described in this paper. Measurements were taken in order to implement a model in MATLAB. Datasheet parameters were used as input into the equation describing the current output of the solar panel. They used the model in order to simulate the MPP and graphed the current versus voltage and power versus voltage, showing the higher output panel producing more peak power than the lower rated panel. Their experiments confirmed that the simulation was well matched to the datasheet information.[19]

## **2.4 Advantage of Boost versus Buck Topology for Maximum Power Point Tracker in Photovoltaic Systems**

Since the buck converter was used to step down the voltage of the solar array, the drawbacks of using buck with a solar array was analyzed. In this paper, they discussed how the use of a buck converter is not optimal for solar arrays. The most important aspect of the experiment is getting as much power out of the panels as possible. While a buck converter is connected to a solar array, it operates the solar array in a state of source discontinuity. This means that while the switch is ‘off’, the panel is disconnected and no current is flowing from the panel to the converter. This state can be considered pure loss. Without a continuous connection to harness the output of the panel, all energy that would have been collected while the switch is in the ‘off’ position is lost. The way to circumvent this problem is to add a large input capacitor, which can store at least the same amount of charge that is generated while the panel is disconnected from the converter.

In general the buck converter has a control advantage. While the boost has a right-half plane zero, the buck does not. This right-half plane zero causes the response of the boost converter to first fluctuate in the opposite direction prior to correcting itself.[20]

## **2.5 Comparison of MPPT Algorithms for DC-DC Converter Based PV Systems**

The differences between two popular MPPT algorithms, P&O and InC were described in this paper. In order to get a good metric for comparison, the authors designed both power

conversion circuits to be optimal for that specific algorithm. This was done to compare the algorithms on an even footing. The conclusion they draw is that the best controller is InC, but if you consider increased cost of implementation of the optimal circuit, then P&O gains favor. Due to the lower cost of measurement devices needed for the algorithm, Perturb and Observe is the most cost effective and efficient MPPT algorithm.[21]

## **2.6 High Efficiency Switched Capacitor Buck-boost Converter For PV Application**

A switching capacitor buck-boost hybrid converter for module level distributed-MPPT PV applications was introduced and described in this paper. The operation principle of the proposed converter is covered including the detailed operating of a resonant charge pump converter. This converter achieved 92.5% efficiency in the experiment. While not very similar to the application described in this thesis, it is good to have a few sources which discuss other methods of implementation of power converters.[22]

## **2.7 A Novel MPPT Charge Regulator for a Photovoltaic Stand-alone Telecommunication System**

A commercial MPPT, SIELTE S4007 with their own converter which uses a two-phase synchronous buck topology was discussed in this paper. They found that there was a significant loss in power when using the SIELTE module to track the MPP. Its error from ideal was always greater than 5%. It is interesting to note the way that they implemented the two-phase synchronous buck topology. They used Kyocera 125-G2 panel as the basis for their circuit simulator model.[23]

## **2.8 Improved Circuit Model of Photovoltaic Array**

In this paper, the authors first explain the current circuit model of how a photovoltaic array functions. They improve upon the model by using a next order piecewise linear mathematical model. They were able to accomplish this by measuring the output of a real panel under known insolation and temperature. By using those measurements as data points on a piecewise function to model the photovoltaic array, they showed that this model was able to account for mismatched panels connected together as well as partial shading of sections of the

array.[24]

## **2.9 Comparative Study of Maximum Power Point Tracking**

### **Algorithms**

The most common algorithm for MPPT is P&O, yet it is explained in this paper that it is not the most efficient algorithm. The most common reason for using P&O is the simplicity of the circuit. This leads to the negation of need for a complicated processing unit. Their main goal was to evenly compare the algorithms across equivalently optimized hardware as well as with the algorithms optimized for that hardware. They conclude that the increase in cost of implementation of InC greatly outweighs any improvement in efficiency gained.[25]

## **2.10 Design and Implementation of Maximum Power Point Tracking Algorithm for a Standalone PV System**

Using a model based on Simulink blocks in MATLAB, the authors simulated the action of an MPPT system. With a variable irradiance from the solar array, the authors use an MPPT algorithm to control a boost converter driving a resistive load. In this paper, the authors compare P&O with InC. They note that tuning the algorithm using incremental changes is important for both algorithms. InC uses far more complicated calculations and, thus, requires more powerful hardware when physically implemented.[26]

THIS PAGE INTENTIONALLY LEFT BLANK

## **CHAPTER 3**

### **SYSTEM OVERVIEW**

#### **3.1 System Diagram and Description**

In this chapter, the use of MATLAB with Simscape, SimPowerSystems and SimElectronics toolboxes to simulate the complete system as seen in Figure 3.1 are described.

Initially, sunlight hits the solar panel array. After being recombined in the active region of the solar cell, the electrons flow into a buck-boost converter. The buck-boost converter then changes the voltage and current. Control of this converter is provided by an MPPT algorithm, which monitors the solar array output and uses the current and voltage measurements from the array to track the highest power output of the array.

One such MPPT algorithm will perturb the output setting and then observe by measurement the change in output power. When the power reaches the MPP, the algorithm will stop changing the setpoint for the duty cycle (D). One of the parameters to investigate how it effects the overall system is the sampling rate and how often the MPPT will change the D of the buck-boost converter. If the sampling rate is too fast, the new D might oscillate around the actual MPP, thereby, never extracting the maximum amount of power. On top of that, there might be a transient instability created by not allowing the step response of the output voltage to settle after changing the setpoint of D. [19]

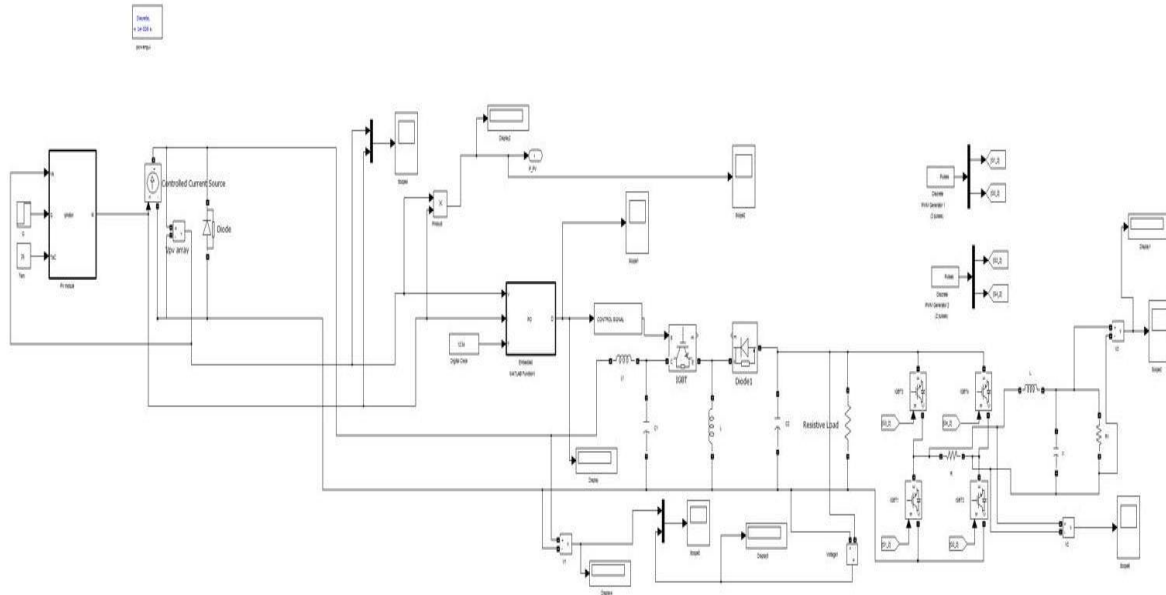


Figure 3.1: The functional portion of the model under test in Simulink, which includes the solar array, buck-boost converter, resistive load, inverter and LC filter.

The algorithm will use the MPP to set the D of the pulse width modulation (PWM) for the buck-boost converter. Under proper conditions, the greatest amount of power is transferred to the load with minimal losses. The losses of efficiency in the system are due to MPP tracking error, buck-boost converter efficiency, and solar cell conversion efficiency. When the panels react to changes in irradiance, there is a disturbance in the setpoint needed to keep the panels at their MPP. During the time while the algorithm is tracking the new MPP, there is a small amount of inefficiency attributed to tracking error. This error is based on the irradiance, making it a difficult error to account for in the physical world. In simulation it can be quite easy to measure since we can control the illumination of the panel in a controlled manner. The tracking error will be tested in simulation to use as a metric for comparison of the MPPT algorithms.

Measurement of the input and output power are the best metric to determine how well the buck-boost converter, IGBT, gate drive, and MPPT algorithm work together.



## 3.2 Modeling of Components Under Test

In order to simulate the analog components which are in use for this thesis, we need to use mathematical approximations to what the elements actually do. Without this step, it is difficult to compare these circuits. By using these models we are then able to do discrete analysis with the assistance of a computer for calculations. Calculating these by hand is time prohibitive. In MATLAB there are many blocksets already created to ease the use of their software environment. By connecting these mathematical models, we are able to simulate the circuit and extract close to real-world data. Once the correct tuning has been done in simulation, the data can then use the data to instantiate a real-world device.

### 3.2.1 Solar Array

For this component, we created a model of the solar array based on

$$I_d = I_{sat} (e^{\frac{qV_d}{kT}} - 1) \quad (3.1)$$

where  $I_d$  is the diode current (A),  $V_d$  is the voltage across the diode (V),  $I_{sat}$  is the diode reverse saturation current (A),  $q$  is the electron charge ( $1.602 \times 10^{-19} C$ ),  $k$  is Boltzmann's constant ( $1.381 \times 10^{-23} J/K$ ),  $T$  is the junction temperature (K), and  $e$  is Napier's Constant (approximately 2.71828).

The solar panel made for simulation is seen in figure 3.2.

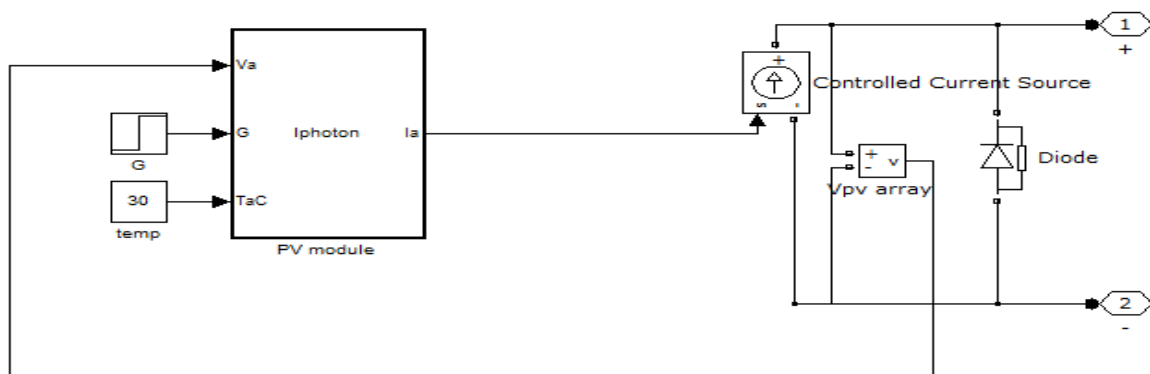


Figure 3.2: The pv panel used for the simulation of the system

The cell characteristic at a given irradiance and temperature basically consists of two segments: the constant-voltage segment and the constant-current segment. The current is

limited as the cell is short-circuited. The maximum power condition occurs at the knee of the characteristic where the two segments meet. It is desirable to operate at the MPP. Ideally, a pure DC current should be drawn from the solar array, though the reduction in delivered power is not very large even in the presence of a fair amount of ripple current. To ensure that the array continues operating at the MPP, a P&O method is used where at regular intervals the amount of current drawn is perturbed and the resulting power output is observed. If an increased current results in a higher power, it is further increased until power output begins to decline. On the other hand, if an increase in current results in less power than before, then the current is increased until the power output stops increasing and begins to go down.[3]

For this simulation, a solar array that could output greater than 100W of power was selected. This panel has an open circuit voltage  $V_{oc}$  of 37.51V with a short circuit current  $I_{sc}$  of 8.63A. The voltage at maximum power  $V_{mp}$  is 33.52V while the current at maximum power  $I_{mp}$  is 8.53A. By plugging these values into

$$P = I \times V \quad (3.2)$$

we attain 286W of output power from the solar array under full solar illumination.

In order to model the varying amount of shading and cloud cover, a profile of illumination was devised that will check the MPPT's ability to change setpoints within a reasonable amount of time.

By varying the incident illumination of the solar array as well as the output resistance, we can extract the Current versus Voltage and Power versus Voltage graphs to find the MPP of the solar array. The peak of the Power versus Voltage graph is the MPP.

The mathematical model of a diode, given in Equation 3.1, was used and integrated with a controlled current source from SimPowerSystems. With this block, the buck-boost converter can modulate the output power.

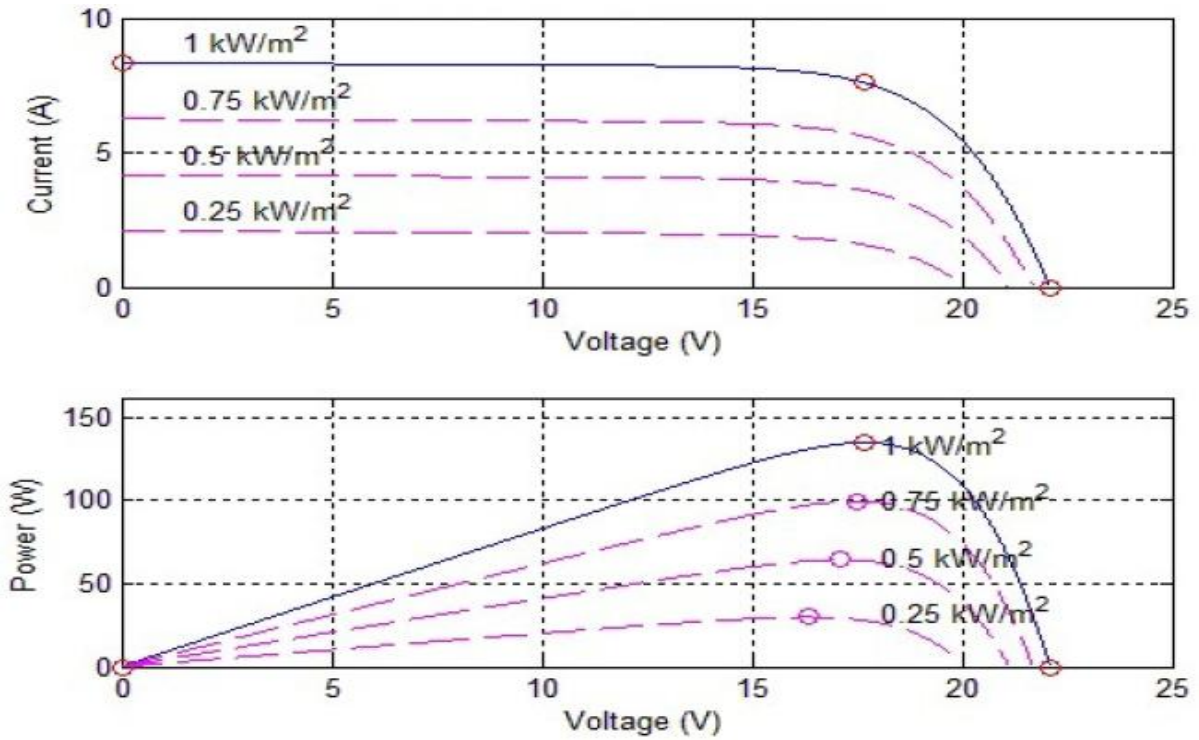


Figure 3.3: The Current versus Voltage and Power versus Voltage plots from the Panel modeled. Image from [10]

### 3.2.2 Buck-boost Converter

The buck–boost converter is a type of DC-to-DC converter that has an output voltage magnitude that is either greater than or less than the input voltage magnitude. The MATLAB circuit model for the buck-boost converter can be seen in Figure 3.4.

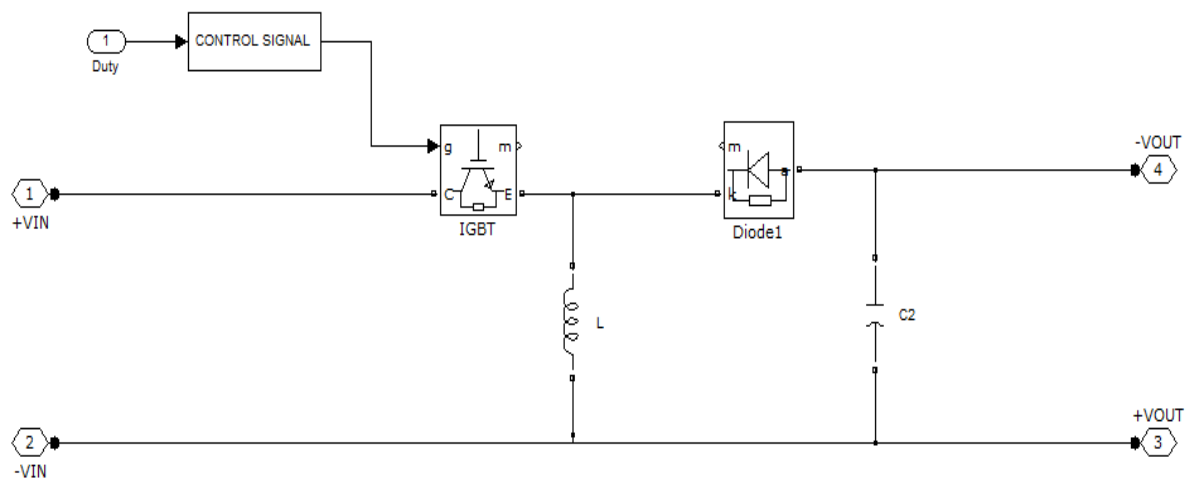


Figure 3.4: Overview of the buck-boost converter model in Simulink.

Two different topologies are called buck–boost converter. Both of them can produce a range of output voltages, from an output voltage much larger (in absolute magnitude) than the input voltage, down to almost zero.

### **The inverting topology:**

The output voltage is of the opposite polarity than the input. This is a switched-mode power supply with a similar circuit topology to the boost converter and the buck converter. The output voltage is adjustable based on the duty cycle of the switching transistor. One possible drawback of this converter is that the switch does not have a terminal at ground; this complicates the driving circuitry. Neither drawback is of any consequence if the power supply is isolated from the load circuit (if, for example, the supply is a battery) because the supply and diode polarity can simply be reversed. The switch can be on either the ground side or the supply side.[20]

### **A buck (step-down) converter followed by a boost (step-up) converter:**

The output voltage is of the same polarity of the input, and can be lower or higher than the input. Such a non-inverting buck-boost converter may use a single inductor which is used for both the buck inductor and the boost inductor.

For the buck-boost converter, we modified the standard topology by moving the IGBT to the ground leg of the circuit. This was done to reduce the large voltage spikes which might cause damage to the components. The input is coming from the solar array. The output is being modeled as a resistive load for simplicity. [20]

The buck-boost converter is a switched mode power supply, meaning it provides digital control through PWM of a switch resulting in a linear response in output voltage. It uses a two switches, a transistor and a diode, and an inductor to continually maintain a voltage on the output capacitor. Buck-boost converters are commonly used when the input voltage is too high and needs to be lowered to an appropriate level. A step down converter produces a lower average output voltage than the DC input voltage  $V_d$ . Its main application is in regulated DC power supplies and DC motor speed control.

The average output voltage can be calculated in terms of switch's D using

$$V_0 = \frac{1}{T_s} \int_0^{T_s} v_0(t) dt = \frac{1}{T_s} \left( \int_0^{t_{on}} V_d dt + \int_{t_{on}}^{T_s} 0 dt \right) = \frac{t_{on}}{T_s} V_d = DV_d \quad (3.3)$$

where,  $V_o$  is the DC output voltage,  $T_s$  is the switching period,  $v_o(t)$  is the instantaneous output voltage as a function of time,  $t_{on}$  is the duration the switch is on per switching period,  $V_d$  is the DC input voltage, and  $D$  is the duty cycle of the converter. When the active time of the switch  $t_{on}$  increases, it increases the DC voltage at the output.

The  $D$  is related to the ‘on’ time of the switch divided by the period of switching:

$$D = \frac{t_{on}}{t_s}$$

Any linear change in the duty cycle parameter causes a linear change in the output voltage  $V_o$ .

The basic principle of the buck–boost converter is fairly simple as seen in figure 3.5.

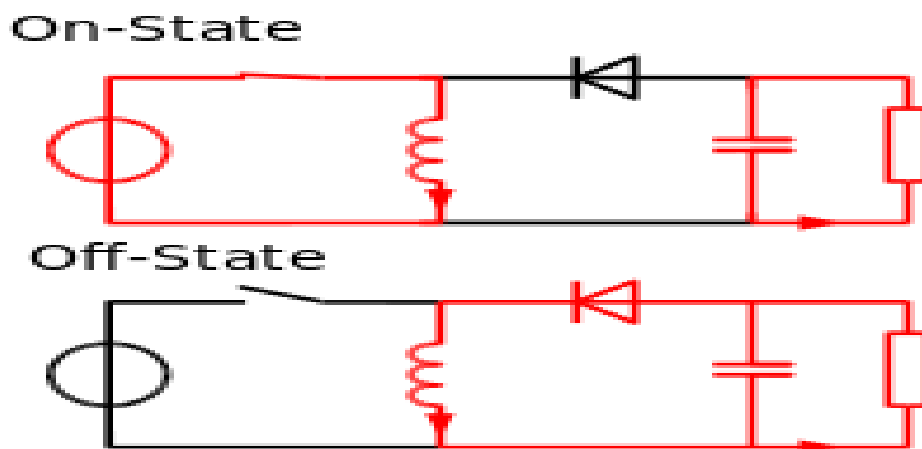


Figure 3.5: The two operating states of a buck–boost converter. Image from [20]

When the switch is in On-state, the input voltage source is directly connected to the inductor ( $L$ ).The diode is in reversed biased mode. So all the current flows through the inductor. The inductor stores energy in the form of magnetic field. In this stage, the capacitor supplies energy to the output load.

When the switch is in Off-state,the inductor is connected to the output load and capacitor and energy is transferred from the inductor to the capacitor and the load.[20]

### 3.2.3 Load

Simulating an active load can be very complex. In order to optimize the buck-boost converter and MPPT algorithm during simulation, a resistive load that remains constant through each test was used. The first order model of the output load can be seen in Figure 3.6. The MPPT

controller adjusts the D of the buck-boost converter to match the MPP of the array, thereby, optimizing output power. By analyzing the output voltage, we can evaluate the effectiveness of the buck-boost converter.

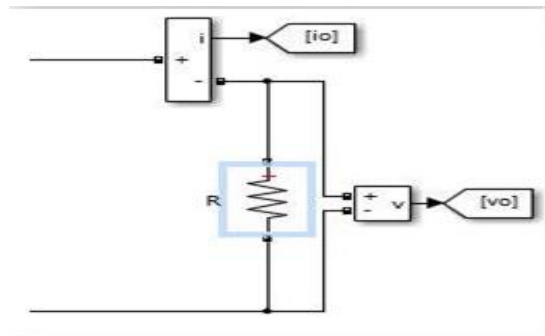


Figure 3.6: Output load resistor with measurement blocks connected.

### 3.2.4 IGBT

The MATLAB model as seen in Figure 3.7 for a IGBT is quite extensive. The adjustable parameters are the IGBT resistance  $R_{on}$ , the internal diode inductance  $L_{on}$ , the internal diode resistance  $R_d$ , the internal diode forward voltage  $V_f$ , the snubber resistance  $R_s$ , and the snubber capacitance  $C_s$ .

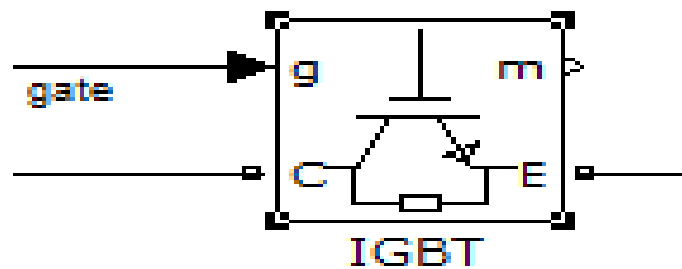


Figure 3.7: IGBT block from MATLAB SimPowerSystems

### 3.2.5 Pulse Width Modulation Generation

For simulations in MATLAB, a gate drive circuit model is not necessary since the gating function assumes an ideal switch. The model for a IGBT was found in the MATLAB blockset SimPowerSystems.

The IGBT gate control for the model can be seen in Figure 3.8. The percentage of time the switch is ‘on’ for a set switching speed is D. We can use the comparison of D with a triangle wave that ranges from zero to one. When the value of the triangle waveform is higher than D, the IGBT is ‘off’. Similarly, when the value of the triangle waveform is lower than D, the IGBT is ‘on’.

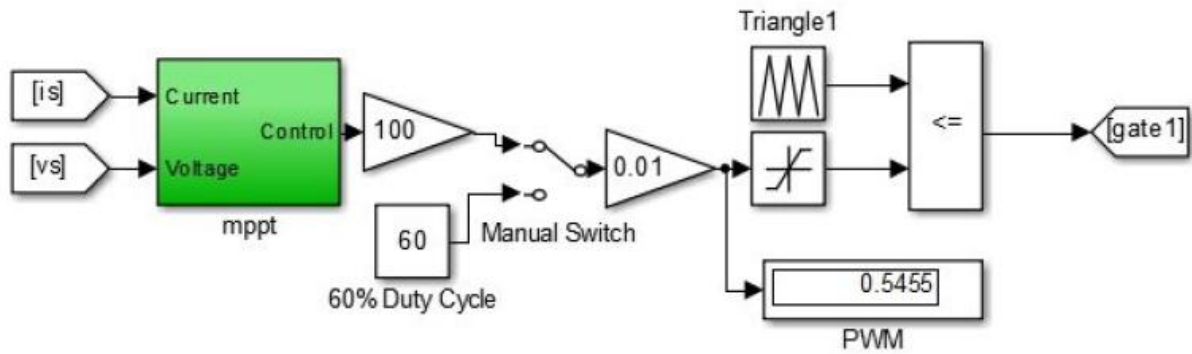


Figure 3.8: PWM signal with triangle wave and duty cycle example. Image from [17]

For the MATLAB model, only a binary signal is needed to control the gate. Using this simplified idea of the gate, we can compare the duty cycle with a triangle waveform set to repeat every 40 ms with the peak of the triangle at 20 ms. This gives a control frequency  $f_s$  of 25 kHz when calculated with

$$f_s = \frac{1}{T_s}$$

When the value of D is less than the triangle waveform the output goes to ‘one’.

### 3.2.6 DC-AC Converter

A dc-ac converter is also known as an inverter. A single phase transistor inverter made on simulink can be seen in figure 3.9. If transistors 1 and 4 conduct for one half of a period and 2 and 3 conduct for the other half, the output voltage is of the alternating form. The output voltage can be controlled by varying the conduction time of transistors.

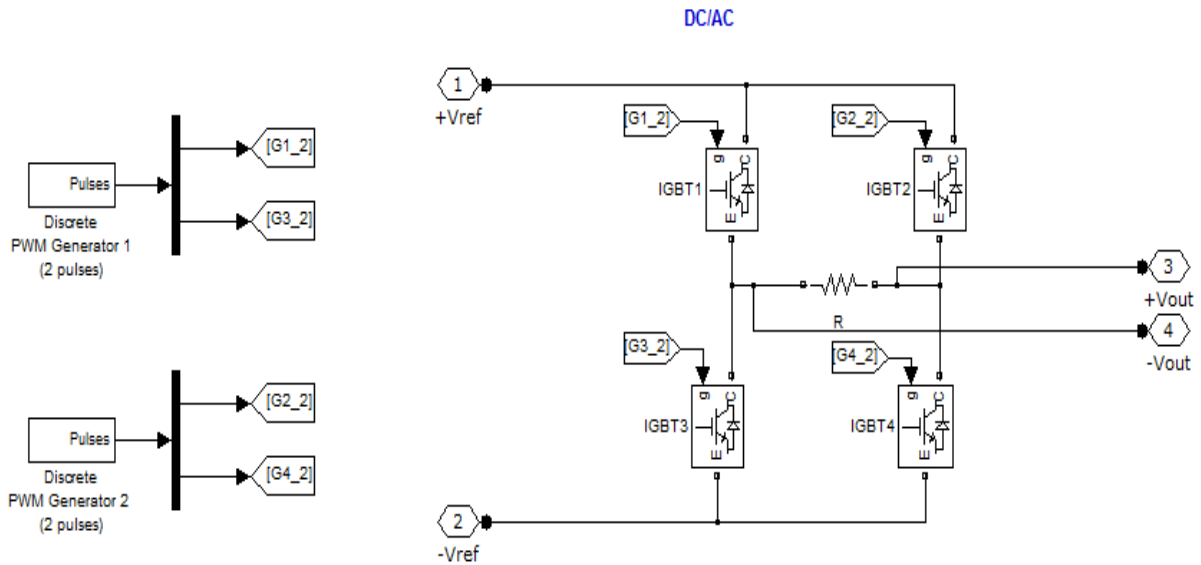


Fig 3.9: Single phase DC-AC Converter used in the system

The inverter does not produce any power, the power is provided. Most of the time DC voltage becomes High voltage. The inverter translates the form of the power from direct current to an alternating current waveform. The converter has not produced a pure sine wave. The resulting waveform is usually called a “Modified Sine Wave”. So a low-pass LC filter has been connector to its end.

### 3.2.7 Low-pass Filter

A low-pass filter has been used in the system to pass low-frequency signals and to attenuate (to reduce the amplitude of) signals with frequencies higher than the cut-off frequency. Low-pass filters provide a smoother form of a signal, removing the short-term fluctuations, and leaving the longer-term trend. By employing the use of a low-pass filter, an inductor and capacitor combination as shown in Figure 3.10, the output voltage and current fluctuations delivered to the load have been greatly reduced.



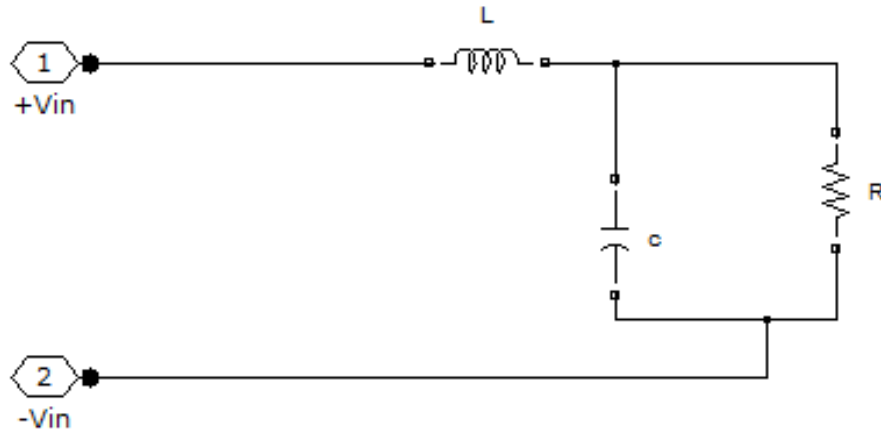


Fig 3.10: Low-pass Filter used in the system

The corner frequency  $f_c$  of this low-pass filter is calculated from

$$f_c = \frac{1}{2\pi\sqrt{LC}}$$

The filter cut-off frequency is selected to be much lower than the switching frequency of the converter, which reduces the output voltage ripple to a reasonable level.

### 3.2.8 MPPT Algorithms

There are many ways to track an MPP. In this section, two of the most popular MPPT algorithms P&O and InC are compared. The perturb and observe (P&O) algorithm for finding the MPP is widely used in commercial applications. This method uses current and voltage sensors to measure the output of a solar array. The P&O algorithm can be the cheapest to implement. Generally, P&O is also the simplest to implement due to its reliance on passive element circuits to measure the current and voltage. These measurements are the only outside data sources the MPPT algorithm needs to determine whether to increase or decrease the duty cycle. By comparing the input power to the previously measured input power, we can determine whether to lower or raise the duty cycle to continue tracking the MPP.[27]

By changing the duty cycle after a set amount of time, the P&O algorithm checks the previously measured input power. If the newly measured input power is greater than the previously measured input power and the new input voltage is greater than the old input voltage, it decreases  $D$  to move closer to the peak power. If the input voltage was less than previously measured and it had greater input power, the algorithm increases  $D$ .

If the new power measured is less than previously measured and the new voltage is greater than the old voltage,  $D$  decreases to converge to an MPP. Finally, if the power and voltage are less than previously measured, the algorithm decreases  $D$ . This algorithmic flow chart can be seen in Figure 3.11.

There are a few optimizable parameters within this algorithm. First, the  $f_s$  can affect the size requirement for the inductor and capacitor. If  $f_s$  increases, then the sizes of the inductor and capacitor decreases. Secondly, the amount of change in duty cycle can be modulated to quickly converge from large tracking errors. This  $DD$  is essentially the gain of the controller. [21]

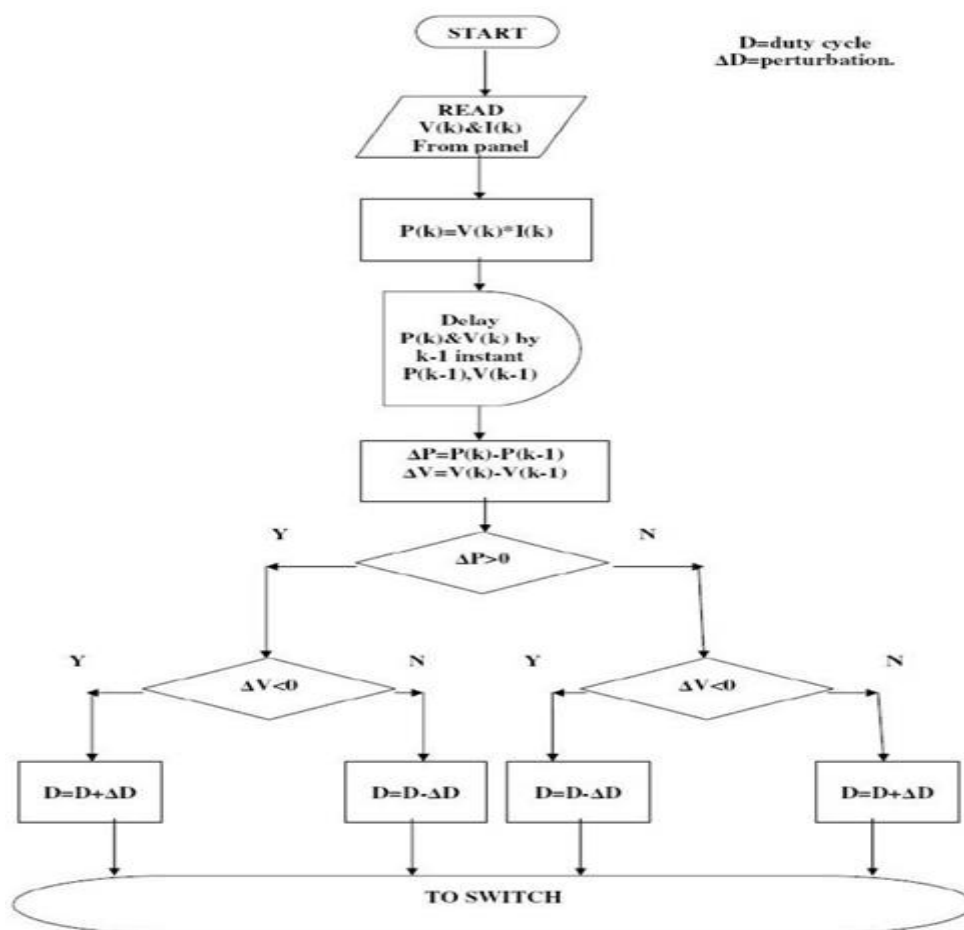


Figure 3.11: Flow chart of Perturb and Observe Algorithm. Image from [27]

If the  $\Delta D$  is too high it can overshoot and oscillate indefinitely around the optimal point, yet never reach it. The perturb and observe algorithm with an example is shown in section 5.1 of chapter 5.

The incremental conductance algorithm (InC) is another method of MPP tracking. The incremental conductance algorithm with an example is shown in section 5.2 of chapter 5.

This algorithm uses incremental measurements on the change in conductance of the photovoltaic array. By comparing these calculated incremental measurements, we can calculate whether there was an increase or decrease in power since it was last measured. The incremental conductance is defined as  $(\Delta I_{PV}/\Delta V_{PV})$ . By comparing this measurement to the actual conductance of the photovoltaic array, one can determine which side of the MPP the current operating point is located. "InC can track rapidly increasing and decreasing irradiance conditions with higher accuracy than P&O. One disadvantage of this is the increased complexity when compared with P&O."

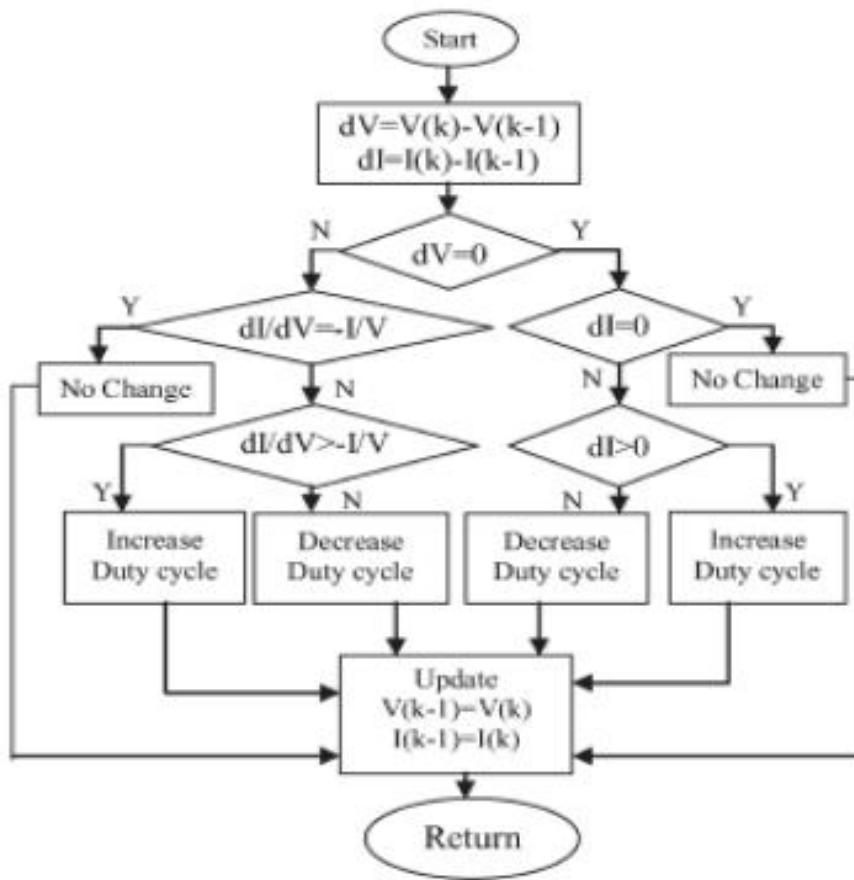


Figure 3.12: Flow chart of the InC Algorithm. Image from [28]

The algorithm used is seen as a flow chart in Figure 3.12. This algorithm has fewer branches for each node and is less complicated than the P&O algorithm's flowchart; however, the simplicity of the algorithm flowchart does not account for the increased complexity of binary calculations required for this algorithm.

Since calculation of both the InC and conductance requires the use of division, a large amount of processing power is necessary in order to acquire the result before the next sample

time. If the calculation to find the InC carries over into the next sample time, the controller will be controlling the buck-boost converter further in the past the longer the system runs. If we have each calculation occur as fast as possible by using more power hungry processors with the hardware to perform division, we will be able to appropriately use the calculations for this algorithm and, thereby, optimize the output power. [28]

THIS PAGE INTENTIONALLY LEFT BLANK

# **CHAPTER 4**

## **Maximum Power Point Tracker**

### **4.1 Maximum Power Point Tracking**

The efficiency of a solar cell is very low. In order to increase the efficiency, methods are to be undertaken to match the source and load properly. One such method is the Maximum Power Point Tracking (MPPT). This is a technique used to obtain the maximum possible power from a varying source. In photovoltaic systems the I-V curve is non-linear, thereby making it difficult to be used to power a certain load. This is done by utilizing a boost converter whose duty cycle is varied by using a mppt algorithm. A MPPT, or maximum power point tracker is an electronic DC to DC converter that optimizes the match between the solar array (PV panels), and the battery bank or utility grid. They convert a higher voltage DC output from solar panels (and a few wind generators) down to the lower voltage needed to charge batteries. The Power point tracker is a high frequency DC to DC converter. They take the DC input from the solar panels, change it to high frequency AC, and convert it back down to a different DC voltage and current to exactly match the panels to the batteries. MPPT's operate at very high audio frequencies, usually in the 20-80 kHz range. The advantage of high frequency circuits is that they can be designed with very high efficiency transformers and small components.[4]

The dc-dc converter is placed between the solar panel and the load in order to draw the maximum power from the solar panel. The converter is an essential section as it operates the solar array at the maximum point while also providing a constant voltage to the battery. It is operated in boost mode, which step-up the output voltage. The regulation of the output voltage is achieved by varying the duty cycle of the switch (MOSFET). The PWM signal generated by 89C51 microcontroller is used to control the transistor switch operation (on & off). The converter has all of the array energy flowing through it so component choice is important for maximum efficiency. The converter also carries out impedance matching so that the impedance of the source is equal to the impedance of the load to ensure maximum power transfer.[12]

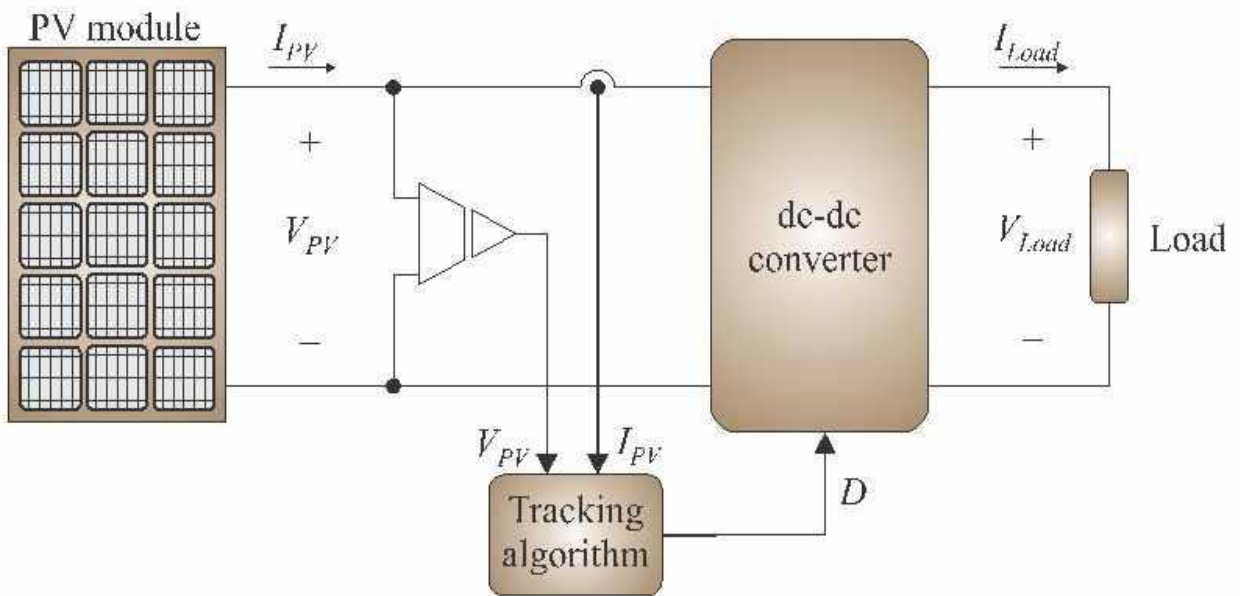


Fig 4.1: Solar Photovoltaic system with maximum power point tracker. Image from[14]

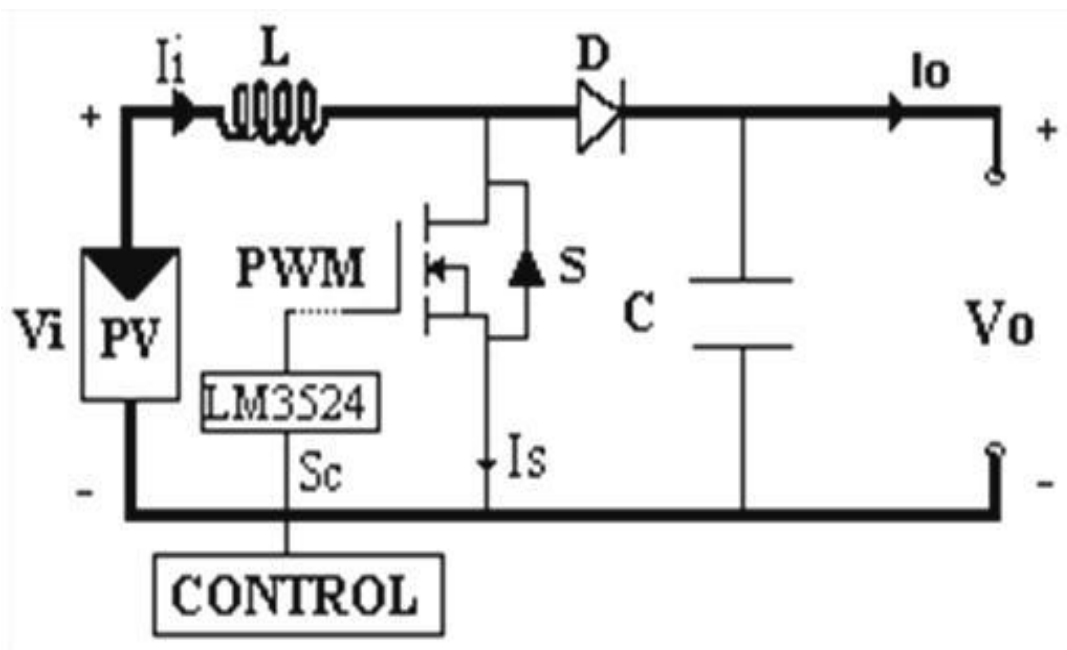


Figure 4.2: Maximum power point tracker: DC-DC converter. Image from[14]

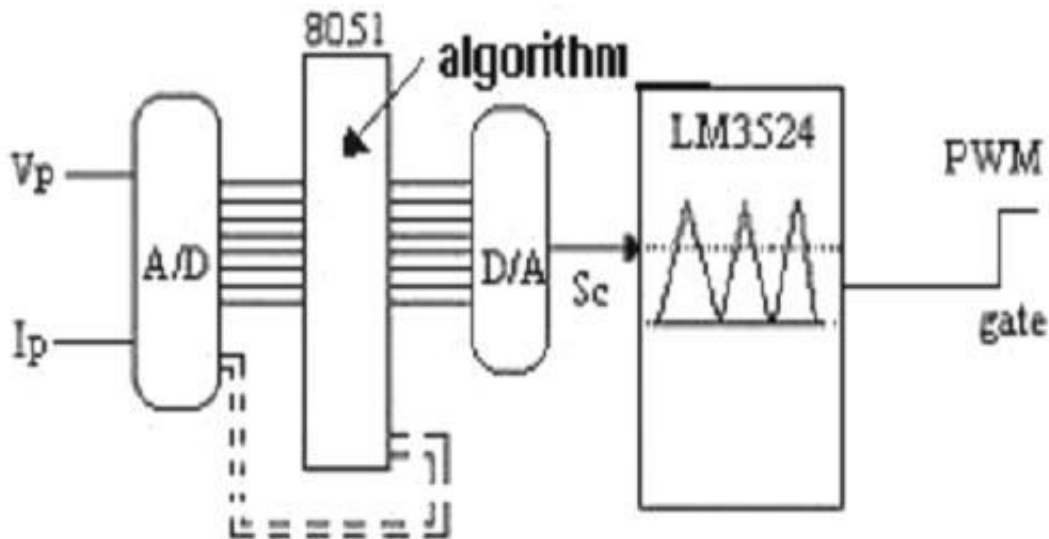


Fig 4.3: Control circuit diagram. Image from[14]

Assume the battery is low, at 12 volts. A MPPT takes that 17.6 volts at 7.4 amps and converts it down, so that now the battery gets is 10.8 amps at 12 volts. Now you still have almost 130 watts. A MPPT tracks the maximum power point, which is going to be different from the STC (Standard Test Conditions) rating under almost all situations. Under very cold conditions a 120 watt panel is actually capable of putting over 130+ watts because the power output goes up as panel temperature goes down - but if you don't have some way of tracking that power point, you are going to lose it. On the other hand under very hot conditions, the power drops - you will lose power as the temperature goes up. That is why you get less gain in summer.

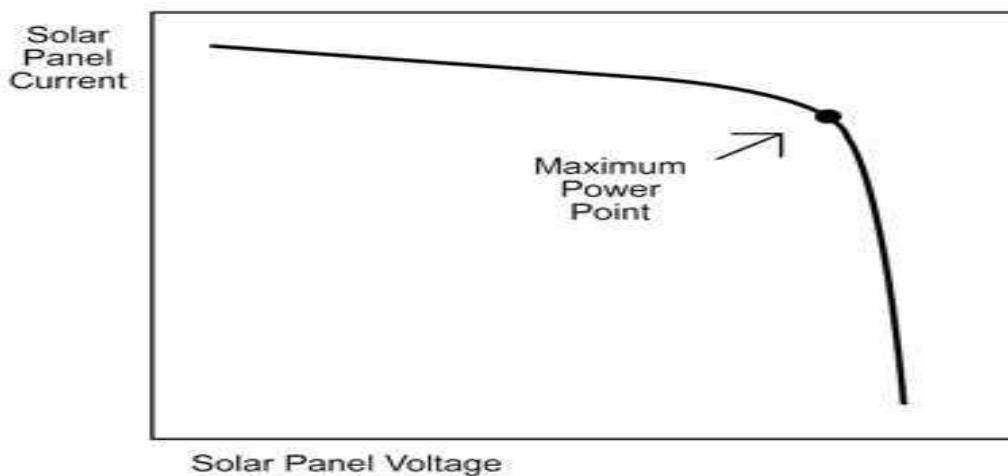


Fig 4.4: I-V characteristics curve. Image from [6]



MPPT's are most effective under these conditions: Cold weather - Low battery charge - Long wire runs.

## 4.2 Effect of Variation of Solar Irradiation

The P-V and I-V curves of a solar cell are highly dependent on the solar irradiation values. The solar irradiation as a result of the environmental changes keeps on fluctuating, but control mechanisms are available that can track this change and can alter the working of the solar cell to meet the required load demands. Higher is the solar irradiation, higher would be the solar input to the solar cell and hence power magnitude would increase for the same voltage value. With increase in the solar irradiation the open circuit voltage increases. This is due to the fact that, when more sunlight incidents on to the solar cell, the electrons are supplied with higher excitation energy, thereby increasing the electron mobility and thus more power is generated. [29]

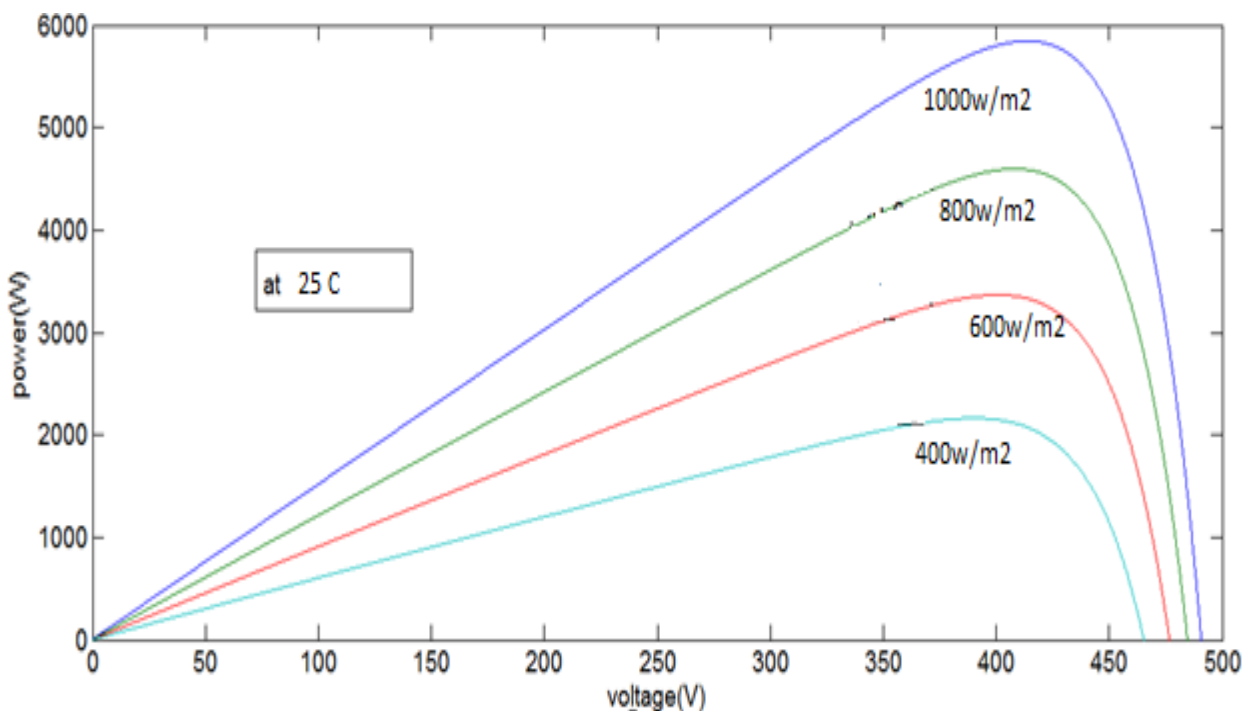


Figure 4.5: Variation of P-V curve with solar irradiation. Image from [29]

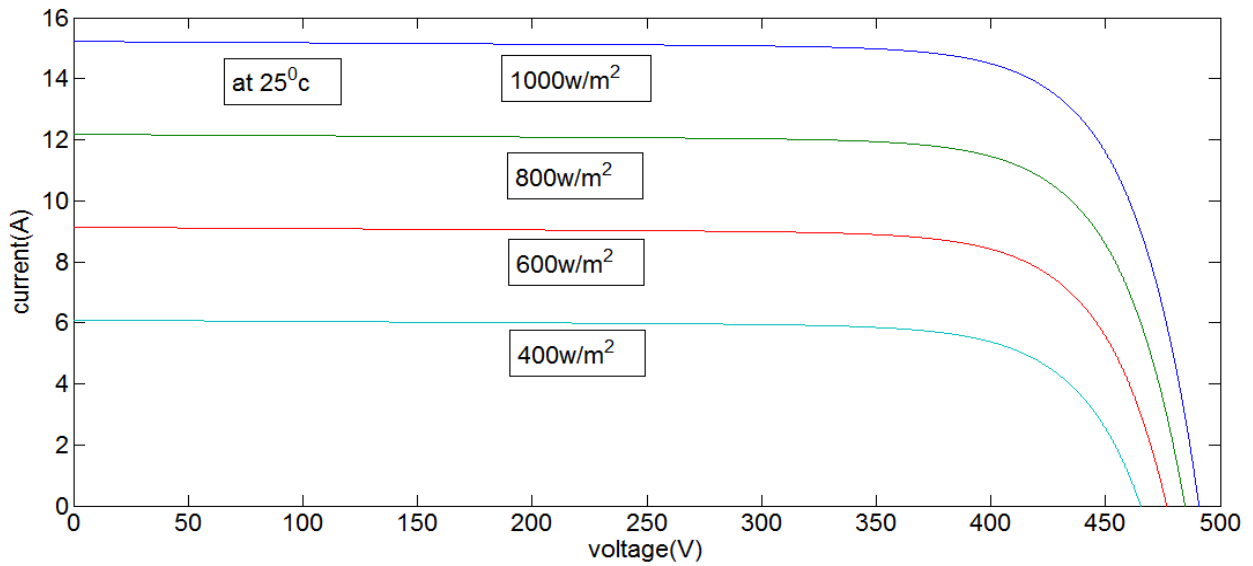


Figure 4.6: Variation of I-V curve with solar irradiation. Image from [29]

### 4.3 Effect of Variation of Temperature

On the contrary the temperature increase around the solar cell has a negative impact on the power generation capability. Increase in temperature is accompanied by a decrease in the open circuit voltage value. Increase in temperature causes increase in the band gap of the material and thus more energy is required to cross this barrier. Thus the efficiency of the solar cell is reduced. [6]

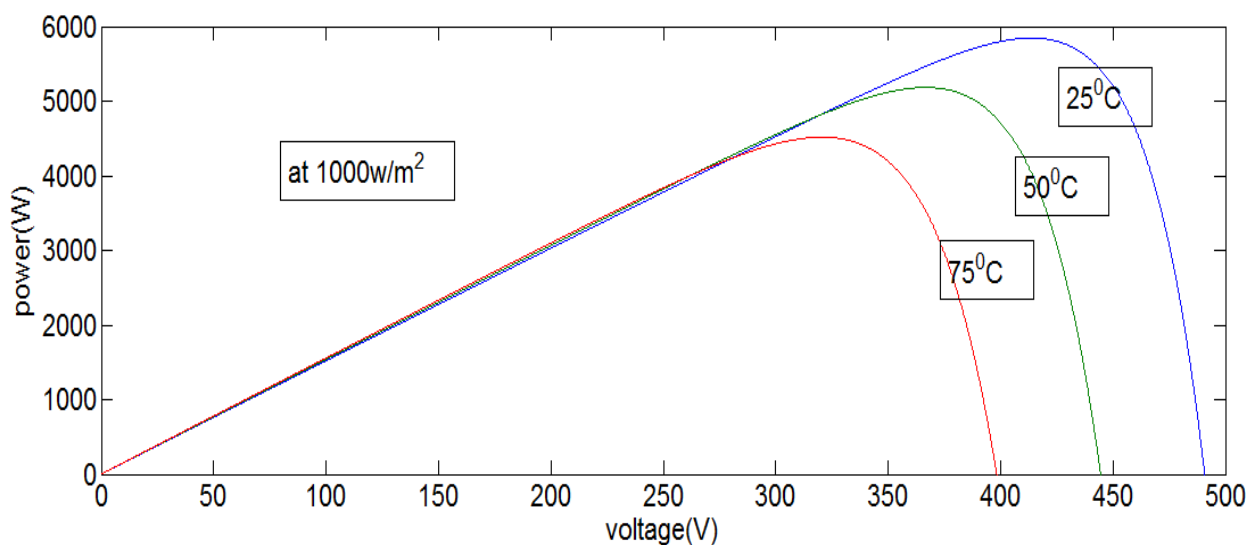


Figure 4.7: Variation of P-V curve with temperature. Image from [30]

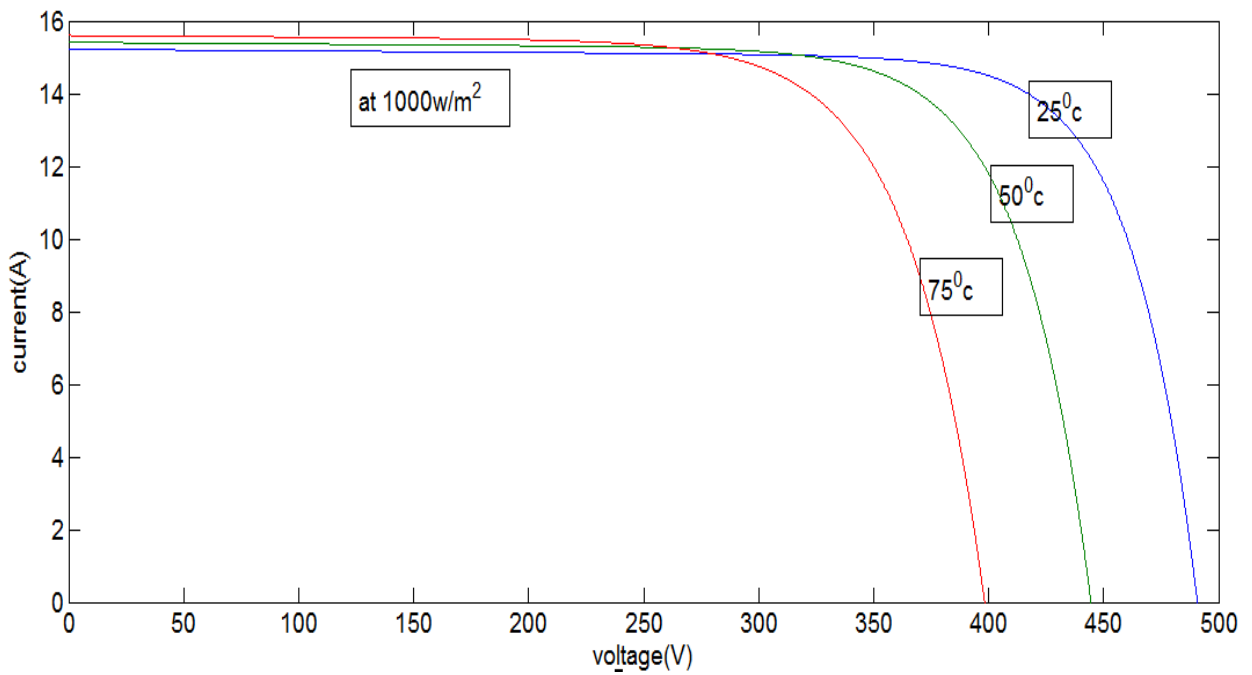


Figure 4.8: Variation of I-V with temperature. Image from[30]

#### 4.4 Comparison of the tracking power for different MPPT system

Table 4.4: Comparison of the tracking power for different MPPT system

Irradiance	600w/m <sup>2</sup>	800w/m <sup>2</sup>	1000w/m <sup>2</sup>
Temperature	22°C	25°C	28°C
P & O	110.2W	190.2W	285.7W
INC	110.9W	191.4W	285.7W

## 4.5 Sensing Circuits

### 4.5.1 Voltage Sensor

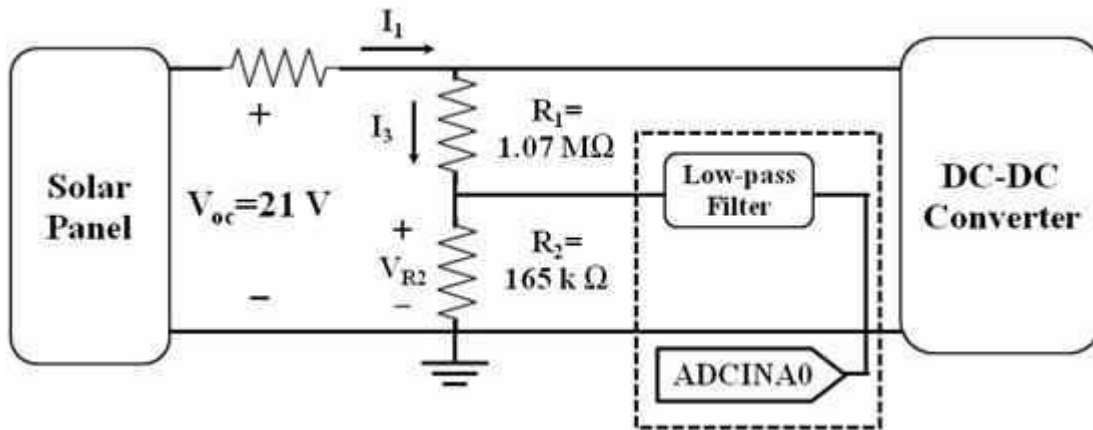


Fig 4.9: Voltage Sensor. Image from[4]

In order for the MPPT controller to measure the voltage provided by the solar panel, two resistors  $R_1$  and  $R_2$  are employed in parallel with the solar panel to act as a voltage divider. The voltage across  $R_2$  in the voltage divider is fed into an analog-to-digital converter (ADC) driver circuit (op-amp in a voltage follower configuration that feeds into a low-pass filter) before being delivered to the ADCINA0 channel of the MPPT controller. By choosing the values of  $R_1$  and  $R_2$  as  $1.07\text{ M}\Omega$  and  $165\text{ k}\Omega$ , respectively the maximum amount of current diverted from the load,  $I_2$  is small enough, even in a worst-case scenario, to be considered negligible.

The allowable voltage range for each ADC channel of the MPPT controller is 0-3 Vdc. Therefore, the voltage across  $R_2$  (which serves as a scaled-down representation of the solar panel's voltage) should not exceed 3 Vdc. Based on the chosen value of  $R_2$  as  $165\text{ k}\Omega$ , the maximum voltage,  $V(R_2, \text{max})$ , sent to the ADC driver circuit (and thus ADC channel ADCINA0) is 2.81 Vdc.

## 4.5.2 Current Sensor

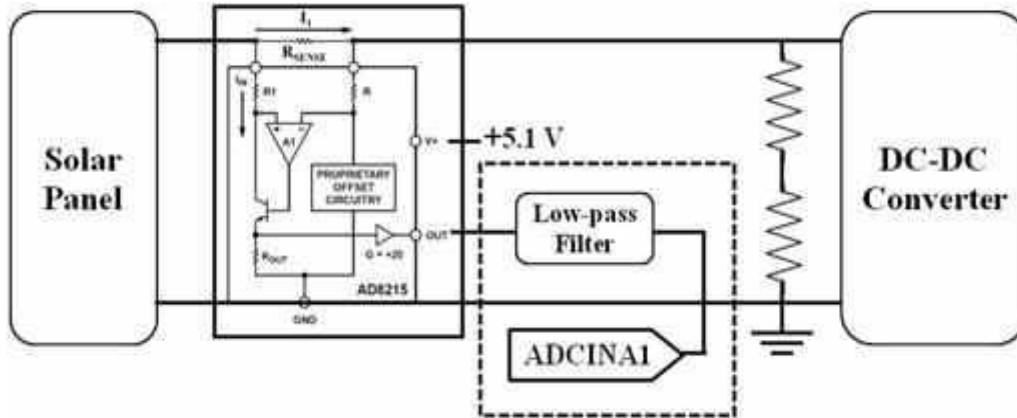


Fig 4.10: Current Sensor. Image from [4]

In order for the MPPT controller to measure the current provided by the solar panel, a single resistor ( $R_{sense}$ ) is placed in series between the solar panel and the DC-DC converter. The voltage across  $R_{sense}$  is fed into an AD8215 current sensor manufactured by Analog Devices whose output voltage is then fed into an ADC driver circuit (op-amp in a voltage follower configuration that feeds into a low-pass filter) before being delivered to the ADCINA1 channel of the MPPT controller. By choosing the value of  $R_{sense}$  as  $51\text{ m}\Omega$ , the maximum voltage drop across  $R_{sense}$ ,  $V_{R_{sense}}$ , is small enough, even in a worst-case scenario, to be considered negligible.

## 4.6 Duty Cycle

A duty cycle is the percentage of one period in which a signal is active. A period is the time it takes for a signal to complete an on-and-off cycle. As a formula, a duty cycle may be expressed as:

$$D = \frac{T}{P} \times 100\%$$

where  $D$  is the duty cycle,  $T$  is the time the signal is active, and  $P$  is the total period of the signal. Thus, a 60% duty cycle means the signal is on 60% of the time but off 40% of the time. The "on time" for a 60% duty cycle could be a fraction of a second, a day, or even a week, depending on the length of the period.

Duty cycles can be used to describe the percent time of an active signal in an electrical device such as the power switch in a switching power supply or the firing of action potentials by a living system such as a neuron.

## **4.7 Methods for MPPT**

There are many methods used for maximum power point tracking. A few are listed below:

Perturb and Observe method

Incremental Conductance method

Parasitic Capacitance method

Constant Voltage method

Constant Current method

### **4.7.1 Perturb and Observe Method**

This method is the most common. In this method very less number of sensors are utilized. The operating voltage is sampled and the algorithm changes the operating voltage in the required direction and samples  $dP/dV$ . If  $dP/dV$  is positive, then the algorithm increases the voltage value towards the MPP until  $dP/dV$  is negative. This iteration is continued until the algorithm finally reaches the MPP. This algorithm is not suitable when the variation in the solar irradiation is high. The voltage never actually reaches an exact value but perturbs around the maximum power point (MPP). [21]

### **4.7.2 Incremental Conductance Method**

This method uses the PV array's incremental conductance  $dI/dV$  to compute the sign of  $dP/dV$ . When  $dI/dV$  is equal and opposite to the value of  $I/V$  (where  $dP/dV=0$ ) the algorithm knows that the maximum power point is reached and thus it terminates and returns the corresponding value of operating voltage for MPP. This method tracks rapidly changing irradiation conditions more accurately than P&O method. One complexity in this method is that it requires many sensors to operate and hence is economically less effective. [21]

### **4.7.3 Parasitic Capacitance Method**

This method is an improved version of the incremental conductance method, with the improvement being that the effect of the PV cell's parasitic junction capacitance is included into the voltage calculation. [21]

### **4.7.4 Constant Voltage Method**

This method which is a not so widely used method because of the losses during operation is dependent on the relation between the open circuit voltage and the maximum power point voltage. The ratio of these two voltages is generally constant for a solar cell, roughly around 0.76. Thus the open circuit voltage is obtained experimentally and the operating voltage is adjusted to 76% of this value. [21]

### **4.7.5 Constant Current Method**

Similar to the constant voltage method, this method is dependent on the relation between the open circuit current and the maximum power point current. The ratio of these two currents is generally constant for a solar cell, roughly around 0.95. Thus the short circuit current is obtained experimentally and the operating current is adjusted to 95% of this value. The methods have certain advantages and certain disadvantages. Choice is to be made regarding which algorithm to be utilized looking at the need of the algorithm and the operating conditions. For example, if the required algorithm is to be simple and not much effort is given on the reduction of the voltage ripple then P&O is suitable. But if the algorithm is to give a definite operating point and the voltage fluctuation near the MPP is to be reduced then the IC method is suitable, but this would make the operation complex and more costly. [21]

THIS PAGE INTENTIONALLY LEFT BLANK



# CHAPTER 5

## MPPT ALGORITHMS TEST AND DATA ANALYSIS

### 5.1 Matlab Code for Perturb and Observe Algorithm

```
clear all;
close all;
clc;
V=zeros(1,50);
I=zeros(1,50);

V=[318 287 287 259 242 123 271 235 267 300 300 331 329 343 339 340 336 341 339 332
333 327 338 321 350 338 338 329 329 327 343 348 355 346 354 334 336 311 299 304 293
283 239 267 232 258 326 313 258 261];Data from[31]

I=[.155 0 0 0 0 0 0 .008 .045 .126 .264 .463 .544 .774 1.12 1.231 1.161 1.249 1.427 1.289
1.374 1.481 1.511 2.173 3.994 4.669 3.802 2.840 2.324 2.308 1.786 1.695 1.581 1.467 .765
.488 .582 .501 .175 .125 .008 0 0 0 .031 .159 .372 .572 .953 1.336];Data from[31]

D=.22;
P=V.*I;

figure(1)
plot(V,P,'-');
figure(2)
plot(V,I,'-');

n=50;
for k=n:-1:2

    dP=P(k)-P(k-1);
    dV=V(k)-V(k-1);
```

```

dD=.0038;

if dP>0
    if dV<0
        D=D+dD;
    else D=D-dD;
    end
else
    if dP<0
        if dV<0
            D=D-dD;
        else D=D+dD;
        end
    end
end
D
end
D
P

```

### 5.1.1 Run Result

```

P=[49.3 0 0 0 0 0 0 1.9 12 37.8 79.2 153.3 179 265.5 397.7 418.5 390.1 425.9 483.8 427.9
457.5 484.3 510.7 697.5 1397.9 1578.1 1285.1 934.4 764.6 754.7 612.6 589.9 561.3 507.6
270.8 163.0 195.6 155.8 52.3 38 2.3 0 0 0 7.2 41 121.3 179 245.9 348.7];

```

```

D=[0.186 0.1896 0.1934 0.1934 0.1934 0.1934 0.1934 0.1934 0.1896 0.1934 0.1972 0.2010
0.2048 0.2010 0.2048 0.2010 0.2048 0.2086 0.2124 0.2086 0.2124 0.2162 0.2124 0.2162
0.2124 0.2162 0.2124 0.2086 0.2124 0.2086 0.2124 0.2086 0.2048 0.2010 0.2048 0.2010
0.2048 0.2086 0.2124 0.2162 0.2124 0.2162 0.2200 0.2200 0.2200 0.2162 0.2200 0.2238
0.2200 0.2162];

```

Table 5.1: Input Current, Input Voltage, Input Power and Corresponding Duty Cycle after Each Step for P&O Algorithm

SL. NO.	INPUT CURRENT	INPUT VOLTAGE	INPUT POWER	DUTY CYCLE
1	0.1550	318	49.3	0.1896
2	0	287	0	0.1896
3	0	287	0	0.1934
4	0	259	0	0.1934
5	0	242	0	0.1934
6	0	123	0	0.1934
7	0	271	0	0.1934
8	0.0080	235	1.9	0.1934
9	0.0450	267	12	0.1896
10	0.1260	300	37.8	0.1934
11	0.2640	300	79.2	0.1972
12	0.4630	331	153.3	0.2010
13	0.5440	329	179	0.2048
14	0.7740	343	265.5	0.2010
15	1.1200	339	397.7	0.2048
16	1.2310	340	418.5	0.2010
17	1.1610	336	390.1	0.2048
18	1.2490	341	425.9	0.2086
19	1.4270	339	483.8	0.2124
20	1.2890	332	427.9	0.2086
21	1.3740	333	457.5	0.2124
22	1.4810	327	484.3	0.2162
23	1.5110	338	510.7	0.2124
24	2.1730	321	697.5	0.2162
25	3.9940	350	1397.9	0.2124
26	4.6690	338	1578.1	0.2162
27	3.8020	338	1285.1	0.2124
28	2.8400	329	934.4	0.2086
29	2.3240	329	764.6	0.2124
30	2.3080	327	754.7	0.2086
31	1.7860	343	612.6	0.2124
32	1.6950	348	589.9	0.2086
33	1.5810	355	561.3	0.2048
34	1.4670	346	507.6	0.2010
35	0.7650	354	270.8	0.2048
36	0.4880	334	163.0	0.2010
37	0.5820	336	195.6	0.2048
38	0.5010	311	155.8	0.2086
39	0.1750	299	52.3	0.2124
40	0.1250	304	38	0.2162
41	0.0080	293	2.3	0.2124
42	0	283	0	0.2162
43	0	239	0	0.2200

44	0	267	0	0.2200
45	0.0310	232	7.2	0.2200
46	0.1590	258	41	0.2162
47	0.3720	326	121.3	0.2200
48	0.5720	313	179	0.2238
49	0.9530	258	245.9	0.2200
50	1.3360	261	348.7	0.2162

### 5.1.2 Duty Cycle versus Power

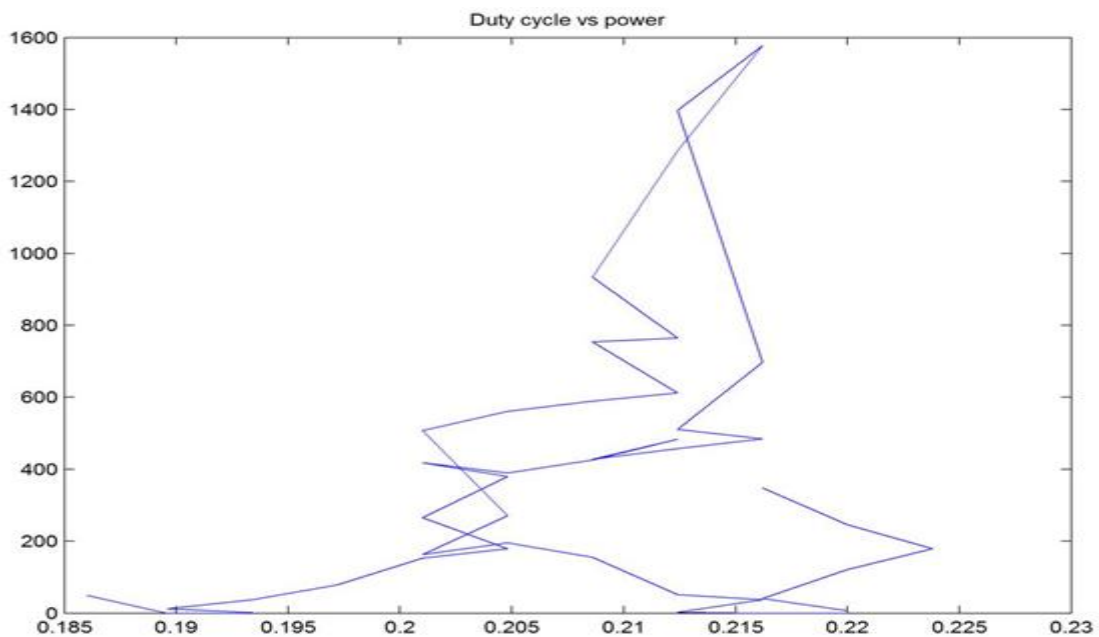


Fig 5.1: Perturb and Observe-Duty cycle versus Power

### 5.2 Matlab Code for Incremental Conductance Algorithm

```
close all;
clear all;
clc;
V=zeros(1,50);
I=zeros(1,50)
```

```
V=[318 287 287 259 242 123 271 235 267 300 300 331 329 343 339 340 336 341 339 332  
333 327 338 321 350 338 338 329 329 327 343 348 355 346 354 334 336 311 299 304 293  
283 239 267 232 258 326 313 258 261];Data from[31]
```

```
I=[.155 0 0 0 0 0 0 .008 .045 .126 .264 .463 .544 .774 1.120 1.231 1.161 1.249 1.427 1.289  
1.374 1.481 1.511 2.173 3.994 4.669 3.802 2.840 2.324 2.308 1.786 1.695 1.581 1.467 .765  
.488 .582 .501 .175 .125 .008 0 0 0 .031 .159 .372 .572 .953 1.336];Data from[31]
```

```
D=.22;
```

```
P=V.*I;
```

```
n=50;
```

```
for k=n:-1:2
```

```
    dV=V(k)-V(k-1);
```

```
    dI=I(k)-I(k-1);
```

```
    dD=.0038;
```

```
    if dV==0
```

```
        if dI==0
```

```
            D=D;
```

```
        else
```

```
            if (dI/dV)>(-I(k)/V(k))
```

```
                D=D+dD;
```

```
            else
```

```
                D=D-dD;
```

```
            end
```

```
        end
```

```
    else
```

```
        if (dI/dV)==(-I(k)/V(k))
```

```
            D=D;
```

```
        else
```

```
            if dI>0
```

```
                D=D+dD;
```

```

else
    D=D-dD;
end
end
end
end
D
end
D
P

```

### 5.2.1 Run Result

D=[0.2504 0.2504 0.2466 0.2466 0.2466 0.2466 0.2466 0.2466 0.2504 0.2466 0.2428 0.2390  
0.2352 0.2390 0.2352 0.2390 0.2352 0.2314 0.2276 0.2314 0.2276 0.2238 0.2276 0.2238  
0.2276 0.2238 0.2276 0.2314 0.2276 0.2314 0.2276 0.2314 0.2352 0.2390 0.2352 0.2390  
0.2352 0.2314 0.2276 0.2238 0.2276 0.2238 0.2200 0.2200 0.2200 0.2238 0.2200 0.2162  
0.2200 0.2238];

P=[49.3 0 0 0 0 0 0 1.9 12 37.8 79.2 153.3 179 265.5 397.7 418.5 390.1 425.9 483.8 427.9  
457.5 484.3 510.7 697.5 1397.9 1578.1 1285.1 934.4 764.6 754.7 612.6 589.9 561.3 507.6  
270.8 163.0 195.6 155.8 52.3 38 2.3 0 0 0 7.2 41 121.3 179 245.9 348.7];

Table 5.2: Input Current, Input Voltage, Input Power and Corresponding Duty Cycle after Each Step for Inc Conductance Algorithm

SL. NO.	INPUT CURRENT	INPUT VOLTAGE	INPUT POWER	DUTY CYCLE
1	0.1550	318	49.3	0.2504
2	0	287	0	0.2504
3	0	287	0	0.2466
4	0	259	0	0.2466

5	0	242	0	0.2466
6	0	123	0	0.2466
7	0	271	0	0.2466
8	0.0080	235	1.9	0.2466
9	0.0450	267	12	0.2504
10	0.1260	300	37.8	0.2466
11	0.2640	300	79.2	0.2428
12	0.4630	331	153.3	0.2390
13	0.5440	329	179	0.2352
14	0.7740	343	265.5	0.2390
15	1.1200	339	397.7	0.2352
16	1.2310	340	418.5	0.2390
17	1.1610	336	390.1	0.2352
18	1.2490	341	425.9	0.2314
19	1.4270	339	483.8	0.2276
20	1.2890	332	427.9	0.2314
21	1.3740	333	457.5	0.2276
22	1.4810	327	484.3	0.2238
23	1.5110	338	510.7	0.2276
24	2.1730	321	697.5	0.2238
25	3.9940	350	1397.9	0.2276
26	4.6690	338	1578.1	0.2238
27	3.8020	338	1285.1	0.2276
28	2.8400	329	934.4	0.2314
29	2.3240	329	764.6	0.2276
30	2.3080	327	754.7	0.2314
31	1.7860	343	612.6	0.2276
32	1.6950	348	589.9	0.2314
33	1.5810	355	561.3	0.2352
34	1.4670	346	507.6	0.2390
35	0.7650	354	270.8	0.2352
36	0.4880	334	163.0	0.2390
37	0.5820	336	195.6	0.2352
38	0.5010	311	155.8	0.2314
39	0.1750	299	52.3	0.2276
40	0.1250	304	38	0.2238
41	0.0080	293	2.3	0.2276
42	0	283	0	0.2238
43	0	239	0	0.2200
44	0	267	0	0.2200
45	0.0310	232	7.2	0.2200
46	0.1590	258	41	0.2238
47	0.3720	326	121.3	0.2200
48	0.5720	313	179	0.2162
49	0.9530	258	245.9	0.2200
50	1.3360	261	348.7	0.2238

## 5.2.2 Duty Cycle versus Power

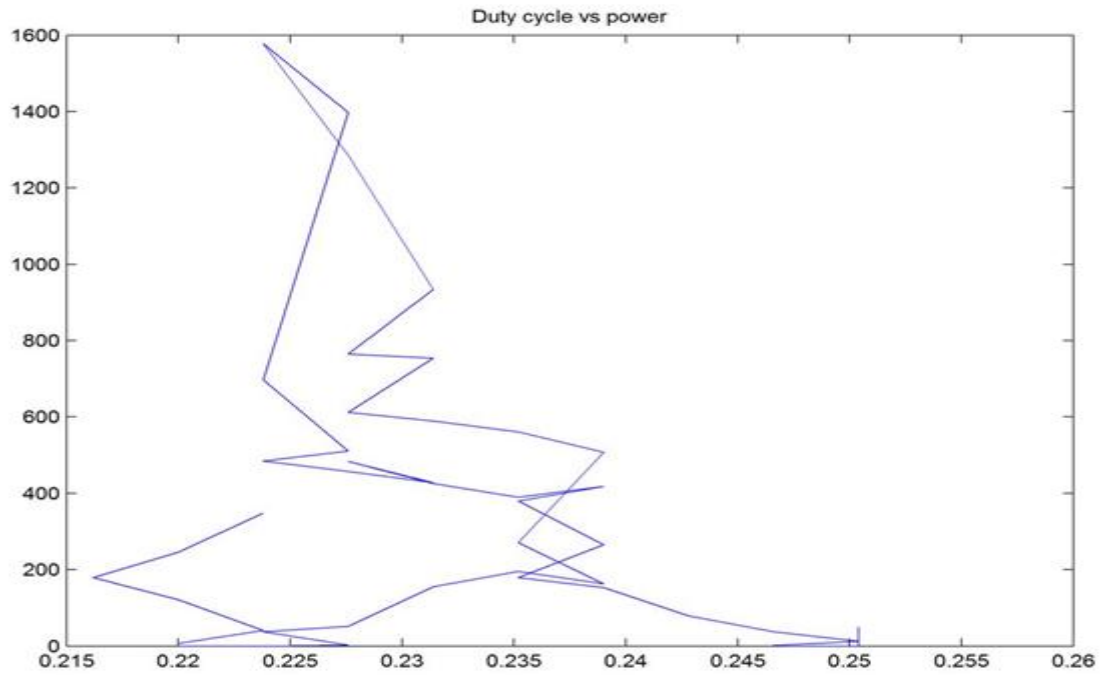


Fig 5.2: Incremental conductance-Duty cycle versus Power

## 5.3. Comparison

### 5.3.1 P&O versus Inc

Table 5.3: Input Current, Input Voltage, Input Power and Corresponding Duty Cycle after Each Step for P&O and Inc Conductance Algorithm

SL. NO.	INPUT CURRENT		INPUT VOLTAGE		INPUT POWER		DUTY CYCLE	
	PO	INC	PO	INC	PO	INC	PO	INC
1	0.1550	0.1550	318	318	49.3	49.3	0.1896	0.2504
2	0	0	287	287	0	0	0.1896	0.2504
3	0	0	287	287	0	0	0.1934	0.2466
4	0	0	259	259	0	0	0.1934	0.2466
5	0	0	242	242	0	0	0.1934	0.2466
6	0	0	123	123	0	0	0.1934	0.2466
7	0	0	271	271	0	0	0.1934	0.2466
8	0.0080	0.0080	235	235	1.9	1.9	0.1934	0.2466



9	0.0450	0.0450	267	267	12	12	0.1896	0.2504
10	0.1260	0.1260	300	300	37.8	37.8	0.1934	0.2466
11	0.2640	0.2640	300	300	79.2	79.2	0.1972	0.2428
12	0.4630	0.4630	331	331	153.3	153.3	0.2010	0.2390
13	0.5440	0.5440	329	329	179	179	0.2048	0.2352
14	0.7740	0.7740	343	343	265.5	265.5	0.2010	0.2390
15	1.1200	1.1200	339	339	397.7	397.7	0.2048	0.2352
16	1.2310	1.2310	340	340	418.5	418.5	0.2010	0.2390
17	1.1610	1.1610	336	336	390.1	390.1	0.2048	0.2352
18	1.2490	1.2490	341	341	425.9	425.9	0.2086	0.2314
19	1.4270	1.4270	339	339	483.8	483.8	0.2124	0.2276
20	1.2890	1.2890	332	332	427.9	427.9	0.2086	0.2314
21	1.3740	1.3740	333	333	457.5	457.5	0.2124	0.2276
22	1.4810	1.4810	327	327	484.3	484.3	0.2162	0.2238
23	1.5110	1.5110	338	338	510.7	510.7	0.2124	0.2276
24	2.1730	2.1730	321	321	697.5	697.5	0.2162	0.2238
25	3.9940	3.9940	350	350	1397.9	1397.9	0.2124	0.2276
26	4.6690	4.6690	338	338	1578.1	1578.1	0.2162	0.2238
27	3.8020	3.8020	338	338	1285.1	1285.1	0.2124	0.2276
28	2.8400	2.8400	329	329	934.4	934.4	0.2086	0.2314
29	2.3240	2.3240	329	329	764.6	764.6	0.2124	0.2276
30	2.3080	2.3080	327	327	754.7	754.7	0.2086	0.2314
31	1.7860	1.7860	343	343	612.6	612.6	0.2124	0.2276
32	1.6950	1.6950	348	348	589.9	589.9	0.2086	0.2314
33	1.5810	1.5810	355	355	561.3	561.3	0.2048	0.2352
34	1.4670	1.4670	346	346	507.6	507.6	0.2010	0.2390
35	0.7650	0.7650	354	354	270.8	270.8	0.2048	0.2352
36	0.4880	0.4880	334	334	163.0	163.0	0.2010	0.2390
37	0.5820	0.5820	336	336	195.6	195.6	0.2048	0.2352
38	0.5010	0.5010	311	311	155.8	155.8	0.2086	0.2314
39	0.1750	0.1750	299	299	52.3	52.3	0.2124	0.2276
40	0.1250	0.1250	304	304	38	38	0.2162	0.2238
41	0.0080	0.0080	293	293	2.3	2.3	0.2124	0.2276
42	0	0	283	283	0	0	0.2162	0.2238
43	0	0	239	239	0	0	0.2200	0.2200
44	0	0	267	267	0	0	0.2200	0.2200
45	0.0310	0.0310	232	232	7.2	7.2	0.2200	0.2200
46	0.1590	0.1590	258	258	41	41	0.2162	0.2238
47	0.3720	0.3720	326	326	121.3	121.3	0.2200	0.2200
48	0.5720	0.5720	313	313	179	179	0.2238	0.2162
49	0.9530	0.9530	258	258	245.9	245.9	0.2200	0.2200
50	1.3360	1.3360	261	261	348.7	348.7	0.2162	0.2238

## 5.4 Verification of the Conditions of the Algorithms

### 5.4.1 Perturb and Observe Algorithm

1.

$$dP=P(12)-P(11)=153.5308-79.3584=74.1724>0$$

$$\text{Now, } dV=V(12)-V(11)=331-300=31>0$$

$$\text{So, } D=D-dD=0.2048-.0038=.2010$$

Here, The difference of power is greater than zero. The difference of voltage is also greater than zero. So, according to the algorithm, the duty cycle measured one step before will get decreased by the fixed duty cycle change 0.0038 and the new duty cycle will be that of the current step. The previously measured duty cycle was 0.2048 and if it is decreased by 0.0038, then the new duty cycle will be 0.2010 .

2.

$$dP=P(11)-P(10)=79.3584-37.8=41.5584>0$$

$$dV=V(11)-V(10)=300-300=0, \text{ which is surely not less than zero}$$

$$\text{So, } D=D-dD=0.2010-.0038=.1972$$

Here, The difference of power is greater than zero. The difference of voltage equals to zero, i.e., it is surely not less than zero. So, according to the algorithm, the duty cycle measured one step before will get decreased by the fixed duty cycle change 0.0038 and the new duty cycle will be that of the current step. The previously measured duty cycle was 0.2010 and if it is decreased by 0.0038, then the new duty cycle will be 0.1972.

3.

$$dP=P(32)-P(31)=589.86-612.598=-22.738<0$$

$$\text{Now, } dV=V(32)-V(31)=348-343=5>0$$

$$\text{So, } D=D+dD=0.2048+.0038=.2086$$

Here, The difference of power is less than zero. The difference of voltage is greater than zero. So, according to the algorithm, the duty cycle measured one step before will get increased by

the fixed duty cycle change 0.0038 and the new duty cycle will be that of the current step. The previously measured duty cycle was 0.2048 and if it is decreased by 0.0038, then the new duty cycle will be 0.2086.

4.

$$dP=P(49)-P(48)=245.874-179.036=66.838>0$$

$$\text{Now, } dV=V(49)-V(48)=258-313=-55<0$$

$$\text{So, } D=D+dD=0.2162+.0038=.2200$$

Here, The difference of power is greater than zero. The difference of voltage is less than zero. So, according to the algorithm, the duty cycle measured one step before will get increased by the fixed duty cycle change 0.0038 and the new duty cycle will be that of the current step. The previously measured duty cycle was 0.2162 and if it is increased by 0.0038, then the new duty cycle will be 0.2200.

5.

$$dP=P(25)-P(24)=1397.9-697.533=700.367>0$$

$$\text{Now, } dV=V(25)-V(24)=350-321=29>0$$

$$\text{So, } D=D-dD=0.2162-.0038=.2124$$

Here, The difference of power is greater than zero. The difference of voltage is also greater than zero. So, according to the algorithm, the duty cycle measured one step before will get decreased by the fixed duty cycle change 0.0038 and the new duty cycle will be that of the current step. The previously measured duty cycle was 0.2162 and if it is decreased by 0.0038, then the new duty cycle will be 0.2124.

## 5.4.2 Incremental Conductance Algorithm

1.

$$dV=V(12)-V(11)=331-300=31, \text{ not equal to zero}$$

$$dI=I(12)-I(11)=.463-.264=.199$$

$$dI/dV=.199/31=.0064$$

$$-I/V=-.463/331=-330.537, \text{ not equal to } dI/dV$$

Now,  $dI/dV > -I/V$

$$\text{So, } D = D + dD = 0.2352 + .0038 = .2390$$

Here, The difference of voltage is not equal to zero. The quotient of difference of current and difference of voltage is .199 and it is not equal to but greater than the negative value of the quotient of current and voltage. So, according to the algorithm, the duty cycle measured one step before will get increased by the fixed duty cycle change 0.0038 and the new duty cycle will be that of the current step. The previously measured duty cycle was 0.2352 and if it is increased by 0.0038, then the new duty cycle will be 0.2390.

2.

$$dV = V(25) - V(24) = 350 - 321 = 29, \text{ not equal to zero}$$

$$dI = I(25) - I(24) = 3.994 - 2.173 = 1.821$$

$$dI/dV = 1.821/29 = .0628$$

$$-I/V = -3.994/350 = -.0114, \text{ not equal to } dI/dV$$

Now,  $dI/dV > -I/V$

$$\text{So, } D = D + dD = 0.2238 + .0038 = .2276$$

Here, The difference of voltage is not equal to zero. The quotient of difference of current and difference of voltage is .0628 and it is not equal to but greater than the negative value of the quotient of current and voltage. So, according to the algorithm, the duty cycle measured one step before will get increased by the fixed duty cycle change 0.0038 and the new duty cycle will be that of the current step. The previously measured duty cycle was 0.2238 and if it is increased by 0.0038, then the new duty cycle will be 0.2276.

3.

$$dV = V(49) - V(48) = 258 - 313 = -55, \text{ not equal to zero}$$

$$dI = I(49) - I(48) = .953 - .572 = .381$$

$$dI/dV = .381/-55 = -.0007$$

$$-I/V = -.953/258 = -.0037, \text{ not equal to } dI/dV$$

Now,  $dI/dV < -I/V$

$$\text{So, } D = D - dD = 0.2238 - .0038 = .2200$$

Here, The difference of voltage is not equal to zero. The quotient of difference of current and difference of voltage is  $-0.0007$  and it is not equal to but less than the negative value of the quotient of current and voltage. So, according to the algorithm, the duty cycle measured one step before will get decreased by the fixed duty cycle change  $0.0038$  and the new duty cycle will be that of the current step. The previously measured duty cycle was  $0.2238$  and if it is decreased by  $0.0038$ , then the new duty cycle will be  $0.2200$ .

4.

$$dV = V(5) - V(4) = 242 - 259 = -17, \text{not equal to zero}$$

$$dI = I(5) - I(4) = 0 - 0 = 0$$

$$dI/dV = 0/-17 = 0$$

$$-I/V = -0/242 = 0$$

$$\text{Now, } dI/dV = -I/V$$

$$\text{So, } D = D = .2466$$

Here, the difference of voltage is not equal to zero. The quotient of difference of current and difference of voltage is zero and it is equal to the negative value of the quotient of current and voltage. So, according to the algorithm, the duty cycle measured one step before will not change and will be that of the current step. The previously measured duty cycle was  $.2466$  and so the new duty cycle will be  $0.2466$ .

5.

$$dV = V(11) - V(10) = 300 - 300 = 0$$

$$dI = I(11) - I(10) = 0.264 - .126 = 0.138, \text{greater than zero}$$

$$\text{So, } D = D + dD = 0.2390 + .0038 = 0.2428$$

Here, the difference of voltage is equal to zero. But, the difference of current is greater than zero. So, according to the algorithm, the duty cycle measured one step before will get increased by the fixed duty cycle change  $0.0038$  and the new duty cycle will be that of the current step. The previously measured duty cycle was  $0.2390$  and if it is increased by  $0.0038$ , then the new duty cycle will be  $0.2428$ .

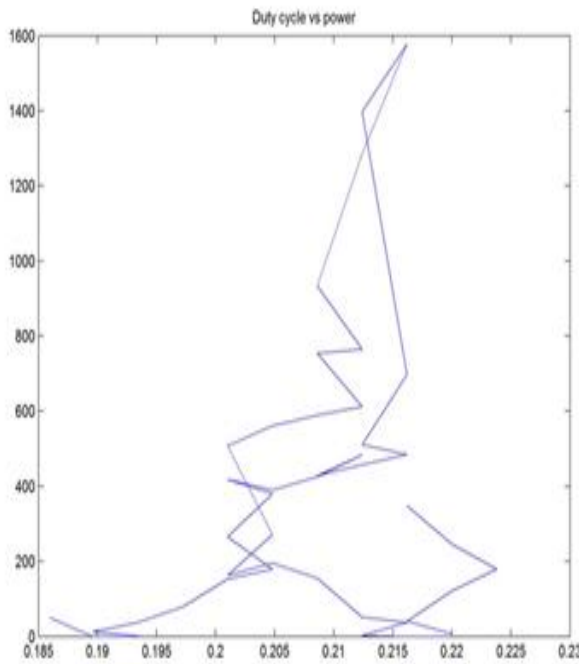


Fig: Perturb and Observe

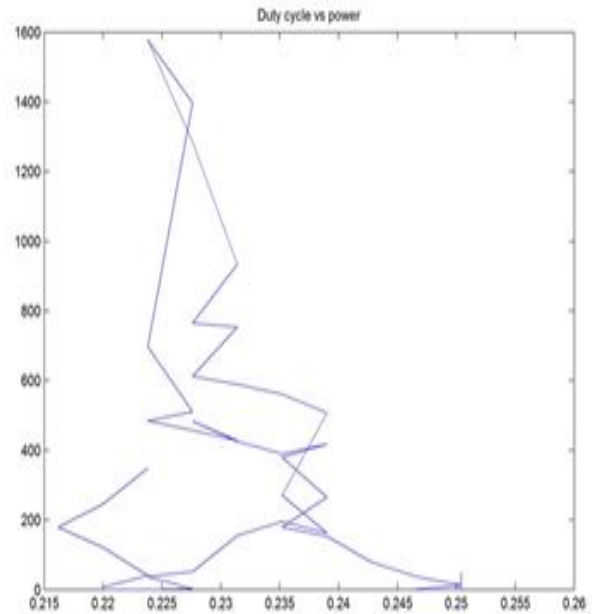


Fig: Incremental conductance

Fig 5.3: Duty Cycle vs Power Curves of P&O & InC Algorithms.

## 5.5 Correlation

### 5.5 1 Correlation between Input Power & Duty Cycle (P & O algorithm)

Table 5.4: Correlation between Input Power & Duty Cycle (P & O algorithm)

SL NO.	Input Power(x)	Duty Cycle (y)	$(x - \bar{x})$	$(y - \bar{y})$	$(x - \bar{x})^2$	$(y - \bar{y})^2$	$(x - \bar{x}) \times (y - \bar{y})$
01	49.29	0.1896	-275.928	-0.01748	76136.2618	0.00030555	4.823221
02	0	0.1896	-325.218	-0.01748	105766.7475	0.00030555	5.684811
03	0	0.1934	-325.218	-0.01368	105766.7475	0.000187142	4.448982
04	0	0.1934	-325.218	-0.01368	105766.7475	0.000187142	4.448982

		4			75	2	
05	0	0.193 4	-325.218	-0.01368	105766.74 75	0.00018714 2	4.448982
06	0	0.193 4	-325.218	-0.01368	105766.74 75	0.00018714 2	4.448982
07	0	0.193 4	-325.218	-0.01368	105766.74 75	0.00018714 2	4.448982
08	1.88	0.193 4	-323.338	-0.01368	104547.46 22	0.00018714 2	4.423264
09	12.015	0.189 6	-313.203	-0.01748	98096.119 21	0.00030555	5.474788
10	37.8	0.193 4	-287.418	-0.01368	82609.106 72	0.00018714 2	3.931878
11	79.2	0.197 2	-246.018	-0.00988	60524.856 32	9.76144E- 05	2.430658
12	153.253	0.201 0	-171.965	-0.00608	29571.961 23	3.69664E- 05	1.045547
13	178.976	0.204 8	-146.242	-0.00228	21386.722 56	5.1984E-06	0.333432
14	265.482	0.201 0	-59.736	-0.00608	3568.3896 96	3.69664E- 05	0.363195
15	379.68	0.204 8	54.462	-0.00228	2966.1094 44	5.1984E-06	-0.12417
16	418.54	0.201 0	93.322	-0.00608	8708.9956 84	3.69664E- 05	-0.5674
17	390.096	0.204 8	64.878	-0.00228	4209.1548 84	5.1984E-06	-0.14792
18	425.909	0.208 6	100.691	0.00152	10138.677 48	2.3104E-06	0.15305
19	483.753	0.212 4	158.535	0.00532	25133.346 23	2.83024E- 05	0.843406
20	427.948	0.208 6	102.73	0.00152	10553.452 9	2.3104E-06	0.15615
21	457.542	0.212 4	132.324	0.00532	17509.640 98	2.83024E- 05	0.703964
22	484.287	0.216 2	159.069	0.00912	25302.946 76	8.31744E- 05	1.450709
23	510.718	0.212 4	185.5	0.00532	34410.25	2.83024E- 05	0.98686
24	697.533	0.216 2	372.315	0.00912	138618.45 92	8.31744E- 05	3.395513
25	1397.9	0.212 4	1072.682	0.00532	1150646.6 73	2.83024E- 05	5.706668
26	1578.12 2	0.216 2	1252.904	0.00912	1569768.4 33	8.31744E- 05	11.42648
27	1285.07 6	0.212 4	959.858	0.00532	921327.38 02	2.83024E- 05	5.106445
28	934.36	0.208 6	609.142	0.00152	371053.97 62	2.3104E-06	0.925896

29	764.596	0.212 4	439.378	0.00532	193053.02 69	2.83024E- 05	2.337491
30	754.716	0.208 6	429.498	0.00152	184468.53 2	2.3104E-06	0.652837
31	612.598	0.212 4	287.38	0.00532	82587.264 4	2.83024E- 05	1.528862
32	589.86	0.208 6	264.642	0.00152	70035.388 16	2.3104E-06	0.402256
33	561.255	0.204 8	236.037	-0.00228	55713.465 37	5.1984E-06	-0.53816
34	507.582	0.201 0	182.364	-0.00608	33256.628 5	3.69664E- 05	-1.10877
35	270.81	0.204 8	-54.408	-0.00228	2960.2304 64	5.1984E-06	0.12405
36	162.992	0.201 0	-162.226	-0.00608	26317.275 08	3.69664E- 05	0.986334
37	195.552	0.204 8	-129.666	-0.00228	16813.271 56	5.1984E-06	0.295638
38	155.811	0.208 6	-169.407	0.00152	28698.731 65	2.3104E-06	-0.2575
39	52.325	0.212 4	-272.893	0.00532	74470.589 45	2.83024E- 05	-1.45179
40	38	0.216 2	-287.218	0.00912	82494.179 52	8.31744E- 05	-2.61943
41	2.344	0.212 4	-322.874	0.00532	104247.61 99	2.83024E- 05	-1.71769
42	0	0.216 2	-325.218	0.00912	105766.74 75	8.31744E- 05	-2.96599
43	0	0.220 0	-325.218	0.01292	105766.74 75	0.00016692 6	-4.20182
44	0	0.220 0	-325.218	0.01292	105766.74 75	0.00016692 6	-4.20182
45	7.192	0.220 0	-318.026	0.01292	101140.53 67	0.00016692 6	-4.1089
46	41.022	0.216 2	-284.196	0.00912	80767.366 42	8.31744E- 05	-2.59187
47	121.272	0.220 0	-203.946	0.01292	41593.970 92	0.00016692 6	-2.63498
48	179.036	0.223 8	-146.182	0.01672	21369.177 12	0.00027955 8	-2.44416
49	245.874	0.220 0	-79.344	0.01292	6295.4703 36	0.00016692 6	-1.02512
50	348.696	0.216 2	23.478	0.00912	551.21648 4	8.31744E- 05	0.214119
n=5 0	$\sum x=$ 16260.8 93	$\sum y=$ 10.35 4	$\sum(x - \bar{x})=$ -0.007	$\sum(y - \bar{y})=$ 8.04912E -16	$\sum(x - \bar{x})^2 =$ 6925523.0 44	$\sum(y - \bar{y})^2 =$ 0.00450528	$\sum(x - \bar{x}) \times (y - \bar{y})$ 55.4449458



Arithmetic Mean:

$$\bar{x} = \frac{\sum x}{n}$$

$$\bar{x} = \frac{16260.893}{50} = 325.218$$

$$\bar{y} = \frac{\sum y}{n}$$

$$\bar{y} = \frac{10.354}{50} = .20708$$

Correlation Coefficient:

$$r = \frac{\sum(x-\bar{x})(y-\bar{y})}{\sqrt{\sum(x-\bar{x})^2 \sum(y-\bar{y})^2}}$$

$$\text{Or, } r = \frac{55.4449458}{\sqrt{(6925523.044 \times 0.00450528)}}$$

So,  $r=.31$

Interpretation: The correlation between duty cycle and power of the perturb and observe algorithm is 0.31. This indicates a low association between the variables.

## 5.5.2 Correlation between Input Power & Duty Cycle (InC algorithm)

Table 5.5: Correlation between Input Power & Duty Cycle (InC algorithm)

SL N O.	x	y	$(x - \bar{x})$	$(y - \bar{y})$	$(x - \bar{x})^2$	$(y - \bar{y})^2$	$(x - \bar{x})(y - \bar{y})$
01	49.29	0.2504	-275.93	0.01748	76136.26	0.00030555	-4.82322144
02	0	0.2504	-325.22	0.01748	105766.7	0.00030555	-5.68481064
03	0	0.2466	-325.22	0.01368	105766.7	0.000187142	-4.44898224
04	0	0.2466	-325.22	0.01368	105766.7	0.000187142	-4.44898224
05	0	0.246	-325.22	0.01368	105766.7	0.00018714	-4.44898224

		6				2	
06	0	0.246 6	-325.22	0.01368	105766.7	0.00018714 2	-4.44898224
07	0	0.246 6	-325.22	0.01368	105766.7	0.00018714 2	-4.44898224
08	1.88	0.246 6	- 323.345	0.01368	104547.5	0.00018714 2	-4.42326384
09	12.015	0.250 4	- 313.178	0.01748	98096.12	0.00030555	-5.47478844
10	37.8	0.246 6	- 287.344	0.01368	82609.11	0.00018714 2	-3.93187824
11	79.2	0.242 8	- 245.862	0.00988	60524.86	9.76144E-05	-2.43065784
12	153.253	0.239 0	- 171.689	0.00608	29571.96	3.69664E-05	-1.0455472
13	178.976	0.235 2	-146.57	0.00228	21386.72	5.1984E-06	-0.33343176
14	265.482	0.239 0	- 59.2736	0.00608	3568.39	3.69664E-05	-0.36319488
15	379.68	0.235 2	53.788	0.00228	2966.109	5.1984E-06	0.12417336
16	418.54	0.239 0	94.0586	0.00608	8708.996	3.69664E-05	0.56739776
17	390.096	0.235 2	65.5726	0.00228	4209.155	5.1984E-06	0.14792184
18	425.909	0.231 4	101.438 4	-0.00152	10138.68	2.3104E-06	-0.15305032
19	483.753	0.227 6	157.676 8	-0.00532	25133.35	2.83024E-05	-0.8434062
20	427.948	0.231 4	103.501 4	-0.00152	10553.45	2.3104E-06	-0.1561496
21	457.542	0.227 6	133.146 4	-0.00532	17509.64	2.83024E-05	-0.70396368
22	484.287	0.223 8	158.178 4	-0.00912	25302.95	8.31744E-05	-1.45070928
23	510.718	0.227 6	186.404 6	-0.00532	34410.25	2.83024E-05	-0.98686
24	697.533	0.223 8	371.009 2	-0.00912	138618.5	8.31744E-05	-3.3955128
25	1397.9	0.227 6	1075.07 6	-0.00532	1150647	2.83024E-05	-5.70666824
26	1578.12 2	0.223 8	1250.10 1	-0.00912	1569768	8.31744E-05	-11.42648448
27	1285.07 6	0.227 6	957.574 8	-0.00532	921327.4	2.83024E-05	-5.10644456
28	934.36	0.231 4	610.844	-0.00152	371054	2.3104E-06	-0.92589584
29	764.596	0.227 6	437.981 6	-0.00532	193053	2.83024E-05	-2.33749096

30	754.716	0.231 4	430.880 8	-0.00152	184468.5	2.3104E-06	-0.65283696
31	612.598	0.227 6	286.306 4	-0.00532	82587.26	2.83024E-05	-1.5288616
32	589.86	0.231 4	263.623	-0.00152	70035.39	2.3104E-06	-0.40225584
33	561.255	0.235 2	235.086 4	0.00228	55713.47	5.1984E-06	0.53816436
34	507.582	0.239 0	183.242 2	0.00608	33256.63	3.69664E-05	1.10877312
35	270.81	0.235 2	-54.869	0.00228	2960.23	5.1984E-06	-0.12405024
36	162.992	0.239 0	- 161.935	0.00608	26317.28	3.69664E-05	-0.98633408
37	195.552	0.235 2	- 129.319	0.00228	16813.27	5.1984E-06	-0.29563848
38	155.811	0.231 4	- 169.108	-0.00152	28698.73	2.3104E-06	0.25749864
39	52.325	0.227 6	-272.79	-0.00532	74470.59	2.83024E-05	1.45179076
40	38	0.223 8	- 287.295	-0.00912	82494.18	8.31744E-05	2.61942816
41	2.344	0.227 6	- 322.871	-0.00532	104247.6	2.83024E-05	1.71768968
42	0	0.223 8	-325.22	-0.00912	105766.7	8.31744E-05	2.96598816
43	0	0.220 0	-325.22	-0.01292	105766.7	0.00016692 6	4.20181656
44	0	0.220 0	-325.22	-0.01292	105766.7	0.00016692 6	4.20181656
45	7.192	0.220 0	- 318.047	-0.01292	101140.5	0.00016692 6	4.10889592
46	41.022	0.223 8	- 284.103	-0.00912	80767.37	8.31744E-05	2.59186752
47	121.272	0.220 0	- 203.725	-0.01292	41593.97	0.00016692 6	2.63498232
48	179.036	0.216 2	- 146.527	-0.01672	21369.18	0.00027955 8	2.44416304
49	245.874	0.220 0	- 79.9178	-0.01292	6295.47	0.00016692 6	1.02512448
50	348.696	0.223 8	24.2776	-0.00912	551.2165	8.31744E-05	-0.21411936
n= 50	$\sum x =$ 16260.8 93	$\sum y =$ 11.64 6	$\sum(x - \bar{x}) =$ -0.007	$\sum(y - \bar{y}) =$ 5.55112 E-16	$\sum(x - \bar{x})^2 =$ 6925523. 044	$\sum(y - \bar{y})^2 =$ 0.00450528	$\sum(x - \bar{x})(y - \bar{y}) =$ -55.44494576

Arithmetic Mean:

$$\bar{x} = \frac{\sum x}{n}$$

$$\bar{x} = \frac{16260.893}{50} = 325.218$$

$$\bar{y} = \frac{\sum y}{n}$$

$$\bar{y} = \frac{11.646}{50} = .23292$$

Correlation Coefficient:

$$r = \frac{\sum(x-\bar{x})(y-\bar{y})}{\sqrt{\sum(x-\bar{x})^2 \sum(y-\bar{y})^2}}$$

$$\text{Or, } r = \frac{-55.44494576}{\sqrt{(6925523.044 \times 0.00450528)}}$$

So,  $r = -0.31$

Interpretation: The correlation between duty cycle and power of the Incremental conductance algorithm is -0.31. This indicates a low association between the variable.

### 5.5.3 Correlation between Duty Cycles obtained from P&O and InC algorithms

Table 5.6: Correlation between Duty Cycles obtained from P&O and InC algorithms

SL N O.	P&O DUTY CYCLE (x)	InC DUTY CYCLE (y)	$(x - \bar{x})$	$(y - \bar{y})$	$(x - \bar{x})^2$	$(y - \bar{y})^2$	$(x - \bar{x}) \times (y - \bar{y})$
01	0.1896	0.2504	-0.01741	0.01748	0.000303108	0.00030555	-0.000304327
02	0.1896	0.2504	-0.01741	0.01748	0.000303108	0.00030555	-0.000304327
03	0.1934	0.2466	-0.01361	0.01368	0.000185232	0.000187142	-0.000186185

04	0.1934	0.2466	-0.01361	0.01368	0.00018523 2	0.00018714 2	- 0.000186185
05	0.1934	0.2466	-0.01361	0.01368	0.00018523 2	0.00018714 2	- 0.000186185
06	0.1934	0.2466	-0.01361	0.01368	0.00018523 2	0.00018714 2	- 0.000186185
07	0.1934	0.2466	-0.01361	0.01368	0.00018523 2	0.00018714 2	- 0.000186185
08	0.1934	0.2466	-0.01361	0.01368	0.00018523 2	0.00018714 2	- 0.000186185
09	0.1896	0.2504	-0.01741	0.01748	0.00030310 8	0.00030555	- 0.000304327
10	0.1934	0.2466	-0.01361	0.01368	0.00018523 2	0.00018714 2	- 0.000186185
11	0.1972	0.2428	-0.00981	0.00988	9.62361E- 05	9.76144E- 05	-9.69228E- 05
12	0.2010	0.2390	-0.00601	0.00608	3.61201E- 05	3.69664E- 05	-3.65408E- 05
13	0.2048	0.2352	-0.00221	0.00228	4.8841E-06	5.1984E-06	-5.0388E-06
14	0.2010	0.2390	-0.00601	0.00608	3.61201E- 05	3.69664E- 05	-3.65408E- 05
15	0.2048	0.2352	-0.00221	0.00228	4.8841E-06	5.1984E-06	-5.0388E-06
16	0.2010	0.2390	-0.00601	0.00608	3.61201E- 05	3.69664E- 05	-3.65408E- 05
17	0.2048	0.2352	-0.00221	0.00228	4.8841E-06	5.1984E-06	-5.0388E-06
18	0.2086	0.2314	0.00159	-0.00152	2.5281E-06	2.3104E-06	-2.4168E-06
19	0.2124	0.2276	0.00539	-0.00532	2.90521E- 05	2.83024E- 05	-2.86748E- 05
20	0.2086	0.2314	0.00159	-0.00152	2.5281E-06	2.3104E-06	-2.4168E-06
21	0.2124	0.2276	0.00539	-0.00532	2.90521E- 05	2.83024E- 05	-2.86748E- 05
22	0.2162	0.2238	0.00919	-0.00912	8.44561E- 05	8.31744E- 05	-8.38128E- 05
23	0.2124	0.2276	0.00539	-0.00532	2.90521E- 05	2.83024E- 05	-2.86748E- 05
24	0.2162	0.2238	0.00919	-0.00912	8.44561E- 05	8.31744E- 05	-8.38128E- 05
25	0.2124	0.2276	0.00539	-0.00532	2.90521E- 05	2.83024E- 05	-2.86748E- 05
26	0.2162	0.2238	0.00919	-0.00912	8.44561E- 05	8.31744E- 05	-8.38128E- 05
27	0.2124	0.2276	0.00539	-0.00532	2.90521E- 05	2.83024E- 05	-2.86748E- 05
28	0.2086	0.2314	0.00159	-0.00152	2.5281E-06	2.3104E-06	-2.4168E-06
29	0.2124	0.2276	0.00539	-0.00532	2.90521E- 05	2.83024E- 05	-2.86748E- 05
30	0.2086	0.2314	0.00159	-0.00152	2.5281E-06	2.3104E-06	-2.4168E-06
31	0.2124	0.2276	0.00539	-0.00532	2.90521E- 05	2.83024E- 05	-2.86748E- 05

32	0.2086	0.2314	0.00159	-0.00152	2.5281E-06	2.3104E-06	-2.4168E-06
33	0.2048	0.2352	-0.00221	0.00228	4.8841E-06	5.1984E-06	-5.0388E-06
34	0.2010	0.2390	-0.00601	0.00608	3.61201E-05	3.69664E-05	-3.65408E-05
35	0.2048	0.2352	-0.00221	0.00228	4.8841E-06	5.1984E-06	-5.0388E-06
36	0.2010	0.2390	-0.00601	0.00608	3.61201E-05	3.69664E-05	-3.65408E-05
37	0.2048	0.2352	-0.00221	0.00228	4.8841E-06	5.1984E-06	-5.0388E-06
38	0.2086	0.2314	0.00159	-0.00152	2.5281E-06	2.3104E-06	-2.4168E-06
39	0.2124	0.2276	0.00539	-0.00532	2.90521E-05	2.83024E-05	-2.86748E-05
40	0.2162	0.2238	0.00919	-0.00912	8.44561E-05	8.31744E-05	-8.38128E-05
41	0.2124	0.2276	0.00539	-0.00532	2.90521E-05	2.83024E-05	-2.86748E-05
42	0.2162	0.2238	0.00919	-0.00912	8.44561E-05	8.31744E-05	-8.38128E-05
43	0.2200	0.2200	0.01299	-0.01292	0.00016874	0.000166926	-0.000167831
44	0.2200	0.2200	0.01299	-0.01292	0.00016874	0.000166926	-0.000167831
45	0.2200	0.2200	0.01299	-0.01292	0.00016874	0.000166926	-0.000167831
46	0.2162	0.2238	0.00919	-0.00912	8.44561E-05	8.31744E-05	-8.38128E-05
47	0.2200	0.2200	0.01299	-0.01292	0.00016874	0.000166926	-0.000167831
48	0.2238	0.2162	0.01679	-0.01672	0.000281904	0.000279558	-0.000280729
49	0.2200	0.2200	0.01299	-0.01292	0.00016874	0.000166926	-0.000167831
50	0.2162	0.2238	0.00919	-0.00912	8.44561E-05	8.31744E-05	-8.38128E-05
n=50	$\sum x=10.354$	$\sum y=11.646$	$\sum(x - \bar{x})=0.0035$	$\sum(y - \bar{y})=5.55112E-16$	$\sum(x - \bar{x})^2=0.004505525$	$\sum(y - \bar{y})^2=0.00450528$	$\sum(x - \bar{x})(y - \bar{y})=-0.00450528$

Arithmetic Mean:

$$\bar{x} = \frac{\sum x}{n}$$

$$\bar{x} = \frac{10.354}{50} = .20708$$

$$\bar{y} = \frac{\sum y}{n}$$

$$\bar{y} = \frac{11.646}{50} = .23292$$

Correlation Coefficient:

$$r = \frac{\Sigma(x-\bar{x})(y-\bar{y})}{\sqrt{\Sigma(x-\bar{x})^2 \Sigma(y-\bar{y})^2}}$$

$$\text{Or, } r = \frac{-0.00450528}{\sqrt{(0.004505525 \times 0.00450528)}}$$

So,  $r = -.9999$

Interpretation: The correlation between the duty cycle of the perturb and observe algorithm and the duty cycle of the Incremental conductance algorithm is -0.9999. This indicates a very high association between the variable.

THIS PAGE INTENTIONALLY LEFT BLANK







## 6.2 Effect of Irradiance and Temperature on PV Voltage, Current and Power

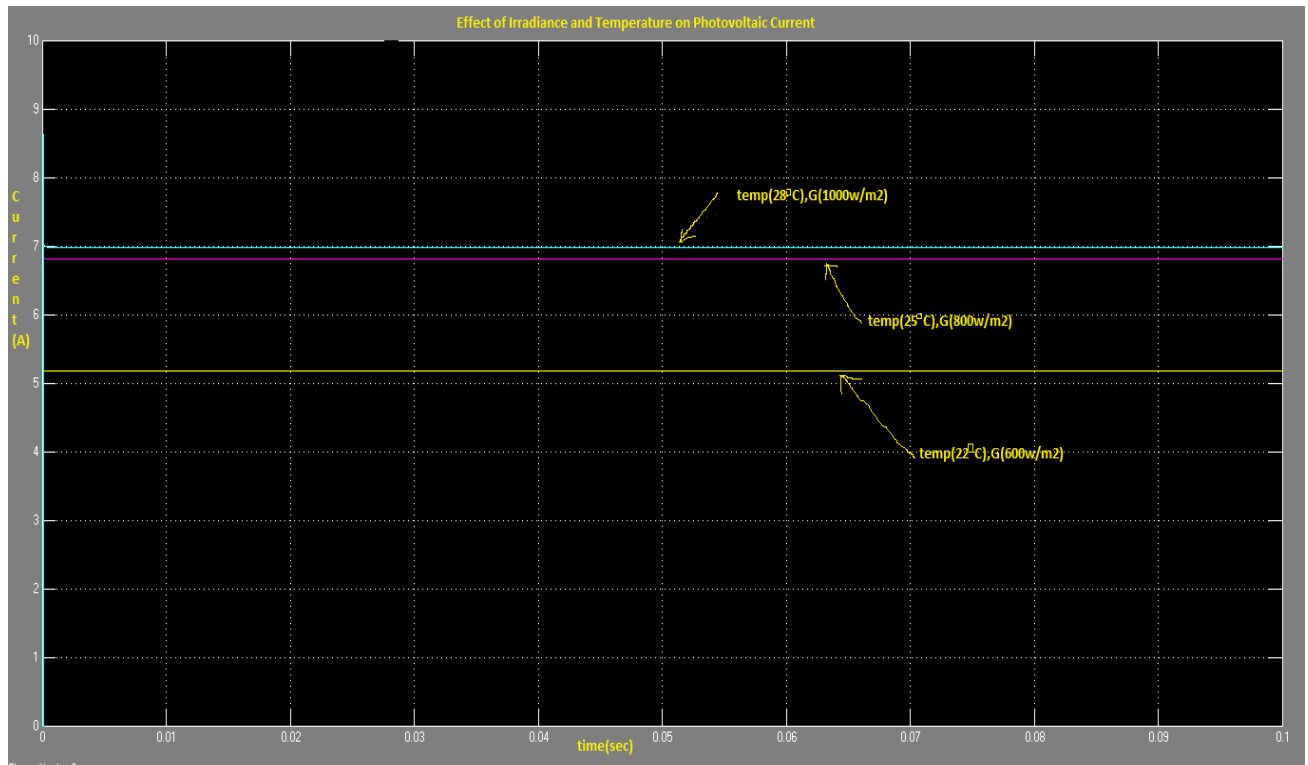


Fig 6.3: Effect of Irradiance and Temperature on PV Current

In figure 6.3 it is seen, when the temperature of the cells is 22°C and the irradiance is 600w/m<sup>2</sup>, then the pv current is 5.178A. When the temperature of the cells is 25°C and the irradiance is 800w/m<sup>2</sup>, then the pv current is 6.804A. When the temperature of the cells is 28°C and the irradiance is 1000w/m<sup>2</sup>, then the current is 6.98A.

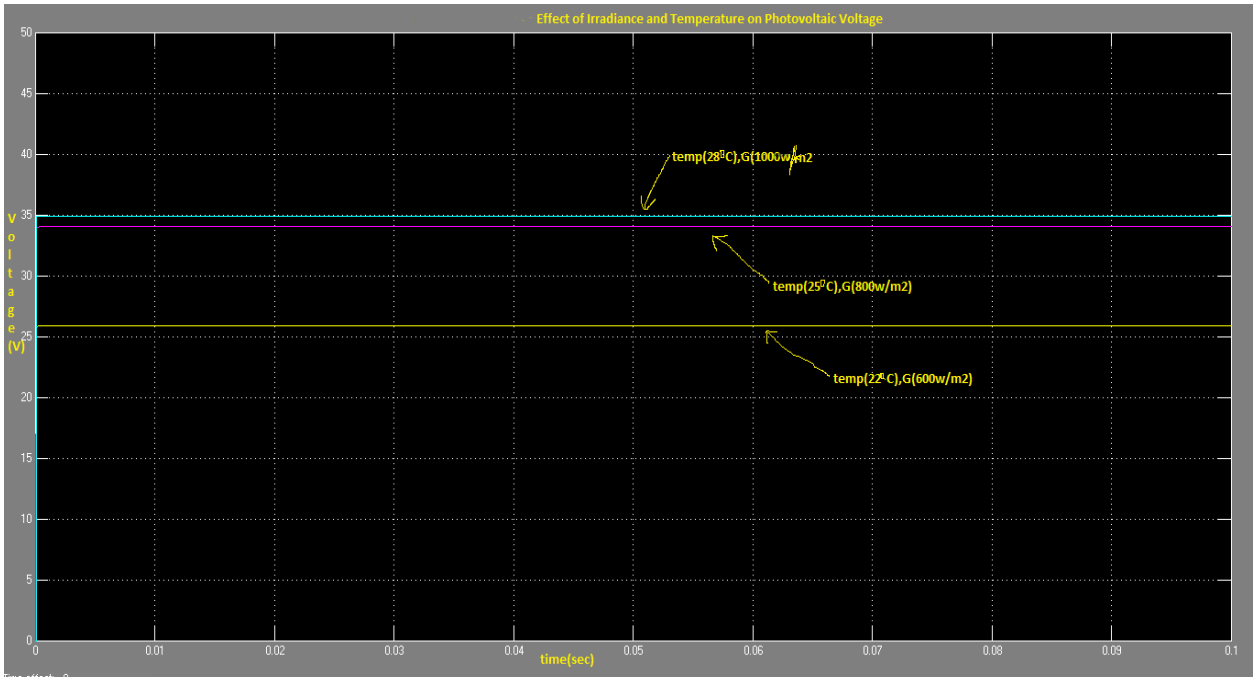


Fig 6.4: Effect of Irradiance and Temperature on PV Voltage

In figure 6.4 it is seen, when the temperature of the cells is 22 °C and the irradiance is 600w/m<sup>2</sup>, then the pv voltage is 25.89V. When the temperature of the cells is 25°C and the irradiance is 800w/m<sup>2</sup>, then the pv voltage is 34.02V. When the temperature of the cells is 28°C and the irradiance is 1000w/m<sup>2</sup>, then the pv voltage is 34.9V.

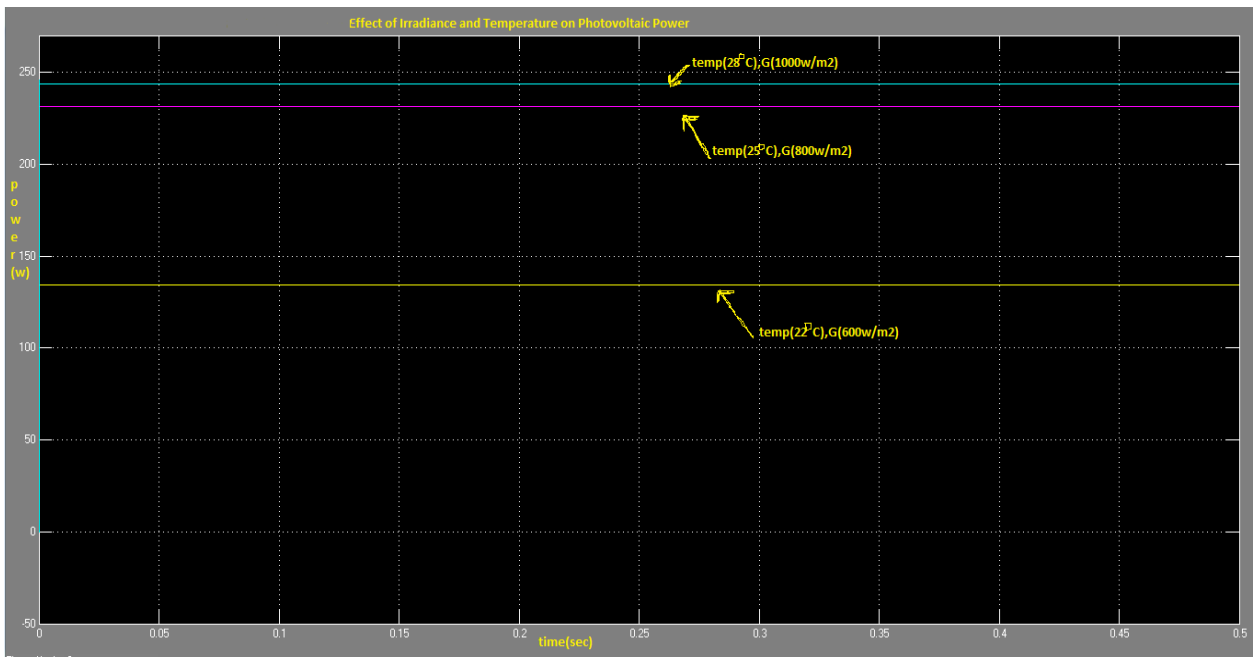


Fig 6.5: Effect of Irradiance and Temperature on PV Power

In figure 6.5 it is seen, when the temperature of the cells is 22°C and the irradiance is 600w/m<sup>2</sup>, then the pv power is 194.1W. When the temperature of the cells is 25°C and the irradiance is 800w/m<sup>2</sup>, then the pv power is 231.4W. When the temperature of the cells is 28°C and the irradiance is 1000w/m<sup>2</sup>, then the pv power is 243.6W.

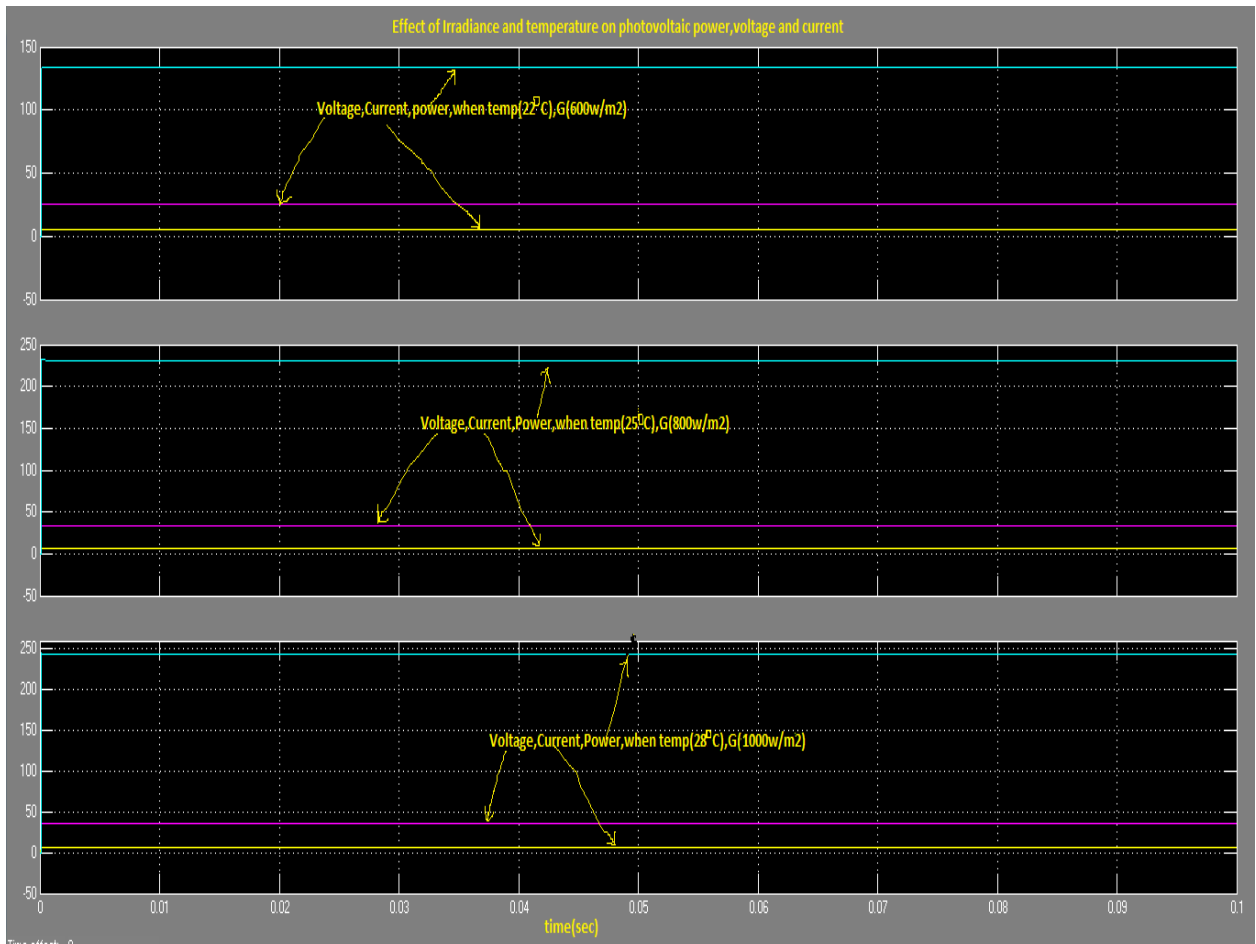


Fig 6.6: Effect of Irradiance and Temperature on PV Voltage, Current and Power

In this figure the effect of changes in irradiance and temperature on pv voltage, current and power have been shown together. When the temperature is 22°C and the irradiance is 600 w/m<sup>2</sup> the pv voltage is 25.89V, the pv current is 5.178A and the pv power is 194.1W. When the temperature is 25°C and the irradiance is 800 w/m<sup>2</sup> the pv voltage is 34.02V, the pv current is 6.804A and the pv power is 231.4W. When the temperature is 28°C and the irradiance is 1000 w/m<sup>2</sup> the pv voltage is 34.9V, the pv current is 6.98A and the pv power is 243.6W.

## 6.3 Waveforms for P&O Algorithm after Simulation

### 6.3.1 PV Voltage and Current

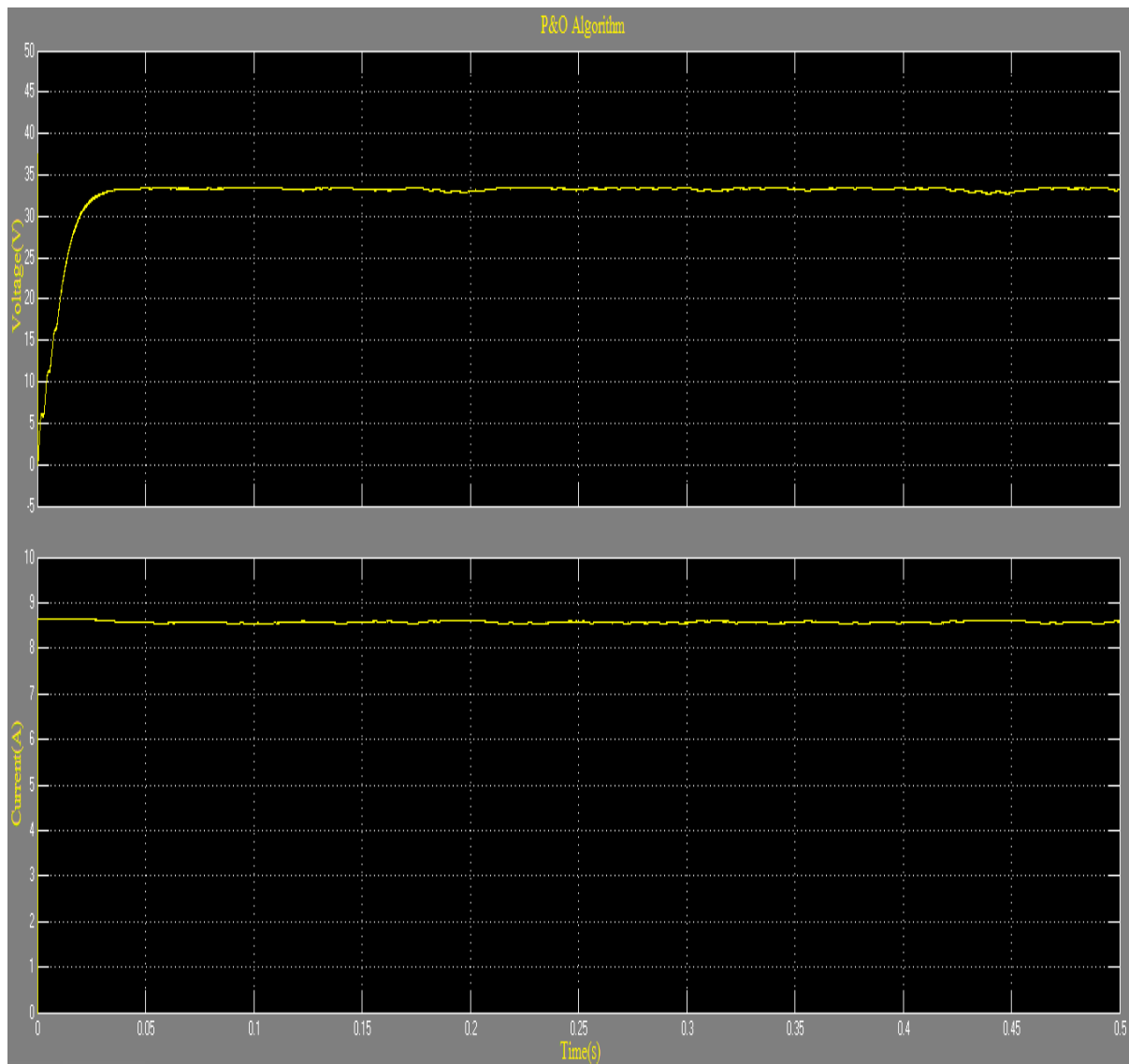


Fig 6.7 : Waveforms of PV Voltage(Top) and Current(Bottom) versus Time.

### 6.3.2 PV Power

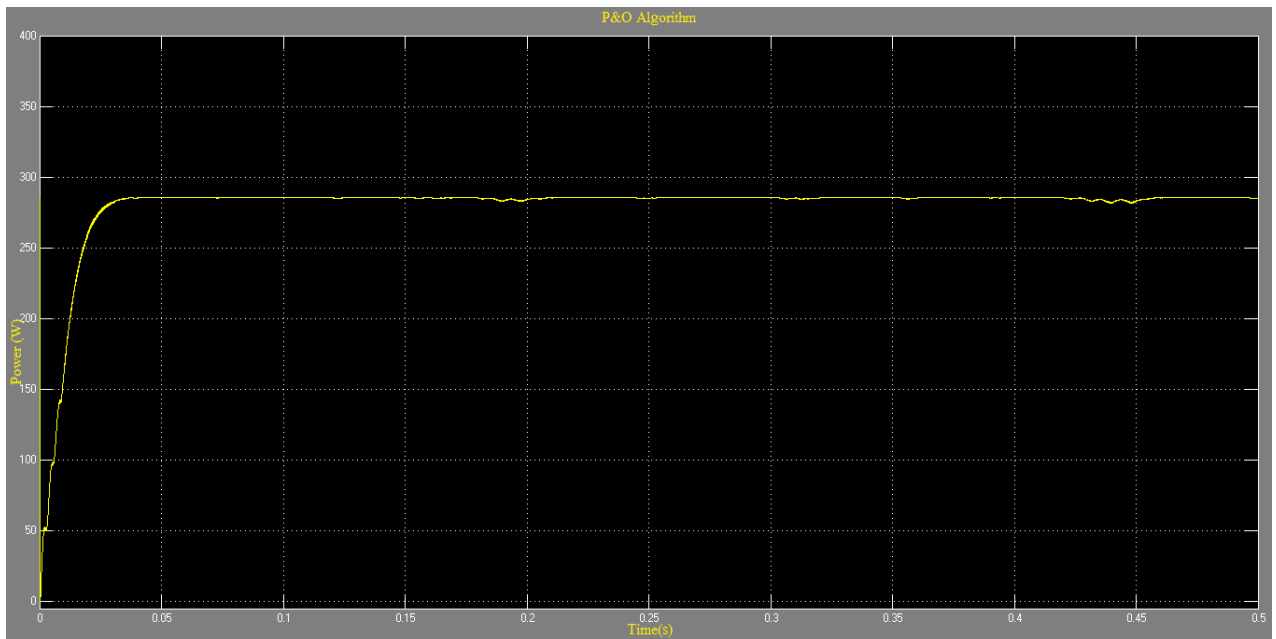


Fig 6.8: Waveform of Photo-Voltaic Power versus Time.

### 6.3.3 Input and Output Voltage of Buck-boost Converter

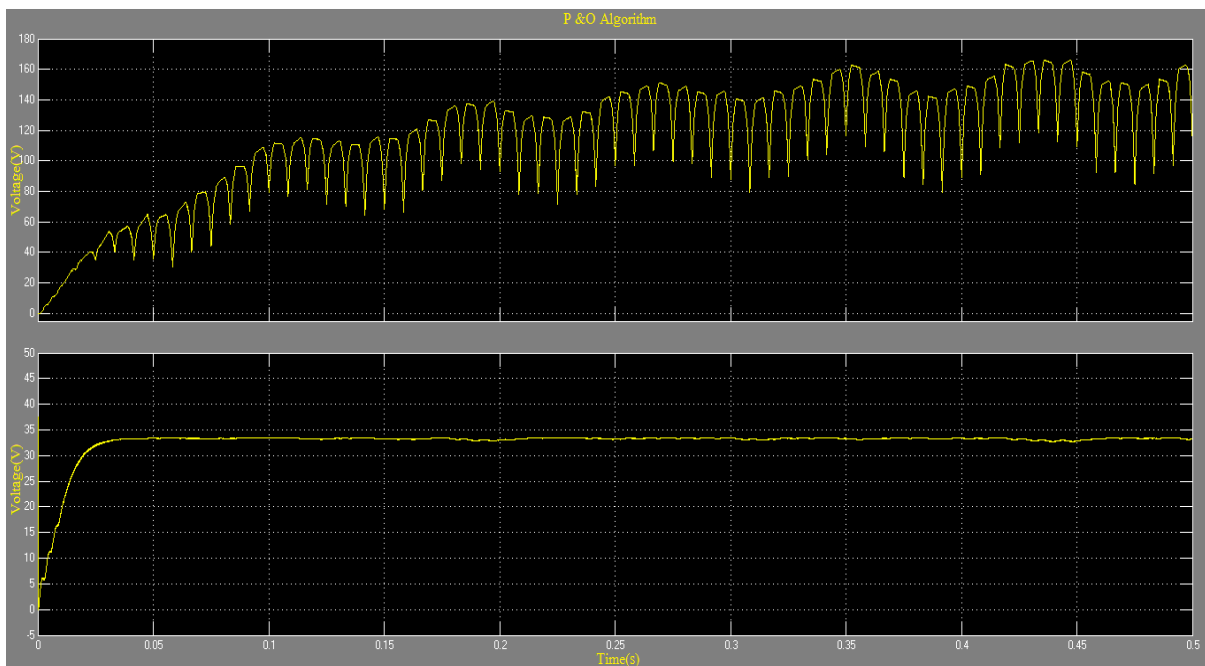


Fig 6.9: Waveforms of Input (Bottom) and Output Voltage (Top) of Buck-Boost Converter versus Time.

### 6.3.4 Duty Cycle

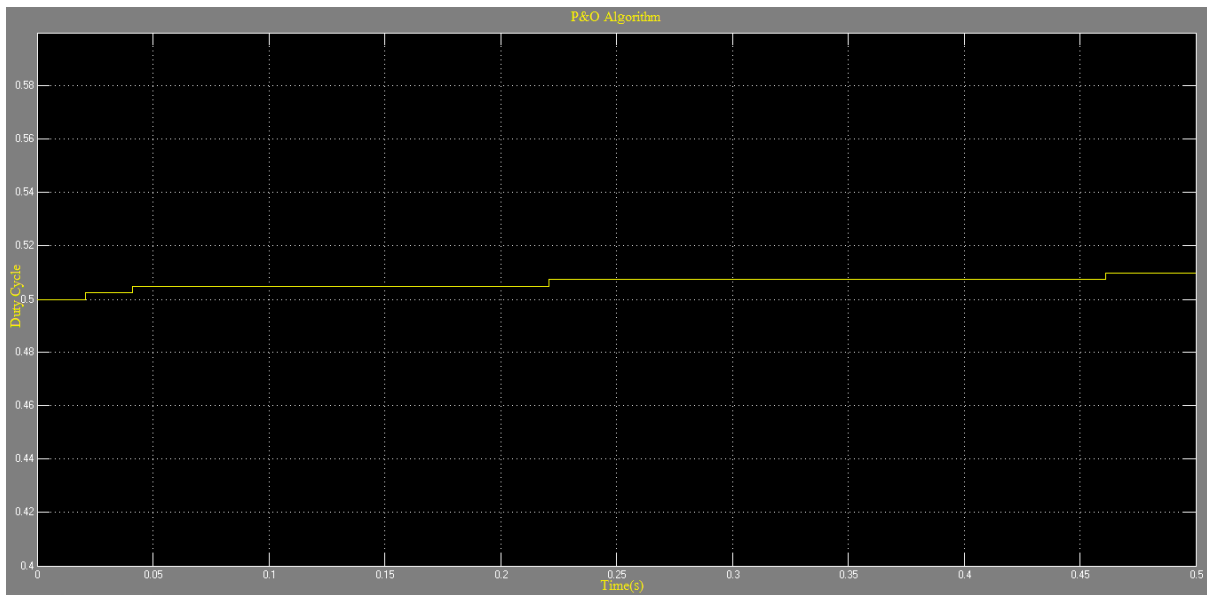


Fig 6.10: Waveform of Duty Cycle versus Time.

### 6.3.5 AC Voltage Output

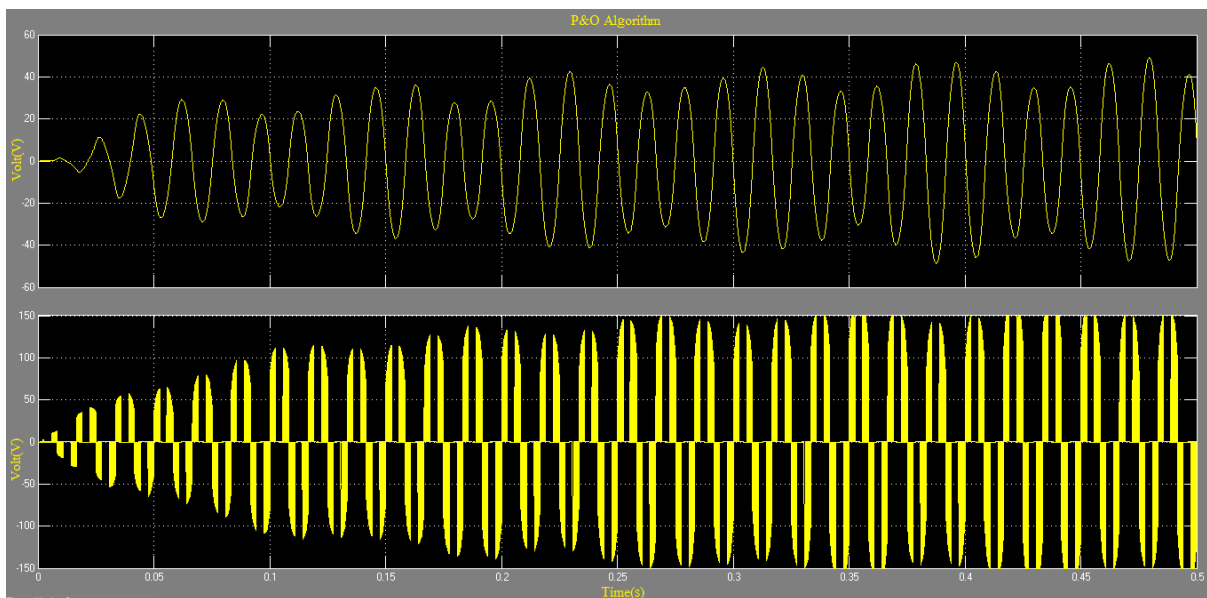


Fig 6.11: Waveforms of AC Voltage after Filtering (Top) and before Filtering (Bottom) versus Time.



## 6.4 Waveforms for Inc Conductance Algorithm

### 6.4.1 PV Voltage and Current

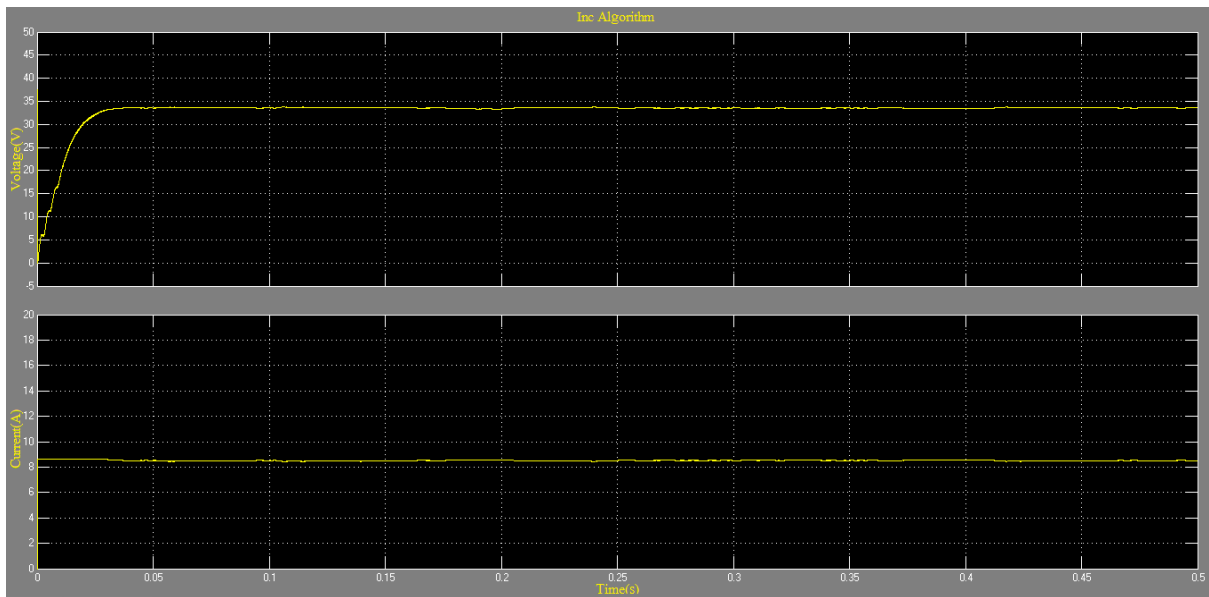


Fig 6.12: Waveforms of PV Voltage (Top) and Current (Bottom) versus Time.

### 6.4.2 PV Power

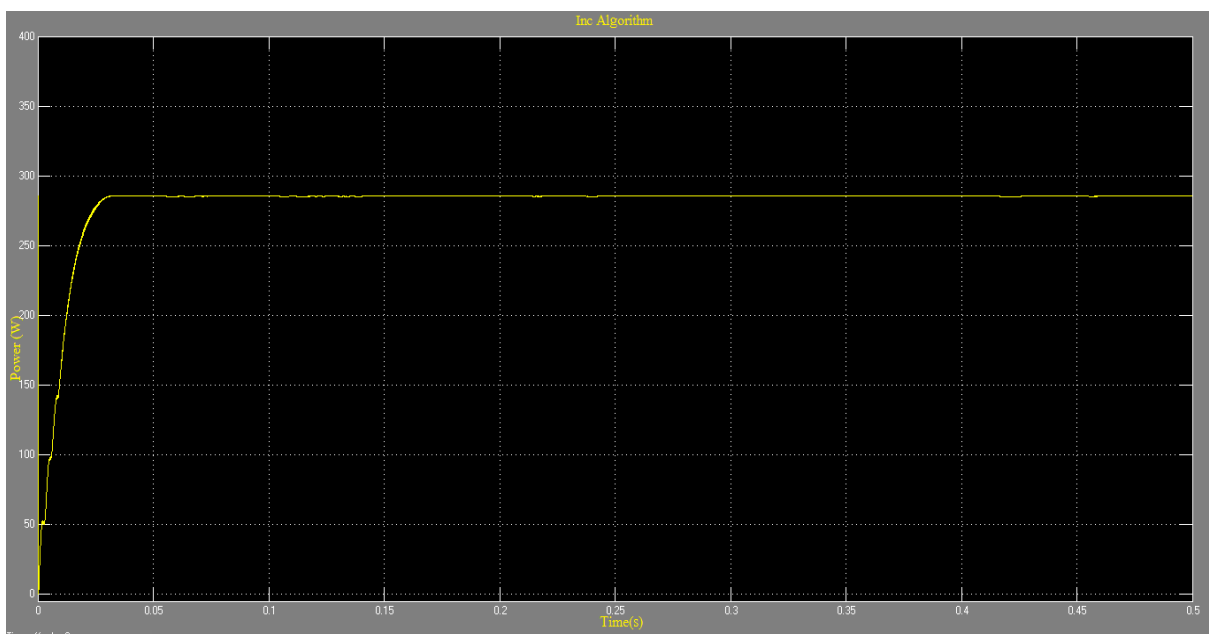


Fig 6.13: Waveform of Photo-Voltaic Power versus Time.

### 6.4.3 Input and Output Voltage of Buck-boost Converter

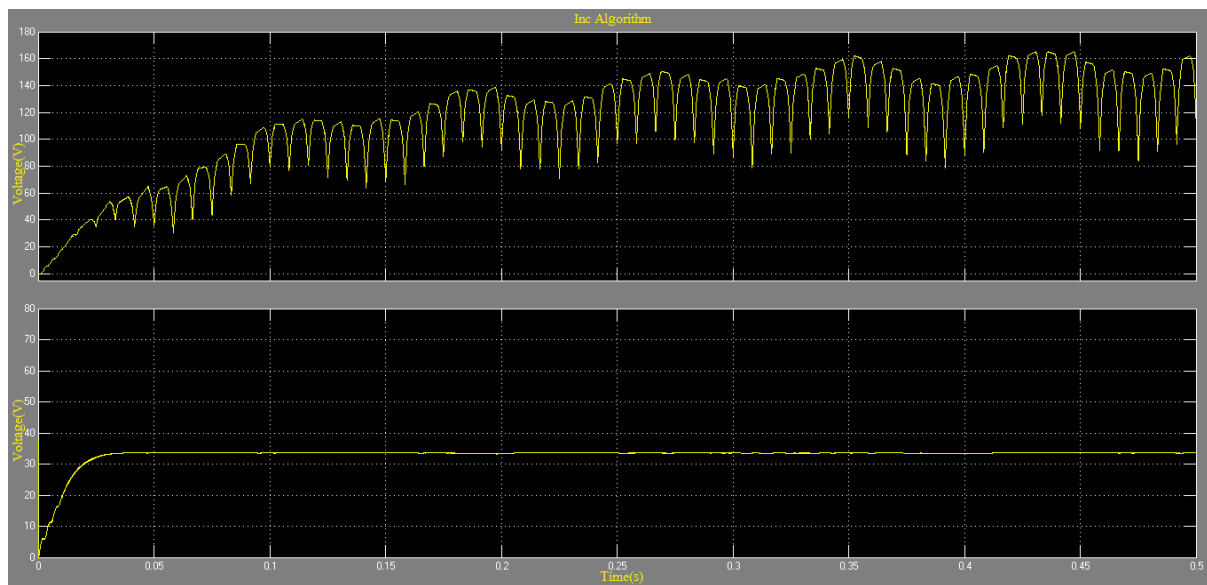


Fig 6.14: Waveforms of Input (Bottom) and Output Voltage (Top) of Buck-Boost Converter versus Time.

### 6.4.4 Duty Cycle

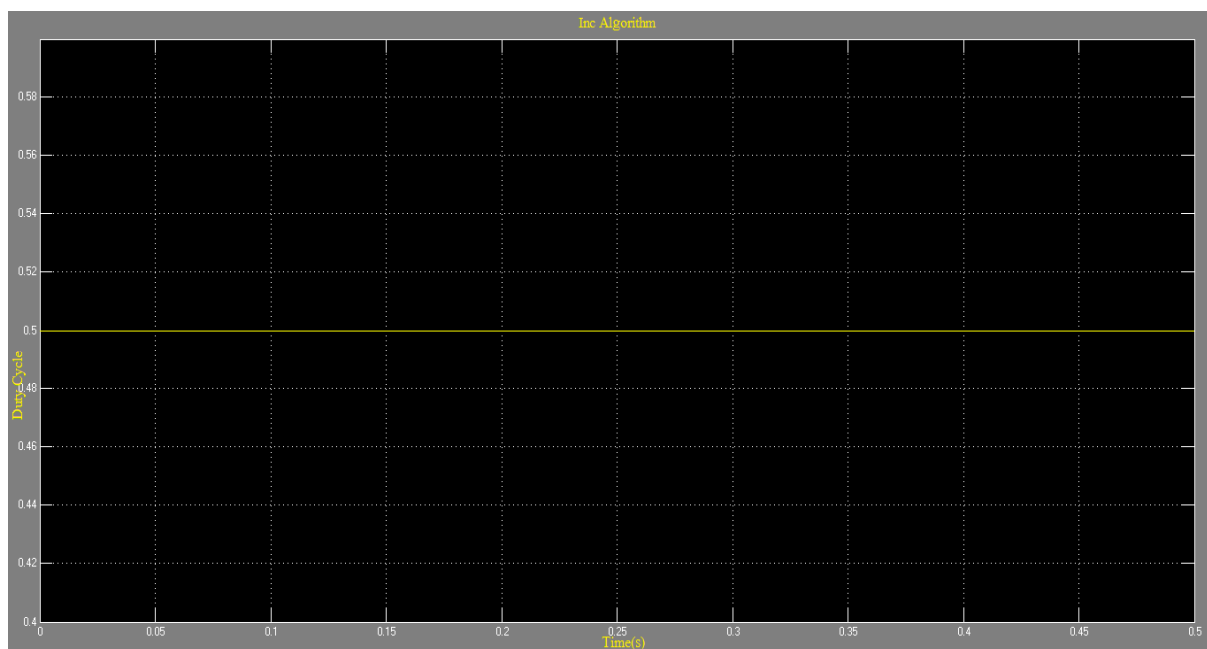


Fig 6.15: Waveform of Duty Cycle versus Time.

## 6.4.5 AC Voltage Output

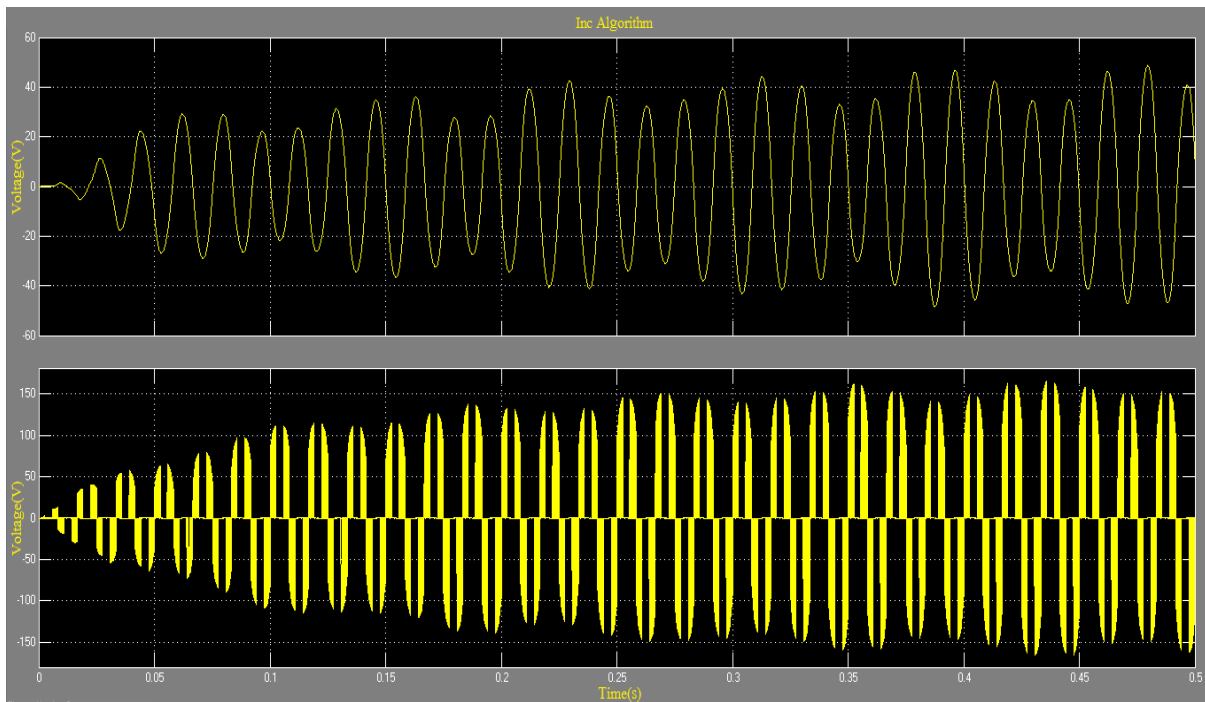


Fig 6.16: Waveforms of AC Voltage after Filtering (Top) and before Filtering (Bottom) versus Time.

## 6.5 COMPARISON

### 6.5.1 Comparison of the tracking power,voltage,current with different MPPT system for different temperature and irradiance

Table 6.5.1: Comparison of the tracking power,voltage,current wiyh different MPPT system for different temperature and irradiance

Irradiance	600w/m <sup>2</sup>	800w/m <sup>2</sup>	1000w/m <sup>2</sup>
Temperature	22°C	25°C	28°C
P&O	P=110.2W	P=190.2W	P=285.7W
INC	P=110.9W	P=191.4W	P=285.7W

P&O	I=5.178A	I=6.904A	I=8.537A
INC	I=5.178A	I=6.904A	I=8.518A
P&O	V=21.29V	V=27.55V	V=33.47V
INC	V=21.41V	V=27.72V	V=33.54V

### 6.5.2 Comparison of the tracking power,voltage,current without MPPT for different temperature and irradiance

Table 6.5.2: Comparison of the tracking power,voltage,current without MPPT system for different temperature and irradiance

Irradiance	600w/m <sup>2</sup>	800w/m <sup>2</sup>	1000w/m <sup>2</sup>
Temperature	22°C	25°C	28°C
Power(W)	P=90.42W	P=154.8W	P=236.3W
Voltage(V)	V=17.46V	V=22.42V	V=27.38V
Current(A)	I=5.178A	I=6.904A	I=8.63A

### 6.5.3 Comparison of the tracking power,voltage,current between NO MPPT and MPPT(PO) for different temperature and irradiance

Table 6.5.3: Comparison of the tracking power,voltage,current between NO MPPT and MPPT(PO) for different temperature and irradiance

Irradiance		600w/m <sup>2</sup>	800w/m <sup>2</sup>	1000w/m <sup>2</sup>
Temperature		22°C	25°C	28°C
Power(W)	NO MPPT	P=90.42W	P=154.8W	P=236.3W
	MPPT(PO)	P=110.2W	P=190.2W	P=285.7W
Voltage(V)	NO MPPT	V=17.46V	V=22.42V	V=27.38V
	MPPT(PO)	V=21.29V	V=27.55V	V=33.47V
Current(A)	NO MPPT	I=5.178A	I=6.904A	I=8.63A
	MPPT(PO)	I=5.178A	I=6.904A	I=8.537A

### 6.5.4 Comparison of the tracking power,voltage,current between NO MPPT and MPPT(INC) for different temperature and irradiance

Table 6.5.4: Comparison of the tracking power,voltage,current between NO MPPT and MPPT(PO) for different temperature and irradiance

Irradiance		600w/m <sup>2</sup>	800w/m <sup>2</sup>	1000w/m <sup>2</sup>
Temperature		22°C	25°C	28°C
Power(W)	NO MPPT	P=90.42W	P=154.8W	P=236.3W
	MPPT(INC)	P=110.9W	P=191.4W	P=285.7W
Voltage(V)	NO MPPT	V=17.46V	V=22.42V	V=27.38V
	MPPT(INC)	V=21.41V	V=27.72V	V=33.54V
Current(A)	NO MPPT	I=5.178A	I=6.904A	I=8.63A
	MPPT(INC)	I=5.178A	I=6.904A	I=8.518A

## 6.5.5 Comparison of the elapsed time for different MPPT system

Table 6.5.5 Comparison of the elapsed time for different MPPT systems

Elapsed time of MPPT (s)			
Irradiance	600w/m <sup>2</sup>	800w/m <sup>2</sup>	1000w/m <sup>2</sup>
Temperature	22°C	25°C	28°C
P&O	51sec	53sec	55sec
	P=110.2W	P=190.2W	P=285.7W
INC	53sec	55sec	56scc
	P=110.9W	P=191.4W	P=285.7W

THIS PAGE INTENTIONALLY LEFT BLANK

# **CHAPTER 7**

## **CONCLUSION AND FUTURE WORK**

### **7.1 Conclusion**

Overall the comparison of the MPPT algorithms was a worthwhile endeavor. Many of the problems inherent in this type of system can be solved or optimized to an acceptable level. This work could benefit future development solar powered UAVs.

In this thesis, the overall operation of the buck-boost converter was covered. The different contributions of each component were discussed and how they each affected the output and functionality of the circuit. By optimizing the buck-boost converter independent of the MPPT and the solar array, the efficiency of the converter was greater than 96% during steady-state operation. This makes the conversion from the solar array quite efficient and attractive.

The MPPT was discussed after the buck-boost boost converter and greatly improved the tracking of the MPP. By having the ability to track the MPP, the MPPT algorithms further optimized the low efficiency solar array output. Since the solar array is the source of power to the system, any improvement in the ability to track the MPP, also greatly improves the overall system performance.

Next, the solar array model was discussed as well as designed around a single diode model. By modeling the solar array based on measured parameters, the output current and voltage were measured and used to drive the buck-boost converter. The actual data gathering runs were done in three parts. The first part included the P&O algorithm with constant 1000W/m<sup>2</sup> irradiance, a step in irradiance from 600W/m<sup>2</sup> to 1000W/m<sup>2</sup> at 0:08 s to 0:01 s, and a random changing of irradiance to the solar array.

Next, the constant D controller was tested with the same three input signals. The constant D was tested as the reference for comparison with the other algorithms. Finally, the InC algorithm was tested; although, the tuning of the parameters for this algorithm was the most difficult. The algorithm leads to either a very fast response to transients or undershoots the MPP. Because of the difficulty optimizing and the amount of time required to actually run each test, the InC algorithm was not optimized to match the performance of the P&O



algorithm. By including a two-stage change in D, the P&O algorithm was further optimized. This innovation was necessary in order to converge quickly to the MPP yet still have fine granularity when approaching the MPP. This addition was not very difficult to implement and overall provided very fast tracking and convergence to the MPP. In the Appendix, the code used for this algorithm is provided. It can be seen that with a multistage MPPT, the overall speed of the system will remain fast and track the MPP well.

Overall, the outcome of the P&O algorithm tests was quite good. Since the algorithm can be optimized to meet certain timing requirements, it responded faster and performed better than the InC algorithm. This can only be accounted for due to the complexities of the InC algorithm computations and speed of operation. Due to the difficulty in optimizing the InC algorithm, the results from those runs do not accurately give the optimal operation of the algorithm. Given more time to properly optimize the DD, the algorithm should have tracked the MPP quicker and with more certainty than the P&O algorithm.

## **7.2 Future Work**

There are a few optimizations that were not integrated into the thesis but would be valuable to include.

### **7.2.1 UAV Flight Endurance**

In the modern UAV, most onboard components are run from a battery. Similar to satellites, UAVs require battery power to be replenished at some point. If all of the power for the system comes from the battery, it seems logical to try and extend the range and time the UAV will be on a mission. In order to accomplish this, thin film solar panels can be laminated to the surface of the wings of these UAVs and used to deliver power to the batteries while in flight. With the inclusion of an MPPT, the solar panels on the wing will be optimized for when the UAV turns to a non-optimal power generation angle[4].

## **7.2.2 Second Stage Constant Voltage Output**

In order to actually use the output power from the MPPT, a second stage constant voltage controller would also be necessary to provide the power required to charge a battery system. This battery system would then have all the equipment connected to that so the voltage would be quite stable at the equipment. Without this extra controller the battery charger attached to the buck-boost converter would not have a high enough voltage if the irradiance dropped too low. Depending on the amount of light and the configuration of the solar panels, a buck-boost-boost converter might be better suited for this application[4].

## **7.2.3 Test MPPT on Real Hardware**

A proof-of-concept for this simulation would be to use real hardware to control a buck -boost converter. Unfortunately, we did not have the required time to change the laboratory setup and run the algorithm.

# APPENDIX: DATASHEET & MATLAB CODE

## Electrical specification of a PV module

Item	Value
Rated maximum power (W)	286
Rated voltage (V)	33.52
Rated current (A)	8.53
Open circuit voltage $V_{OC}$ (V)	37.51
Short circuit current $I_{SC}$ (A)	8.63
$I_{SC}$ temperature coefficient (mA/°C)	1.65
$V_{OC}$ temperature coefficient(V/°C)	- 0.129

## P & O Algorithm

```
function D = PO(V,I,T)
persistent P2 P1 dP d dd n;
if isempty(V)
    V=20;
end
if isempty(I)
    I=0;
end
if isempty(P2)
    P2=0;
end
if isempty(P1)
    P1=0;
end
if isempty(dP)
    dP=0;
end
if isempty(d)
    d=1;
end
if isempty(dd)
    dd=0;
end
if isempty(n)
    n=1;
end

if (T > n*0.02)
    n = n + 1;
    P1=P2;
    P2=V*I;
    dP=P2-P1;
```

```

if (dd==0)
    if dP>1
        dd=0.01;
        d=d+dd;
    else
        if dP<-1
            dd=-0.01;
            d=d+dd;
        else
            dd=0;
        end
    end
end
else
    if ((dP<1)&&(dP>-1))
        dd=0;
        d=d+dd;
    else
        if ((dP/dd)>0)
            dd=0.01;
            d=d+dd;
        else
            dd=-0.01;
            d=d+dd;
        end
    end
end
end
end
D=d/(d+1);
if D<0.1
    D=0.1;
    d=D/(1-D);
else
    if D>0.9
        D=0.9;

```

```

        d=D/(1-D);
    else
    end
end
end
end

```

## Incremental Conductance Algorithm

```

function D = IC(V,I,T)
persistent V2 V1 I2 I1 dV dI d dd n;
if isempty(V)
    V=20;
end
if isempty(I)
    I=0;
end
if isempty(V2)
    V2=0;
end
if isempty(V1)
    V1=0;
end
if isempty(dV)
    dV=0;
end
if isempty(I2)
    I2=0;
end
if isempty(I1)
    I1=0;
end
if isempty(dI)
    dI=0;

```

```

end
if isempty(d)
    d=1;
end
if isempty(dd)
    dd=0;
end
if isempty(n)
    n=1;
end
if (T > n*0.02)
    n = n + 1;
    V1=V2;
    I1=I2;
    dV=V2-V1;
    dI=I2-I1;
    if (dV==0)
        if (dI==0)
            dd=0;
            d=d+dd;
        else
            if (dI/dV)>(-(I/V))
                dd=0.01;
                d=d+dd;
            else
                dd=-0.01;
                d=d+dd;
            end
        end
    end
else
    if (dI/dV)==(-(I/V))
        dd=0;
        d=d+dd;
    else

```

```
    if dI>0
        dd=0.01;
        d=d+dd;
    else
        dd=-0.01;
        d=d+dd;
    end
end
end
end
D=d/(d+1);
if D<0.1
    D=0.1;
else
    if D>0.9
        D=0.9;
    else
end
end
end
```

## REFERENCES



- [1] Mummadi Veerachary, "Control of TI-SEPIC Converter for Optimal Utilization of PV Power", IICPE, 2010 New Delhi.
- [2] M. Berrera, A. Dolara, R. Faranda and S. Leva, "Experimental test of seven widely-adopted MPPT algorithms", 2009 IEEE Bucharest Power Tech Conference, June 28th - July 2nd, Bucharest, Romania.
- [3] Comparative Study of Maximum Power Point Tracking Algorithms;D. P. Hohm and M. E.Ropp.P.47
- [4] Design of a maximum power point tracker with simulation,analysis and comparison of algorithms Jeff Wurz, Civilian, United States Navy,B.S., Electrical Engineering, University of California, Davis, 2008.P.1-3,69
- [5] E. Weston, "Art of utilizing solar radiant energy," September 1888.
- [6] A. Einstein, "Concerning an heuristic point of view toward the emission and transformation of light," American Journal of Physics, vol. 33, no. 5, 1965.
- [7] "BP Solar limited warranty certificate", BP Solar, 2010. [Online]. Available: [http://www.bp.com/liveassets/bp\\_internet/solar/bp\\_solar\\_usa/STAGING/local\\_assets/downloads\\_pdfs/2010\\_Warranty.pdf](http://www.bp.com/liveassets/bp_internet/solar/bp_solar_usa/STAGING/local_assets/downloads_pdfs/2010_Warranty.pdf) [Accessed 14/12/2010].
- [8] D. M. Chapin, C. S. Fuller, and G. L. Pearson, "A new silicon pn junction photocell for converting solar radiation into electrical power," Journal of Applied Physics, vol. 25,p. 676, 1954.
- [9] G. M. S. Azevedo, M. C. Cavalcanti, K. C. Oliveira, F. A. S. Neves, Z. D. Lins, "Evaluation of maximum power point tracking methods for grid connected photovoltaic systems," in *Proc. IEEE PESC*, 2008, pp. 1456-1462.
- [10] "Trends in photovoltaic applications. Survey report of selected IEA countries between 1992 and 2009", International Energy Agency, Report IEA-PVPS Task 1 T1-19:2010, 2010. [Online]. Available: [http://www.iea-pvps.org/products/download/Trends-in-Photovoltaic\\_2010.pdf](http://www.iea-pvps.org/products/download/Trends-in-Photovoltaic_2010.pdf) [Accessed 28/10/2010].
- [11] G. Barca, A. Moschetto, C. Sapuppo, G. M. Tina, R. Giusto, and A. D. Grasso, "A novel mppt charge regulator for photovoltaic stand-alone telecommunication system," pp. 235–238, 2008.
- [12] N. Mohan, Power Electronics: Converters, Applications, and Design. Wiley, 2002.
- [13] M. Azab, "Improved circuit model of photovoltaic array," International journal of electrical power and energy systems engineering, vol. 2, no. 3, pp. 185–188, 2009.
- [14] A. P. K. Yadav, S. Thirumaliah, and G. Haritha, "Comparison of mppt algorithms for dc-dc converters based pv systems," International Journal of Advanced Research

- in *Electrical, Electronics, and Instrumentation Engineering*, vol. 1, no. 1, pp. 18–23, 2012.
- [15] G. M. S. Azevedo, M. C. Cavalcanti, K. C. Oliveira, F. A. S. Neves, Z. D. Lins, "Evaluation of maximum power point tracking methods for grid connected photovoltaic systems," in *Proc. IEEE PESC*, 2008, pp. 1456-1462.
- [16] Norjasmi Bin Abdul Rahman, "Inverter Topologies for Photovoltaic Systems", Master's Thesis, Dept. Electrical Engineering, Aalto University School of Science and Technology, Espoo, Finland, 2010.
- [17] W. Hurd, "Applicaion of copper indium gallium diselenide photovoltaic cells to extend the endurance and capabilities of unmanned aerial vehicles," Master's thesis, Naval Postgraduate School, Monterey, CA, 2009.
- [18] J. Coba, "Design of solar powered airplanes for continuous flight," Master's thesis, Naval Postgraduate School, Monterey, CA, 2010.
- [19] S. S. Mohammed, "Modeling and simulation of photovoltaic module using matlab/simulink," *International Journal of CHemial and Environmental Engineering*, vol. 2, no. 5, pp. 350–355, 2011.
- [20] I. Glasner and J. Appelbaum, "Advantage of boost vs buck topology for maximum power point tracker in photovoltaic systems," pp. 355–358, 1996.
- [21] A. P. K. Yadav, S. Thirumaliah, and G. Haritha, "Comparison of mppt algorithms for dc-dc converters based pv systems," *International Journal of Advanced Research in Electrical, Electronics, and Instrumentation Engineering*, vol. 1, no. 1, pp. 18–23, 2012.
- [22] Z. Liang and R. Huang, A. Q. and Guo, "High efficiency switched capacitor buckboost converter for pv application," pp. 1951–1958, 2012.
- [23] G. Barca, A. Moschetto, C. Sapuppo, G. M. Tina, R. Giusto, and A. D. Grasso, "A novel mppt charge regulator for photovoltaic stand-alone telecommunication system," pp. 235–238, 2008.
- [24] M. Azab, "Improved circuit model of photovoltaic array," *International journal of electrical power and energy systems engineering*, vol. 2, no. 3, pp. 185–188, 2009.
- [25] D. P. Hohm and M. E. Ropp, "Comparative study of maximum power point tracking algorithms," *Progress in Photovoltaics: Research and Applications*, vol. 11, pp. 47–62, 2003.
- [26] S. Gomathy, S. Saravanan, and D. S. Thangavel, "Design and implimentation of maximum power point tracking algorithm for a standalone pv system," *International journal of scientific and engineering research*, vol. 3, no. 3, 2012.

- [27] V. A. Chaudhari, “Automatic peak power tracker for solar pv modules using dspacer software.” Master’s thesis, MAULANA AZAD NATIONAL INSTITUTE OF TECHNOLOGY, Deemed University, Bhopal, India, 2005.
- [28] V. Salas, E. Olías, A. Barrado, and A. Lázaro, “Review of the maximum power point tracking algorithms for stand-alone photovoltaic systems,” *Solar Energy Materials and Solar Cells*, vol. 90, pp. 1555–1578, July 2006.
- [29] Huan-Liang Tsai, Ci-Siang Tu, and Yi-Jie Su, “Development of Generalized Photovoltaic Model Using MATLAB/SIMULINK”, *Proceedings of the World Congress on Engineering and Computer Science 2008 WCECS 2008*, October 22 - 24, 2008, San Francisco, USA.
- [30] Ramos Hernanz, JA., Campayo Martín, J.J. Zamora Belver, I., Larrañaga Lesaka, J., Zulueta Guerrero, E. Puelles Pérez, E.,” *Modeling of Photovoltaic Module*”, *International Conference on Renewable Energies and Power Quality (ICREPQ’10) Granada (Spain)*, 23th to 25th March, 2010.
- [31] [www.asrite.com:8080/solar/mikebaker\\_SDM\\_0608.xls/WR25U04E](http://www.asrite.com:8080/solar/mikebaker_SDM_0608.xls/WR25U04E) SN 1344403160